The Dissertation Committee for Tieying Hou Certifies that this is the approved version of the following dissertation:

STAT3-Protein Interactions in IL-6/gp130 Signaling

Committee:

John Papaconstantinou, Ph.D.

Allan Brasier, M.D.

Istvan Boldogh, Ph.D.

Chunming Liu, Ph.D.

Kishor Bhakat, Ph.D.

John DiGiovanni, Ph.D.

Dean, Graduate School

STAT3-Protein Interactions in IL-6/gp130 Signaling

by

Tieying Hou, M.S.

Dissertation

Presented to the Faculty of the Graduate School of

The University of Texas Medical Branch

in Partial Fulfillment

of the Requirements

for the Degree of

DOCTOR OF PHILOSOPHY

The University of Texas Medical Branch

December, 2008

Dedication

This dissertation is dedicated to the following people:

My father, who has been my role-model for hard work and persistence.

My mother, who has been giving me endless love and support.

My husband, who has shared the many uncertainties, challenges and complains.

My brother and his family, who have been taking care of my parents and sharing the happiness in my little nephew's growth.

Acknowledgements

I would like to thank everyone who has helped make this dissertation possible.

My deepest gratitude is to my advisor, Dr. Allan R. Brasier for all his guidance, support, patience and encouragement. I am fortunate to have an advisor who has always been there, listens to me and gives advice. His sincere interest in science and education has been a great inspiration to me. He taught me many technical skills and his expertise in cloning was a big help to my project. Dr. Brasier also encouraged me to develop independent thinking and continually stimulated my analytic ability. I would not finish this dissertation without his constant help.

I am also thankful for my committee members: Dr. John Papaconstantinou, Dr. John DiGiovanni, Dr. Istvan Boldogh, Dr. Chunming Liu and Dr. Kishor Bhakat, for their very helpful insights, comments and suggestions.

I extend many thanks to all my colleagues especially Dr. Sutapa Ray, Chang Lee, Ping Liu, Ruwen Cui and Muping Lu for providing technical support. I am fortunate to work in such a friendly environment.

I want to acknowledge Dr. Lillian Chan and Debora Botting for constant assistance throughout my doctoral study. I also own a note of gratitude to Dr. Kathleen O'Connor for offering kind help in my visa application and my project.

Finally, I give my thanks to my family and my friends. They have been constant source of love, concern and strength all these years. None of this would be possible without their support.

STAT3-Protein Interaction in IL-6/gp130 Signaling

Publication No._____

Tieying Hou, M.S.

The University of Texas Medical Branch, 2008

Supervisor: Allan R. Brasier

The Signal Transducer and Activator of Transcription 3 (STAT3) is a central transcription factor downstream of IL-6/gp130 signaling. This thesis investigates how STAT3 regulates IL-6 signal transduction by interacting with its coactivators. First, the function of an IL-6 inducible complex of STAT3 with cyclin-dependent kinase 9 (CDK9) was examined by using gamma-Fibrinogen (γ-FBG), an acute phase protein, as a model. IL-6 induces a strong nuclear association of STAT3 with CDK9, which is mediated via both STAT's NH2-terminal and COOH-terminal domains. The induction of γ-FBG by IL-6 is significantly decreased when CDK9 is repressed by kinase inhibitor or downregulated by siRNA. Moreover, an IL-6-inducible STAT3 and CDK9 binding to the proximal γ-FBG promoter is observed. This phenomenon is accompanied by increased loading of RNA Pol II and phospho-Ser2 CTD Pol II on the γ-FBG TATA box and coding regions. Finally, both IL-6-inducible RNA Pol II and phospho-S2 CTD RNA Pol II association with the endogenous γ-FBG gene are significantly decreased when CDK9 kinase activity is inhibited. In this study we provide evidence that activated STAT3 regulates the transcription elongation of the γ-FBG gene by associating with CDK9. The magnitude of IL-6/gp130 signaling is also regulated by p300, another coactivator of STAT3 with histone acetyltransferase

activity (HAT). The p300-STAT3 interaction is partially regulated by the STAT3 NH2-terminal domain. The second part of this thesis investigates the STAT3 NH2-terminal function and how its interaction with p300 regulates STAT3 signal transduction. The STAT3 NH2-terminal domain is required for the downstream gene expression, including *socs3*, *c-fos* and *p21*. Additionally, the recruitment of p300 and RNA Pol II to the *socs3* promoter is reduced in MEFs stably expressing STAT3-ΔN mutant which is deficient in the NH2-terminal domain. We also reported that the binding site of the STAT3 NH2-terminal domain maps to the p300 bromodomain and the STAT3 NH2-terminal acetylation induced by p300 stabilizes this interaction. Finally, the deletion of p300 bromodomain not only reduces its binding affinity to STAT3 but also inhibits its association to the *socs3* promoter. Our data indicates that the STAT3 NH2-terminal domain regulates gp130 signaling by interacting with the p300 bromodomain, thereby stabilizing enhanceosome assembly. In summary, my thesis work has described a mechanism by which the STAT3 NH2-terminal domain controls gene expression by interacting with coactivators and transcriptional elongation factors. The multiple functions of the STAT3 NH2-terminal domain make it a potential target for the therapeutic modulation in inflammatory disease.

Table of Contents

List of Tables

List of Figures

CHAPTER 1: INTRODUCTION

1.1 IL-6 signaling

Cytokines of the Interleukin-6 (IL-6) family include IL-6, IL-11, oncostatin M (OSM), cardiotrophin-1 (CT-1), ciliary neurotrophic factor (CNTF), cardiotophin-like cytokine (CLC), leukemia inhibitory factor (LIF), and the recently identified IL-27p28 (1-5). As a pleiotropic cytokine, IL-6 is widely implicated in multiple processes including immune response, hematopoiesis, neurogenesis, embryogenesis, and oncogenesis (6-10). Because of its central role in a variety of biological responses, mechanisms for IL-6 signaling pathway have been intensely investigated. The classic signaling pathway initiated by the IL-6 cytokine family is via ligand binding to cognate high affinity α chain receptors, e.g., IL-6Rα or OSMRα (11), which lacks intrinsic kinase activity. The liganded IL-6Rα then forms an oligomeric complex with gp130 (transducin) (12), a ubiquitously expressed transmembrane protein shared by all IL-6 family members. Receptor ligation causes conformational changes in the cytoplasmic domain of gp130, which brings gp130-associated tyrosine kinases, the Janus- (JAK) and Tyk, into close proximity. JAK and Tyk phosphorylate gp130 on its cytoplasmic domain (13-15), leading to the binding of the cytoplasmic Signal Transducer and Activator of Transcription (STAT)-1 and -3 isoforms via their src homology (SH)-2 domains (16, 17). As additional substrates of the JAK/Tyk kinases, STATs are also phosphorylated on a specific tyrosine localized on its COOH-terminal transactivation domain (TAD) (18, 19), allowing them to dimerize via intermolecular SH2 interactions, whereupon they are translocated into the nucleus (Figure 1.1).

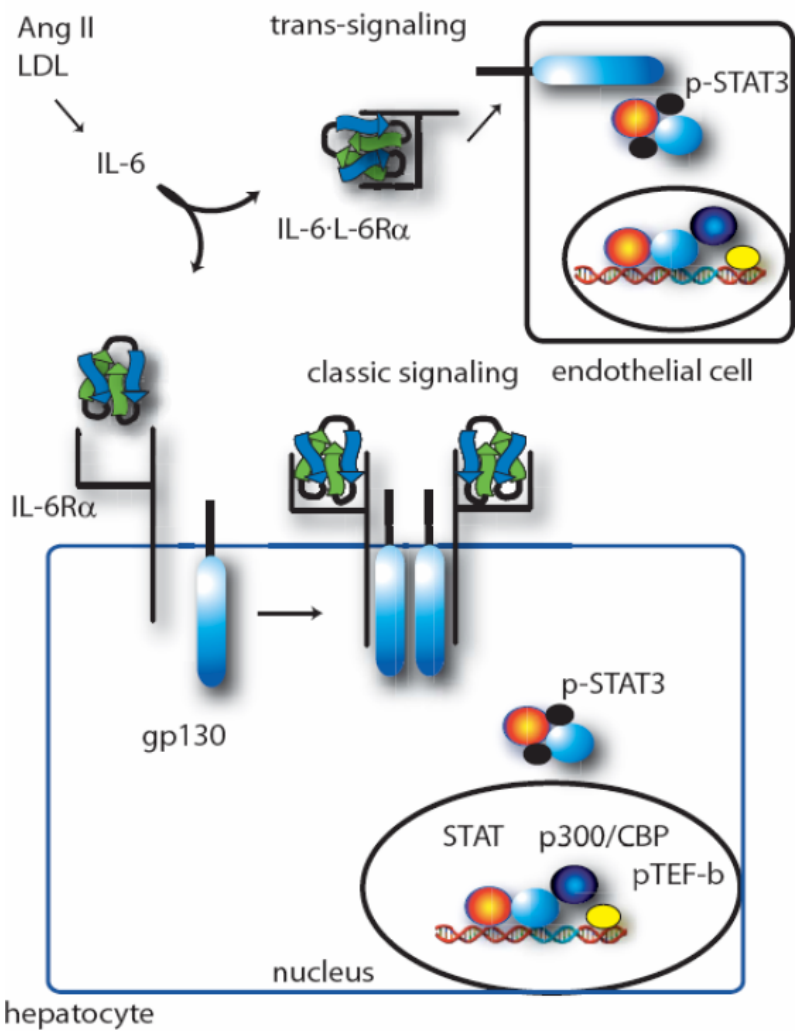

Figure 1.1 IL-6 induced classical and trans-signaling pathways. Shown is a schematic view of classical IL-6 signaling *via* the IL-6Rα receptor and gp130 for a representative hepatocyte. IL-6Rα bound to the IL-6 ligand results in complex formation with gp130, activating tyrosine kinase activity, including and culminating in tyrosine phosphorylation of STAT3. The IL-6 trans-signaling pathway is diagrammed at top, using a representative endothelial cell. Circulating IL-6·IL-6Rα engages with gp130 expressed on cells, enabling activation of the IL-6 signaling pathway in cells lacking IL-6Rα. See text for further details. (Figure adapted from Hou, T., Tieu, B.C., Ray, S.,Recinos, A., Cui, R., Tilton, R.G. and Brasier, A.R. Roles of IL-6-gp130 Signaling in Vascular Inflammation. *Current Cardiology Reviews* 2008, 4: 179-192).

In addition to membrane-bound IL-6R, a soluble form of IL-6R (sIL-6Rα), which has been found in various human fluids (20, 21), significantly enhances IL-6 tissue response by a process termed "trans-signaling" (Figure 1.1). The sIL-6Rα is produced by two mechanisms: translation from an alternative spliced mRNA transcript (22) or metalloprotease-dependent proteolytic cleavage of a membrane-anchored protein at a site close to the cell surface (23). The soluble IL-6-IL-6Rα complex can initiate IL-6 signaling on any cell type that only express gp130 (5). Because gp130 is ubiquitously expressed, IL-6 trans-signaling expands the repertoire of IL-6 responsive cells to virtually any cell in the body. IL-6 trans-signaling has been shown play a key role in the development of chronic inflammatory disorder and cancer (24, 25).

1.2 CDK9 and P-TEFb

The mechanism how tyrosine-phosphorylated STAT3 (pY-STAT3) induces gene expression is partly understood. Upon entry into the nucleus, STAT3 undergoes additional post-translational modifications that permit interactions with co-factors, which positively or negatively regulate STAT3 activity. There is a growing list of STAT3 coactivators that have been identified up to now, including the relatively general transcriptional coactivators, like p300/CBP (26, 27), and the more specific ones, like Crif1 (28). In Chapter 1, we report our finding that cyclin-Dependent Kinase 9 (CDK9) also functions as coactivator of STAT3 and its kinase activity is indispensable for STAT3 downstream gene expression.

Cyclin-Dependent Kinase 9 (CDK9) was first identified in searching for putative controllers of the mammalian cell cycle. It was regarded as a CDC2-related kinase and named PITALRE for its Pro-Ile-Thr-Ala-Leu-Arg-Glu motif (29). The function of CDK9 was unknown until Zhu *et al* (30) cloned the small subunit of *Drosophila* P-TEFb and

found that it was the homologue of the human PITALRE protein. Their data also showed that PITALRE was associated with HIV-1 Tat, the virus-encoded transcription factor, and the association was required for the effect of Tat on transcription elongation (30).

There are two isoforms of CDK9 in mammalian cells, named CDK942 and CDK955 according to the distinct molecular weight (31). Subsequently, the regulatory subunit of CDK9 is identified, which contains a cyclin box motif and is named cyclin T (32, 33). Thus far, two cyclin T genes have been found, encoding cyclin T1 and T2, and alternative splicing of cyclin T2 gene produces two variants called cyclin T2a and cyclin T2b. Another cyclin subunit, cyclin K, has also been shown in association with CDK9 (34). Therefore, there are eight different CDK9/cyclin complexes resulting from the combination from two CDK9 isoforms and four regulatory cyclin subunits (35). The CDK9/cyclin T complex is known as P-TEFb because the T type cyclins contain a His-rich motif that helps recoganize the COOH-terminal domain (CTD) of RNA polymerase II (RNA pol II) (33) and facilitates the CTD phosphorylation by CDK9. In contrast, cyclin K lacks the essential His-rich motif and cyclin K/CDK9 can only activate transcription when tethered to RNA not DNA (34).

The mRNA transcription cycle includes the following steps: preinitiation, initiation, promoter clearance, elongation and termination. After the preinitiation complex is assembled, the CTD of RNA Pol II in unphosphorylated form is targeted on S5 by the kinase subunit, Kin28, of TFIIH (36, 37), which initiate transcription and early elongation (38-40). At this moment, only short and abortive RNA transcripts can be produced. Shortly after transcription initiation, RNA Pol II activity is inhibited by the recruitment of negative elongation factors, including the DRB-sensitivity-inducing factor (DSIF) and the negative elongation factor (NELF) (41, 42). This pause allows the capping enzyme (CE) binding to add a 5'-cap to the nascent transcript. The subsequent release of RNA Pol II

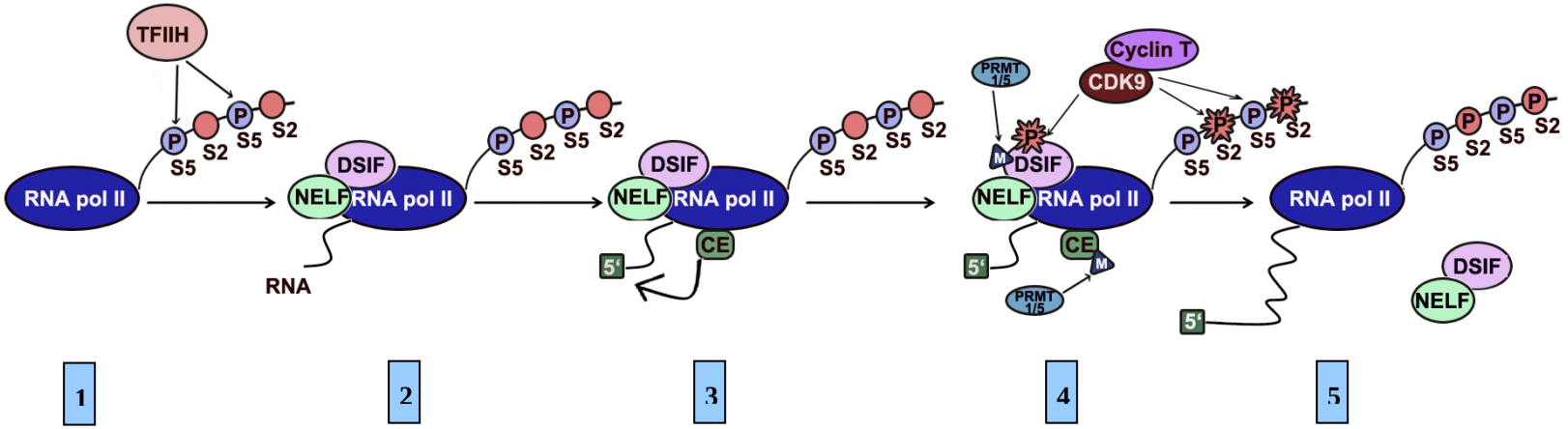

Figure 1.2 Function of CDK9/cyclin T in mRNA transcription (1). The unphosphorylated RNA Pol II is first targeted by TFIIH on S5 of the CTD, which initiates transcription and early elongation (2). Shortly after transcription initiation, negative elongation factors, NELF and DSIF, recruit and pause the transcription cycle. Only abortive transcripts are produced (3). The pause of transcription allows the capping enzyme (CE) recruitment, adding 5'-cap to the nascent transcript (4). CDK9 phosphorylates the CTD of RNA Pol II on S2 as well as negative elongation factors, leading to RNA Pol II activation. The disassociation of DSIF also requires methylation on DSIF and CE catalyzed by protein-arginine N-methyltransferase-1/5 (PRMT 1/5) (5). The transcription cycle is reinitiated and RNA Pol II catalyzes the production of long transcripts.

from the repression of negative elongation factors requires the kinase activity of CDK9, a subunit of P-TEFb complex. CDK9 phosphorylates the CTD of RNA pol on ser2 as well as negative elongation factors (43, 44), resulting into their disassociation from transcription apparatus. The transcription cycle is then reinitiated and RNA Pol II becomes engaged into the productive transcript elongation (45, 46) (Figure 1.2).

Although P-TEFb activity is widely required for the transcription of many genes, the regulatory mechanisms by which P-TEFb is recruited to different promoters are not clear. There are eight potential P-TEFb complexes due to the combination of distinct isoforms of CDK9 and cyclin subunits. This implicates that different genes may require specific P-TEFb complexes to activate productive elongation. Another interesting finding is that P-TEFb associates with various protein factors to induce downstream gene expression. For example, a cellular transcription factor, Nuclear Factor-κB (NF-κB) associates with P-TEFb to stimulate transcriptional elongation of IL-8 gene (47). Both CDK9 and cyclin T1 interact with Rel A and TNF-α stimulates the recruitment of P-TEFb complex to the NF-κB-regulated IL-8 promoter(47). A group of transactivators or receptors have been identified that interact with P-TEFb to regulate target gene transcription, such as the class II transactivator (CIITA), which regulates the expression of MHC class II gene (48), and Tat, a transcription factor required for HIV-1 transcription (30).

In Chapter 1, we found that STAT3 also recruits CDK9 in response of IL-6 in human hepatocarcinoma cells. We observed a stable nuclear complex of STAT3 with CDK9 and sought to further understand its role in the hepatic acute phase response (APR) regulation using γ-FBG as a model gene.

1.3 IL-6, APR and γ-FBG

The APR is a coordinated response to tissue injury, infection or malignancy that initiates a global switch in the transcription of secreted proteins expressed by the vertebrate liver (49). Here, cytokines produced at the site of injury activate the *de novo* expression of genes encoding acute phase proteins (APPs), proteins important in homeostasis, opsonization and wound repair. Gene deletion experiments have shown that the actions of STAT3 are necessary for inducible expression of a network of APP genes, including C-reactive protein, serum amyloid A, angiotensinogen (50-52).

Of the APPs, fibrinogen (FBG) is known to play a key role in the APR by mediating hemostasis, participating in clot formation, platelet aggregation and clot retraction (53), processes important in promoting tissue repair at the site of injury. Fibrinogen (FBG) is a large glycoprotein consisting of three pairs of non-identical polypeptides (Aα, Bβ, and γ) which are encoded by separate genes (54). IL-6 can stimulate mammalian hepatocytes to produce FBG in a dose-dependent manner (55). IL-6 response elements have been identified in the promoter regions of all human FBG Aα, Bβ, and γ genes (56-59). Analysis of the 5'-flanking region of human FBG Aα identified six potential IL-6 responsive sequences, among which a single sequence of CTGGGA localized from -122 to -127 bp is a functional element (56). Also, a CCAAT/enhancer binding protein site (C/EBP, -134 to -142 bp) is found adjacent to the functional IL-6 response element (IL-6RE), which might modulate and further increase the magnitude of IL-6 response (56). In addition, a hepatocyte nuclear factor 1 (HNF-1) binding site, present from -47 to -59 bp, is also essential for the activation of the human FBG Aα gene (56). A similar finding is observed in the promoter of the human FBG Bβ gene. The identified DNA sequences essential for full IL-6-induced expression of FBG Bβ included

three distinct *cis*-acting DNA elements: an HNF-1 site at -85 bp upstream of the transcription start site; a C/EBP binding site between nucleotides -124 and -133; and an IL-6RE present just 4 bp upstream of the C/EBP consensus binding site (59-61).

The γ chain of fibrinogen (γ-FBG) plays a crucial role in fibrinogen function. First, it contains binding sites for platelet integrin $\alpha_{IIb}\beta_3$ and leukocyte integrin $\alpha_M\beta_2$, leading to platelet aggregation and leukocyte recruitment in inflammation (62, 63). In addition, its high binding affinities for vascular endothelial growth factor (64), fibroblast growth factor-2 (65) and interleukin-1β (66) contribute to wound healing. Finally, γ-FBG contains a fibrin polymerization site which is involved in fibrin clot formation and platelet aggregation. Because of the key role of γ-FBG in multiple processes, the transcriptional mechanisms controlling inducible γ-FBG expression have been extensively investigated.

The cytokine IL-6 has emerged as a major mediator of *de novo* acute phase reactants synthesis, and for γ-FBG in particular (57, 67-69). Here, IL-6 produced and secreted at the site of injury, circulates and binds to the hepatic high-affinity IL-6Rα. The liganded IL-6Rα then induces phosphorylations, dimerization and nuclear translocation of STAT-1 and -3 isoforms via gp130. Three IL-6 REs are found in the promoter region of the γ-FBG gene (57, 58). Although all of them contribute to the full promoter activity induced by IL-6, one site (site II) is the major functional IL-6 responsive site (57, 58). Further studies using gel mobility shift assays have shown that the binding affinity of STAT3 to these three elements inversely correlated with their functional activities (67). In contrast to Aα and Bβ-FBG genes, the promoter activity of γ-FBG is not affected by overexpression of C/EBPβ and C/EBPδ isoforms (57).

In Chapter 1 we find IL-6 induces STAT3 binding to CDK9 in a mechanism mediated by both the NH2- and COOH-terminal domains of STAT3. Inhibition of CDK9

activity or its expression decrease IL-6 inducible γ-FBG transcription. Chromatin immunoprecipitation (ChIP) experiments provide direct evidence that IL-6 induces CDK9 recruitment to the γ-FBG promoter along with enhanced RNA Pol II and phospho-S2 CTD Pol II loading on the coding region. Moreover, IL-6 inducible Pol II binding is abolished by the CDK9 inhibitor, flavopiridol (FP). Taken together, our data indicate that the IL-6 inducible STAT3·CDK9 complex is essential for γ-FBG induction during the APR. This phenomenon suggests STAT3 promotes transcription elongation as an additional mechanism for induction of APP genes.

1.4 STAT3 and p300/CBP

Like many other transcription factors, nulcear STAT3 also recruits the p300/CBP as a coactivator, a protein with histone acetyltranferase (HAT) activity. The crucial role of HATs in inducing chromatin remodeling and transcription activation has been long recognized (70). Several proteins with intrinsic HAT activity have been identified, including GCN5 (71), p300/CREB-binding protein (CBP) homologs (72), p300/CBP-associated factor (P/CAF) (73), and TAFII250 (74). HATs activate transcription by one or more of the following ways: (1) they are able to relax core nucleosome structure by acetylating the NH2-terminal histone tails (75-77); (2) they can directly acetylate transcription factors and alter their transcription activities (78-82); (3) they function as scaffold proteins to recruit other coactivators to the local transcriptional apparatus (83, 84); (4) they serve as bridging factors to physically connect sequence-specific transcription factors with multiple components in the basal transcription machinery (85, 86) (Figure 1.3). p300 and its homolog CBP are potent transcriptional coactivators that are actively involved in all the four processes mentioned above. They have been shown

interact with several transcription factors, such as MyoD (82), p53 (87) and E2F1 (88), and regulate their activity by reversible acetylation.

Although the HAT activity of p300/CBP is critical for their function, a growing body of evidence indicates several other mechanisms for the transcriptional activation mediated by p300/CBP. First, by interacting simultaneously with sequence-specific transcription factors and the basal transcriptional machinery, including the TATA-box binding protein, TFIIB, TFIIE and TFIIH, as well as RNA Pol II (89, 90), p300/CBP facilitates the transcription initiation. Also, p300/CBP brings diverse cofactors or coactivators into the local transcription complex by direct interaction, thereby promoting the transcriptional synergy between protein-protein and protein-DNA. For example, it has known that p300/CBP complexes with several other HATs, such as P/CAF (72), SRC-1 (91) and P/CIP/ACTR/AIB1 (92). A recent study reported an interaction between p300/CBP with a family of nucleosome assembly proteins (NAP) (90, 93), which enhances p300-dependent transcription by stabilizing the association of p300 to chromatin and increasing the specific transcription factor binding to DNA (90). JMY is another binding partner that was identified by the yeast two-hybrid approach to screen p300-interacting protein (94). JMY is a functional component of p300/CBP coactivator complex and facilitates p53-dependent apoptosis regulated by p300/CBP (94).

There is strong evidence demonstrating the HAT activity of p300 is required for STAT3 target gene activation (27, 95, 96). For example, overexpression of p300 inhibitor, the adenovirus 12S E1A, significantly inhibits the IL-6-induced activation of human angiotensinogen (hAGT), a vasoactive peptide and acute phase protein controlled by STAT3 (27). Conversely, the ectopical expression of p300 enhances the induction of

hAGT reporter gene stimulated by IL-6 (27). However, p300 deficient in HAT activity functions as a dominant-negative inhibitor and strongly inhibits STAT3-dependent transcription (27).

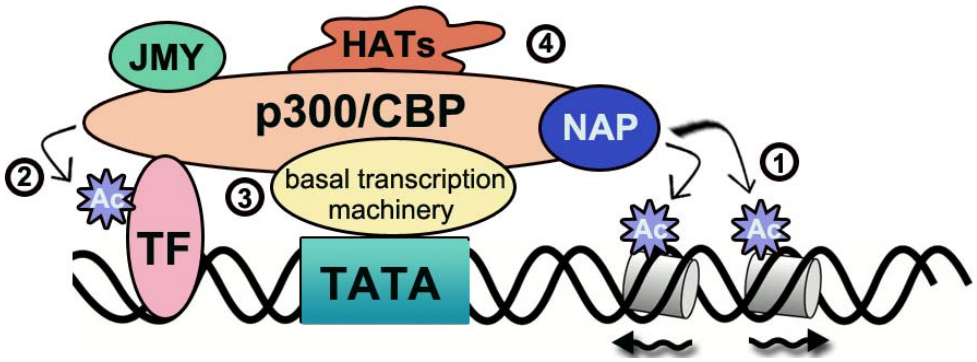

Figure 1.3 Mechanisms of transcriptional activation by p300/CBP. (1) p300/CBP induces chromatin remodeling by acetylating histone tails. (2) p300/CBP targets transcription factors (TF) with the intrinsic HAT activity. Acetylation of TF increases their binding affinity to DNA or affects their interaction with other enhancer binding proteins. (3) p300/CBP functions as a bridge connecting TF with the basal transcription machinery. (4) p300/CBP acts as a scaffold connecting multiple protein components, such as other HATs, JMY and NAP, to facilitate transcriptional activation. See text for more information.

P300 interacts with STAT3 within both its COOH-terminal TAD and NH2-terminal domain (95, 96), and this phenomenon is also confirmed for STAT1 and STAT2 (97, 98). The STAT family share the highly conserved structure that includes an NH2-terminal domain, a coiled-coil domain, a DNA-binding domain, a linker domain, a SH2 domain and a COOH-terminal TAD (99). The coiled-coil domain is actively involved in protein-protein interaction (100) and the SH2 domain mediates the STAT3 dimerization via intermolecular pY-SH2 interactions (101). The COOH-terminal TAD contains a conserved single tyrosine residue that is phosphorylated in STAT activation (13) and facilitates transcriptional activation. The function of NH2-terminal domain in STAT3, however, is poorly understood. In Chapter 3, we investigated the STAT3 NH2-terminal

function by stably expressing a NH2-terminus-deleted mutant (STAT3-ΔN) in *STAT3-/-* MEFs. Both OSM-inducible γ-FBG reporter gene and endogenous mRNA expression including *socs3, c-fos* and *p21*, are significantly reduced in response to STAT3-ΔN expression. Because NH2-terminal domain is involved in p300 binding, the defective activity observed in STAT3-ΔN is probably caused by the reduced cooperation between STAT3 and p300. This hypothesis was then tested in native chromatin by ChIP assays which reveal a reduction in OSM-inducible p300 recruitment to the *socs3* promoter in MEFs stably expressing STAT3-ΔN. At the same time, there is a decrease in RNA pol II binding to the *socs3* promoter, indicating the STAT3 NH2-terminal domain not only stabilizes coactivator association but also facilitates the assembly of transcription preinitiation complex.

Recent studies identified STAT3 not only as a binding partner of p300 but also as a substrate for acetylation. In fact, p300 targets STAT3 at multiple sites. A single acetylation on K685 localized in the COOH-terminal TAD is required for STAT3 dimerization and the subsequent DNA binding activity (96). Our lab independently identified two other Lysine residues, K49 and K87, in the STAT3 NH2-terminal domain that are also inducibly acetylated by p300 in presence of IL-6 and OSM (95). Although these NH2-terminal acetylation have no effect on STAT3 DNA-binding activity, they are essential for STAT3 dependent transcription because K49R/K87R substitutions significantly inhibit STAT3 target gene expression (95). We also noticed that the K49R/K87R mutations decrease the association between p300 and STAT3, indicating that the inducible NH2-terminal acetylation may augment STAT3-p300 interactions. In Chaper 3, we further investigate the interaction between the STAT3 NH2-teriminal domain and p300 and found that the acetyl-lysine mimic substitutions (K49Q/K87Q) increase the STAT3 NH2-terminal binding to p300, confirming the hypothesis that the

NH2-terminal acetylation stabilizes the STAT3-p300 interaction. We also discovered that the STAT3 NH2-terminal binding site maps to the p300 bromodomain. The deletion of the bromodomain in p300 molecule decreases its ability to cooperate with STAT3. In addition, the bromodomain-deficient p300 mutant (p300-ΔB) exhibits weaker chromatin binding.

Taken together, we propose a model in which the IL-6 or OSM-inducible acetylation of STAT3 on K49 and K87 triggers the recognition of NH2-terminal domain by the p300 bromodomain, resulting in a strengthened recruitment of p300 to the promoter of STAT3 target gene, thereby facilitating subsequent enhanceosome assembly.

CHAPTER 2: THE FUNCTIONAL ROLE OF AN IL-6 INDUCIBLE CDK9·STAT3 COMPLEX IN HUMAN γ-FIBRINOGEN GENE EXPRESSION.

2.1. Abstract:

STAT3 is an IL-6 inducible transcription factor that mediates the hepatic acute phase response (APR). Using γ-FBG as a model of the APR, we investigated the requirement of an IL-6 inducible complex of STAT3 with CDK9 on γ-FBG expression in HepG2 hepatocarcinoma cells. IL-6 induces rapid nuclear translocation of Y-phosphorylated STAT3 that forms a nuclear complex with CDK9 in nondenaturing co-immunoprecipitation and confocal colocalization assays. To further understand this interaction, we found that CDK9-STAT3 binding is mediated via both STAT's NH2-terminal modulatory and COOH-terminal transactivation domains. Both IL-6-inducible γ-FBG reporter gene and endogenous mRNA expression are significantly decreased after CDK9 inhibition using the potent CDK inhibitor, flavopiridol (FP), or specific CDK9 siRNA. Moreover, chromatin immunoprecipitation (ChIP) experiments revealed an IL-6 inducible STAT3 and CDK9 binding to the proximal γ-FBG promoter as well as increased loading of RNA Pol II and phospho-S2 CTD Pol II on the TATA box and coding regions. Finally, FP specifically and efficiently inhibits association of phospho-S2 CTD RNA Pol II, indicating that CDK9 kinase activity mediates IL-6 inducible CTD phosphorylation on γ-FBG. Our data indicates that IL-6 induces a STAT3·CDK9 complex mediated by bivalent STAT3 domains and CDK9 kinase activity is necessary for licensing Pol II to enter transcriptional elongation mode. Therefore, disruption of IL-6 signaling by CDK9 inhibitors could be a potential therapeutic strategy for inflammatory disease.

2.2. Results:

2.2.1 IL-6-inducible γ-FBG expression is mediated by STAT3

Previous studies showed that IL-6 potently up-regulates γ-FBG expression in the human hepatoma cell line, HepG2 (57, 67-69). To confirm this finding, γ-FBG expression was measured over a time course of IL-6 stimulation by Q-RT-PCR. A 2.5-fold increase in γ-FBG mRNA abundance was detected as early as 2 h after IL-6 treatment, and the mRNA level continued to increase until a plateau of 12-fold relative to control was observed at 24 h (Fig. 2.1A). To determine the transcriptional contribution, a luciferase reporter driven by 643 bp of the γ-FBG promoter containing three functional type II IL-6 response elements (IL-6REs) was constructed. This -607/+36 γ-FBG-LUC plasmid was transiently transfected into HepG2 cells and stimulated in the absence or presence of various doses of IL-6 (10- and 50 ng/ml) for two different times (12 and 24 h). For the cells stimulated with 10 ng/ml IL-6, we observed an 8-fold induction of normalized luciferase reporter activity relative to control after 12 h, and 13-fold over control after 24 h of stimulation (Fig. 2.1B). At 50 ng/ml IL-6, the inducible activity of the γ-FBG promoter was increased by 15-fold at 12 h and 24-fold at 24 h (Fig. 2.1B). To determine the contribution of IL-6 inducible transcription mediated by STAT3, increasing concentrations of dominant-negative (DN-) STAT3 (Y705F, Ref (52)) were co-transfected with the -607/+36 γ-FBG-LUC reporter gene. As little as 0.1 μg of DN-STAT3 decreased IL-6 inducible reporter activity by more than 70 % (Fig.2.1C). Co-transfected DN-STAT3 had no significant effects on the basal activity of the γ-FBG-LUC reporter gene. Together these data indicated that γ-FBG is an IL-6 inducible gene, mediated, at least in part, by STAT3 dependent transcriptional induction.

Figure 2.1: IL-6 upregulates γ-FBG in HepG2 cells through STAT3.

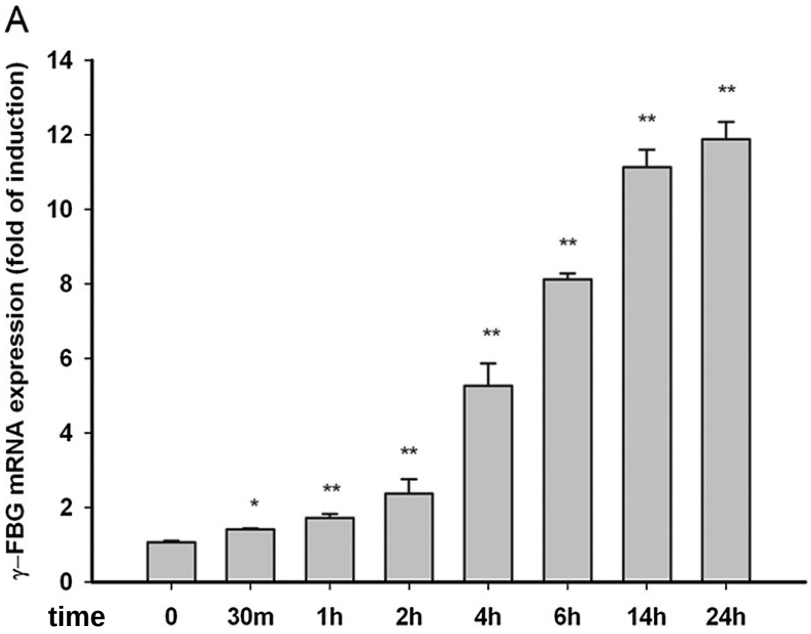

Figure 2.1 A, IL-6 increases endogenous γ-FBG mRNA expression. Serum-starved HepG2 cells were treated with IL-6 (10 ng/ml) for indicated times. Shown is the result of Q-RT-PCR assays plotting the fold change of γ-FBG in IL-6 treated cells normalization to GAPDH. *, p value < 0.05, **, p value < 0.01.

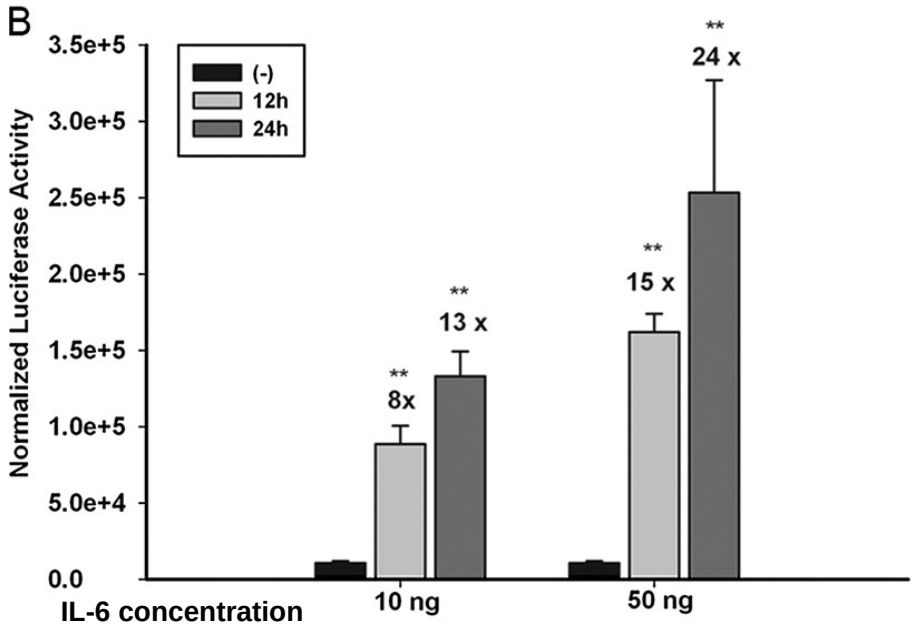

Figure 2.1B, IL-6 induces the reporter activity of γ-FBG in a time- and dose-dependent manner. HepG2 cells were transiently transfected with γ-FBG-LUC reporter and control plasmid pSV2PAP. 24 h after transfection, cells were treated with two different doses of IL-6 (10 ng/ml or 50 ng/ml) for 12 or 24 h followed by assay for reporter gene expression. Fold changes of luciferase activity in IL-6 stimulated cells compared to that of unstimulated cells are shown. *, p value < 0.05, **, p value < 0.01.

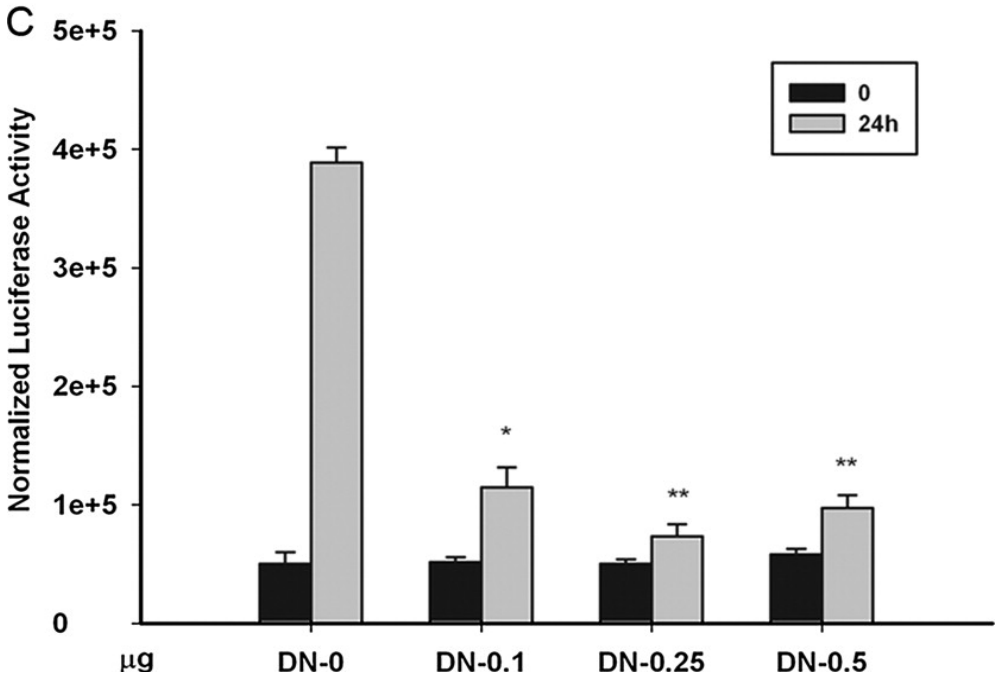

Figure 2.1C, DN-STAT3 inhibits IL-6 induced γ-FBG-LUC reporter activity. Cells were transfected with different amounts of DN-STAT3 together with the reporter gene. Amount of transfected DNA was kept equivalent using an empty expression plasmid. Data shown were means ± SD from three independent transfections. The data was analyzed by Student's t test. *, p value < 0.05, **, p value < 0.01.

2.2.2 IL-6 induces a nuclear STAT3·P-TEFb complex

A series of studies have shown that P-TEFb can interact with various transcription factors or nuclear receptors, such as Nuclear Factor-kappa B (NF-κB) (47), c-Myc (102), androgen receptor (103) and Peroxisome Proliferator-Activated Receptors-gamma (PPARγ) (104). To determine whether STAT3 associates with P-TEFb, HepG2 cells were stimulated in the presence or absence of IL-6 and nuclear extract (NE) was subjected to nondenaturing co-immunoprecipitation assay using anti-CDK9 as the primary Ab. The immune complexes were fractionated on an SDS-PAGE, and STAT3 was detected by Western blot (Fig. 2.2A, upper panel). We observed STAT3 binding only in the IL-6 stimulated NE. By contrast, cyclin T1 was also observed in the complex, but there was no difference in cyclin T1 abundance between IL-6-stimulated and unstimulated NEs (Fig. 2.2A, middle panel), indicating that the CDK9·cyclin T1 complex formation is independent of IL-6 stimulation.

Since IL-6 was required for the association of STAT3 and CDK9, we next asked whether activated STAT3 isoforms were interacting with CDK9. After nondenaturing CDK9 IP, the immune complexes were probed with an antibody that specifically recognized phospho-Y705 STAT3. A strong signal was specifically detected in the IL-6 stimulated CDK9 complexes (Fig. 2.2B, upper panel). By contrast, inactive cytosolic STAT3 failed to interact with CDK9 although CDK9 is expressed constitutively in both the cytosol and nucleus (data not shown). Together, these data suggest that Y phosphorylation and nuclear translocation are essential for the formation of the STAT3·CDK9 complex.

After STAT3 is translocated into the nucleus, it recruits the p300/CBP coactivator, an enzyme with histone acetyltransferase activity. p300/CBP acetylates two lysines (K49, K87) localized at NH2 terminus of STAT3, thereby stabilizing STAT3-

p300/CBP interaction and facilitating downstream gene expression (95). In order to see whether acetylated STAT3 (Ac-STAT3) associates with CDK9, proteins present in the immune complexes precipitated by CDK9 antibody were revealed by immunoblotting with anti-Ac-K87STAT3 Ab (95). We observed that Ac-STAT3 binds CDK9 only in IL-6 stimulated NE (Fig. 2.2C, upper panel).

To exclude the possibility that the Co-immunoprecipitation findings were artifactual due to biochemical fractionation, we confirmed this interaction using confocal colocalization assays. For this purpose, HepG2 cells were transfected with a plasmid encoding CDK9 fused to a monomeric strawberry fluorescence protein pcDNA-FStraw-CDK9, and stimulated with IL-6 prior to fixation. Cells were then stained with anti-STAT3 Ab and secondary FITC labeled Ab. In the transfected cells, straw-CDK9 is diffusely and constitutively localized in nucleus but excluded from the nucleoli (Fig. 2.2D, bottom middle). This distribution pattern of Straw-CDK9 is identical to that of the endogenous CDK9 by immunofluorescence labeling (Fig.2.2D, top middle). In the unstimulated cells, the majority of STAT3 was detected in cytoplasm (Fig. 2.2E, top). By contrast, after IL-6 treatment, there is an obvious accumulation of nuclear STAT3 (Fig. 2.2E, bottom). STAT3-CDK9 co-localization is indicated by the merged overlay (Fig. 2.2E, bottom right). A similar assay was performed staining for phospho-Y705 STAT3. By contrast with anti-STAT3 labeling, no detectable phospho-Y705 STAT3 was observed in unstimulated cells (Fig. 2.2F, top). Upon IL-6 stimulation, phospho-Y705 STAT3 was strongly localized to the nucleus, where it co-localized with nuclear CDK9 (Fig. 2.2F, bottom right). These data confirmed the co-immunoprecipitation studies and indicated that activated STAT3 co-localizes with CDK9 in the nucleus.

Figure 2.2: Activated STAT3 complexes with CDK9 in HepG2 nuclei in presence of IL-6.

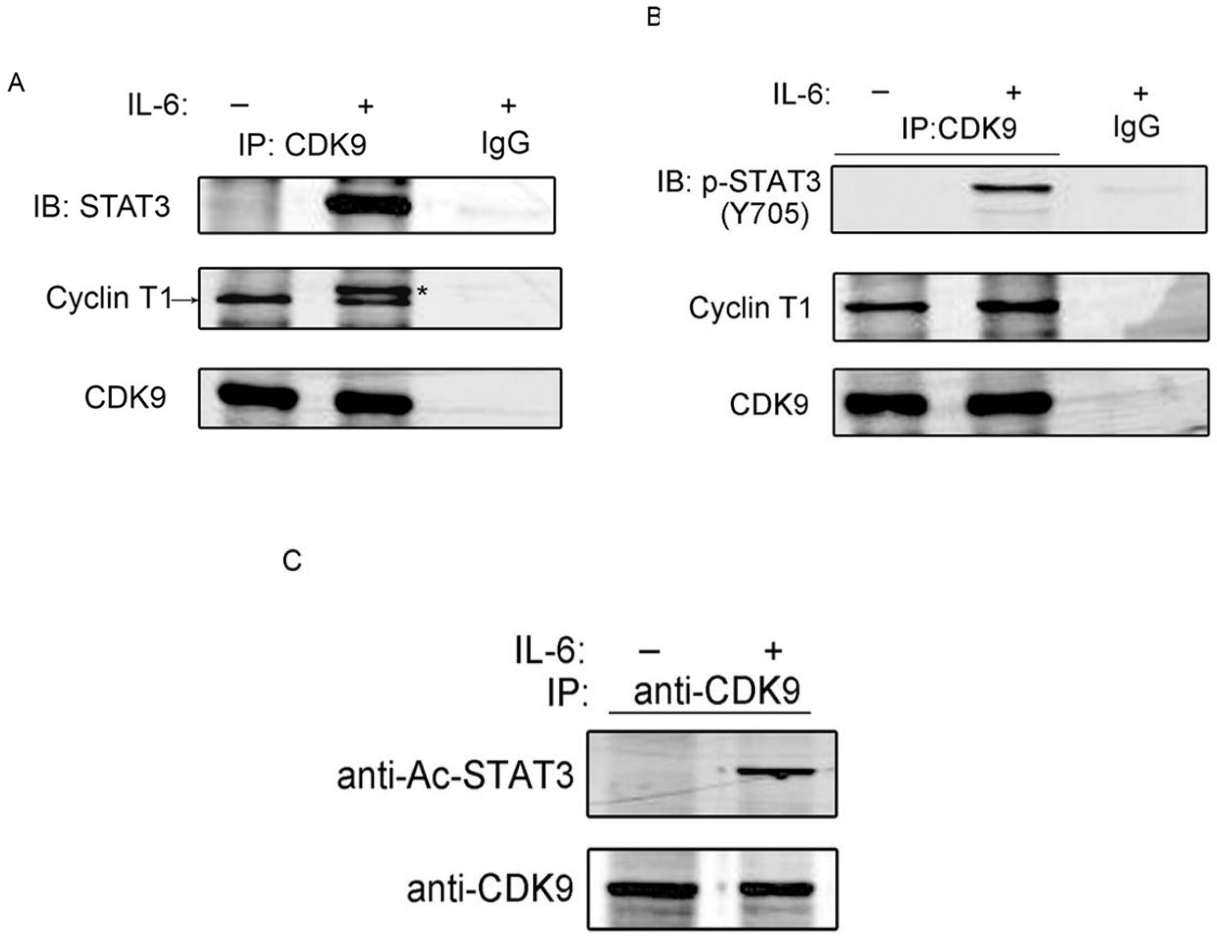

Figure 2.2 A-C, STAT3 and CDK9 form a complex in nuclei in an IL-6-dependent manner. Serum-starved HepG2 cells were treated with IL-6 (10 ng/ml) for 30 min and NEs were isolated using sucrose gradient fractionation. 2 mg of NE was immunoprecipitated by anti-CDK9 Ab or normal rabbit IgG as control. The immune complexes were fractioned by 10% SDS-PAGE and immunoblotted with anti-STAT3 (Fig. 2.2A), anti-phospho-STAT3 (Y705) (Fig. 2.2B), or anti-Ac-K87 STAT3 Abs (Fig. 2.2C). The blots were then reprobed with cyclin T1 and CDK9 Abs. Because the PVDF membrane was reprobed with anti-cyclin T1 antibody without stripping, the STAT3 band (indicated by * in Fig. A, middle panel, second lane) was remained in IL-6-stimulated cells.

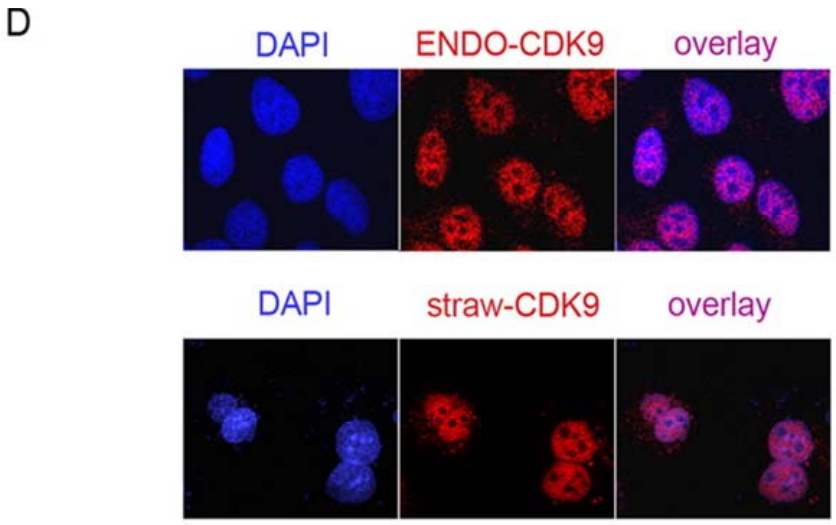

Figure 2.2 D, The distribution of straw-CDK9 is similar to that of endogenous CDK9. Endogenous CDK9 (upper panel) was stained by a polyclonal rabbit IgG directed against CDK9 and Alexa 568 goat anti-rabbit secondary Ab. For straw-CDK9 (lower panel), HepG2 cells were transfected with pcDNA-FStraw-CDK9 and 24h later split into 6-well plates containing sterile coverslips. Nuclei were stained by DAPI.

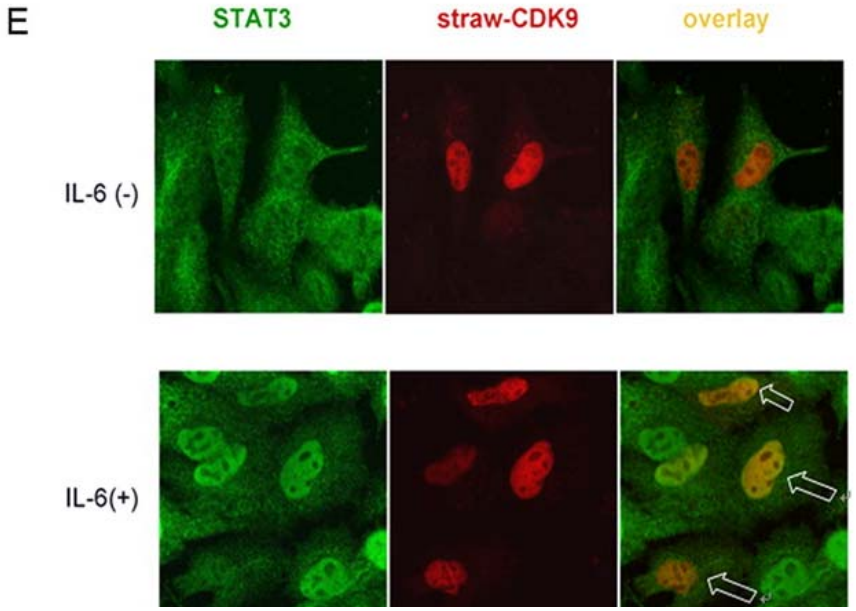

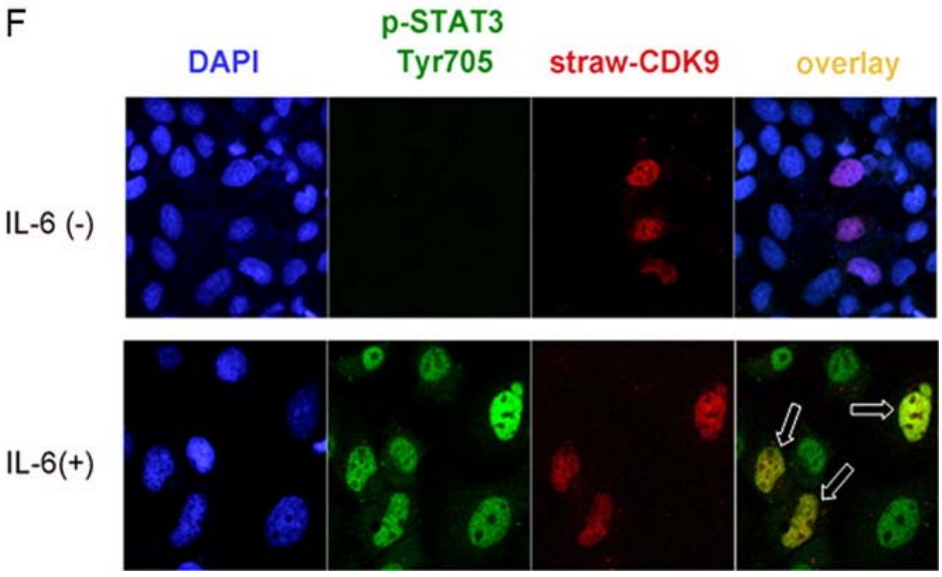

Figure 2.2 E and F, Activated STAT3 co-localizes with CDK9 under IL-6 stimulation. Cells were treated with IL-6 (10 ng/ml) for 30 min and then stained for STAT3 or pY705-STAT3. STAT3 was detected by a rabbit Ab directed against STAT3 (c-20) and a fluorescein isothiocyanate (FITC)-conjugated goat anti-rabbit secondary Ab. pY705-STAT3 was recognized by a mouse anti-phospho-Y705 STAT3 Ab (B7) and a FITC-conjugated goat anti-mouse secondary Ab. Straw-CDK9 was transfected and expressed as described in Fig. 2.2D. Shown is confocal immunofluorescent imaging of representative cells. Empty arrows indicated the co-localization of STAT3 or pY705-STAT3 with CDK9.

2.2.3 The STAT3 NH2-terminus is sufficient for CDK9 complex formation

To map the domain(s) of STAT3 responsible for CDK9 interaction, we sought first to confirm that ectopically expressed V5-epitope tagged STAT3 (V5-STAT3) associated with endogenous CDK9 in an IL-6 dependent manner. For this purpose, an expression vector encoding full length V5-STAT3 was transiently transfected into HepG2 cells. NEs were prepared in the absence or presence of IL-6 stimulation, and subjected to nondenaturing co-immunoprecipitation assays. As seen in Fig. 2.3A, V5-STAT3 is captured by nondenaturing IP of CDK9 in an IL-6 dependent manner. Note that no complex is seen using IgG as the immunoprecipitating Ab, demonstrating assay specificity. Fig. 2.3B shows that cyclin T1 is also captured by nondenaturing IP of V5-tagged STAT3. These data indicated that the ectopic V5-STAT3 also inducibly associated with endogenous P-TEFb, containing CDK9 and cyclin T1.

To identify the regions of STAT3 interacting with CDK9, a series of expression vectors encoding COOH domain-deleted V5-STAT3 proteins were constructed (the relevant domains are schematically shown in Fig. 2.3C). The V5-STAT3 deletion mutants were then expressed in HepG2 cells and the CDK9-bound mutated STAT3 proteins were detected using nondenaturing Co-immunoprecipitation. We observed that all of the STAT3 COOH-terminal-deletion mutants (containing amino acids 1-320, aa 1-465, aa 1-585, and aa 1-688) complexed with endogenous CDK9 (Fig. 2.3D). To further dissect the domain in the NH2 terminus, an expression vector encoding STAT3 (aa1-130) was constructed and tested (Fig. 2.3E). STAT3 (1-130) bound endogenous CDK9 in a manner similar to STAT3 (1-320). This finding suggests that NH_2-terminal domain of STAT3 is sufficient for the association of STAT3 and CDK9. To determine if the NH2 terminus was necessary for CDK9 interaction, we tested whether the NH_2-terminal-deleted STAT3 containing aa131-771 (termed ΔN) could still interact with CDK9. As

seen in Fig. 2.3F, STAT3 (ΔN) still bound CDK9. Previous work has indicated that the STAT3 COOH transactivation domain, spanning aa716-770 could bind to *in vitro*-translated CDK9 (105). We therefore tested whether the STAT3-CDK9 interaction depended on both the NH_2-and COOH-terminal domains. For this purpose, we constructed an expression vector encoding STAT3 (130-688), missing both NH2 and COOH terminal activation domains. As we expected, STAT3 (130-688) did not bind CDK9 (Fig. 2.3G). Together these data indicated that although the STAT3 NH2 terminus was sufficient for CDK9 complex formation, both NH2 and COOH termini participate in complex formation.

To further explore the importance of the NH2-terminal domain for STAT3's transcriptional activation function, STAT3 (ΔN) was co-transfected with γ-FBG-LUC reporter gene and luciferase reporter activity measured. As shown in Figure 2.3H, 0.5 μg of STAT3 (ΔN) decreased IL-6 inducible reporter activity by nearly 30% and 1.0 μg dramatically reduced reporter activity by 97% compared to empty vector controls. In addition, the basal level of luciferase activity was also inhibited by STAT3 (ΔN) in a dose-dependent manner. This result indicates that the NH2 terminus is essential for STAT3 to activate the transcription of downstream genes. Our interpretation of this finding is that STAT3 (ΔN) competes with endogenous STAT3 for promoter binding, and is unable to effectively activate transcription because of its reduced binding affinity for transcriptional elongation factors.

Figure 2.3: Identification of STAT3 domain responsible for STAT3-CDK9 association.

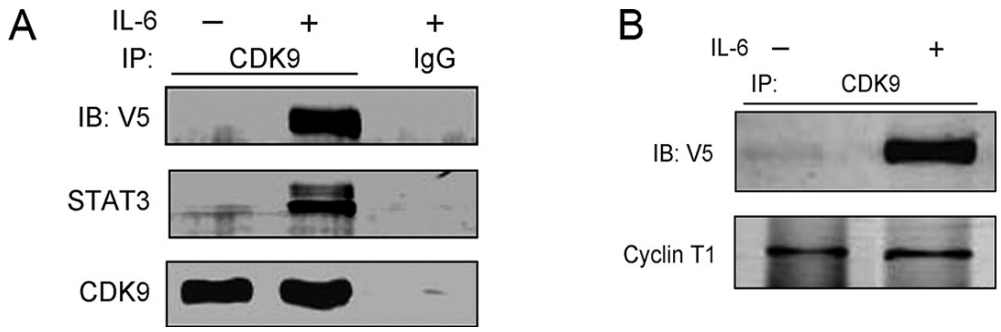

Figure 2.3 A and B, Over-expressed V5-STAT3 associates with P-TEFb. HepG2 cells were transfected with pEF6-V5-STAT3 for 24 h and stimulated with IL-6 for 30 min. Two mg of NE was immunoprecipitated with anti-CDK9 Ab or normal rabbit IgG. CDK9-bound exogenous and endogenous STAT3 was visualized by anti-V5 and anti-STAT3 Abs. The blots were then reprobed with anti-CDK9 and anti-cyclin T1 antibodies.

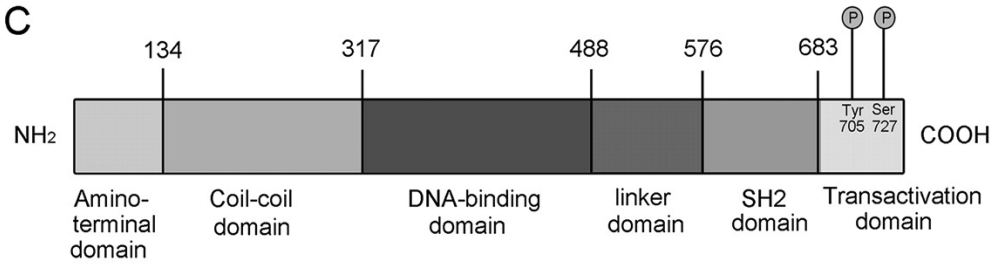

Figure 2.3 C, Schematic diagram of functional domains of STAT3.
The major functional domains of STAT3 include the NH2-terminal domain, the coiled-coil domain, the DNA-binding domain, the linker domain, the SH2 domain and the COOH-terminal TAD. The two phosphorylation sites on the COOH-terminal TAD (Y705 and S727) are shown.

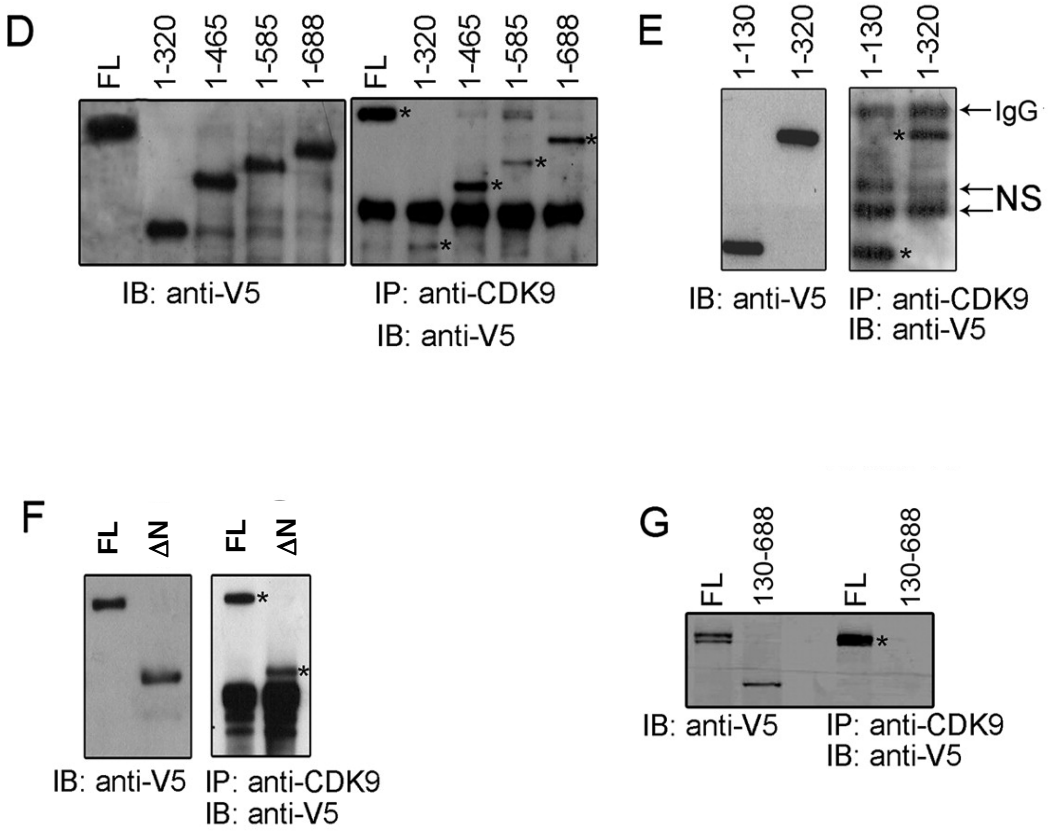

Figure 2.3D,E, F and G, NH_2-terminal domain of STAT3 is sufficient for STAT3-CDK9 interaction. HepG2 cells were transfected with pEF6-V5-STAT3 expression plasmids encoding COOH-deleted STAT3 proteins (1-130, 1-320, 1-465, 1-585, 1-688, ΔN and 130-688). Co-immunoprecipitation was performed as described in *Fig. 2.3A*. The left panels are Western blots for the total protein expression in the cell lysate (specific bands indicated by *), and the right panels show CDK9-bound STAT3 deleted mutations. NS, nonspecific signal.

H

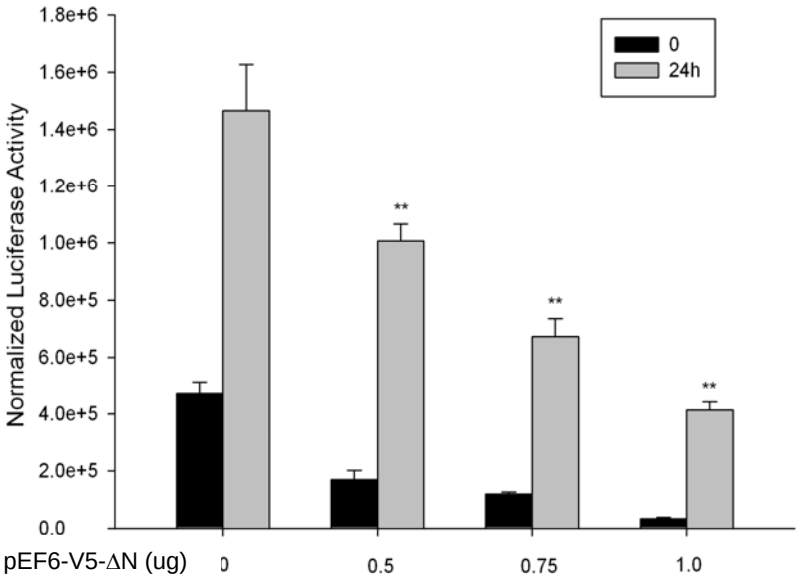

Figure 2.3H, STAT3(ΔN) (aa 130-770) inhibits γ-FBG-LUC transcription in a dose-dependent manner. The indicated amounts of pEF6-V5-ΔN were co-transfected with the γ-FBG-LUC reporter gene. An empty vector was used to keep the total amount of transfected DNA equivalent. Twenty-four hours later, cells were treated or untreated with IL-6 (10 ng/ml). After another 24 h, luciferase activity was measured. Data shown were means ± SD from three independent transfections. The data was analyzed by Student's *t* test. *, *p* value < 0.05, **, *p* value < 0.01.

2.2.4 CDK9 activity is required for IL-6-induced expression of γ-FBG

To investigate the functional role of CDK9 in IL-6-induced expression of γ-FBG, we inhibited CDK9 kinase activity by a chemical inhibitor, flavopiridol (FP). FP is a highly selective P-TEFb inhibitor with a *Ki* of 3 nM (106). We first tested the effect of FP on IL-6 inducible γ-FBG transcription. HepG2 cells transfected with the -607/+36 γ-FBG-LUC reporter plasmid were pretreated with either vehicle (DMSO) or FP (500 nM) for 1 h prior to IL-6 stimulation. Both the basal and IL-6-induced activities of γ-FBG-LUC reporter were dramatically decreased when FP was added (Fig. 2.4A). In addition, FP also inhibited IL-6 induced endogenous γ-FBG mRNA (Fig. 2.4B). Consistent with these results, expression of a kinase-deficient DN-CDK9 also inhibited the induction of γ-FBG-LUC reporter in a dose-dependent manner, with greater than 50% inhibition seen with 0.25 μg of expression vector (Fig. 2.4C). These results indicated that IL-6 inducible expression of γ-FBG was highly dependent on CDK9 kinase activity.

To more specifically confirm the essential role of CDK9 in the γ-FBG induction, short interfering RNA (siRNA) transfection was used to specifically silence endogenous CDK9 expression. As seen in Fig. 2.4D, transfection of CDK9 siRNA (siCDK9) significantly reduced CDK9 protein levels to less than 20% compared to control siRNA. To examine the effect of CDK9 knockdown on IL-6 inducible γ-FBG expression, abundance of γ-FBG mRNA was measured in a time course of stimulation by Q-RT-PCR. In contrast to control transfectants, the induction of γ-FBG mRNA in siCDK9 transfected-cells was significantly decreased at every time point (Fig. 2.4E). From these results, we concluded that IL-6-induced γ-FBG expression requires CDK9 expression and activity.

Figure 2.4: CDK9 activity is required for IL-6-stimulated expression of γ-FBG.

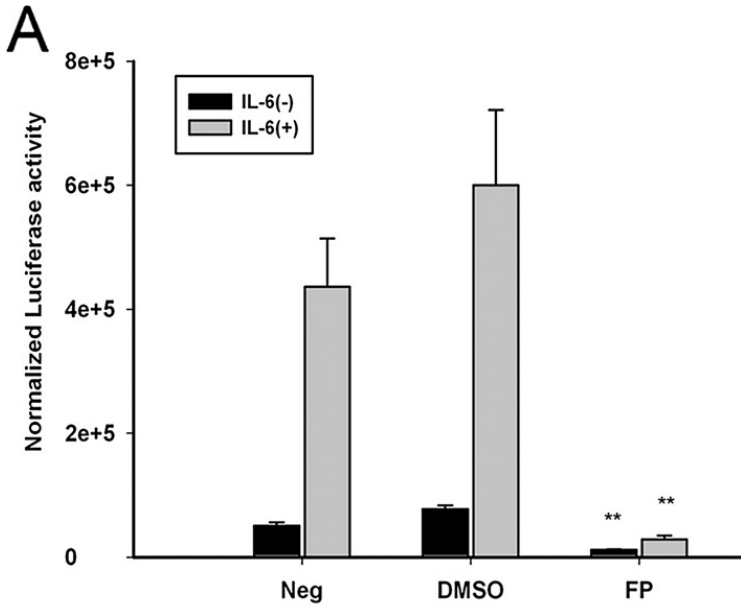

Figure 2.4 A, CDK9 inhibitor, FP, inhibits γ-FBG-LUC reporter gene activity. HepG2 cells were transfected with γ-FBG-LUC reporter gene and pSV2PAP as an internal control. 24 h after transfection, cells were stimulated with IL-6 alone (Neg) or pretreated with FP (500 nM) for 1 h followed by IL-6 stimulation. The control cells were pretreated with the vehicle DMSO. 24 h after IL-6 stimulation, cells were collected to measure reporter gene activity. Shown is normalized reporter activity from three independent transfections. *, p value < 0.05, **, p value < 0.01.

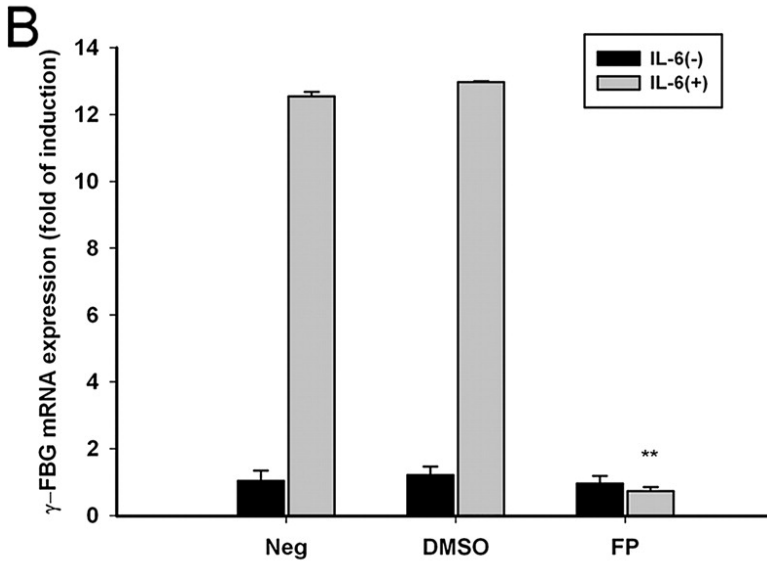

Figure 2.4 B, FP blocks IL-6-induced γ-FBG mRNA expression. HepG2 cells were pretreated with FP or DMSO as described above before 24 h of IL-6 stimulation. γ-FBG and GAPDH mRNA expressions were assayed by Q-RT-PCR. The fold change of γ-FBG in IL-6-treated cells over IL-6-unstimulated control was obtained after correction for the amount of GAPDH. Data shown were means ± SD from triplicates. The data was analyzed by Student's *t* test. *, *p* value < 0.05, **, *p* value < 0.01.

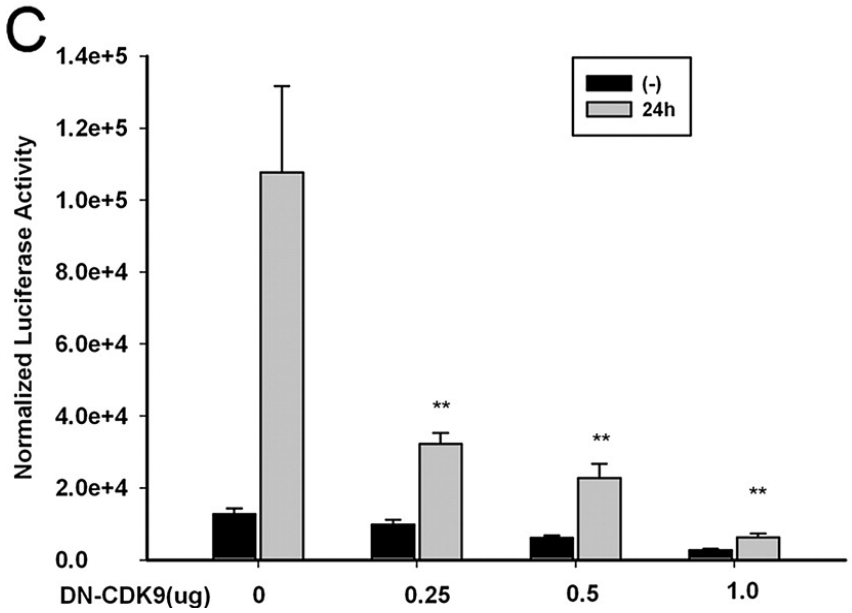

Figure 2.4 C, DN-CDK9 inhibits the IL-6 induction of the γ-FBG reporter gene. Different amounts of DN-CDK9 were cotransfected with γ-FBG-LUC reporter gene. Cells were then treated with IL-6 (10 ng/ml) for 24 h or left unstimulated prior to reporter gene assay. Data shown is means ± SD from three independent transfections. The data was analyzed by Student's *t* test. *, *p* value < 0.05, **, *p* value < 0.01.

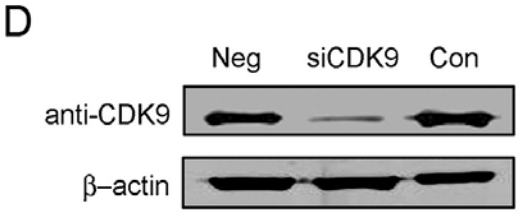

Figure 2.4 D, CDK9 siRNA transfection efficiently inhibits CDK9 expression. HepG2 cells grown in 6-well plates were transiently transfected with 100 nM of CDK9 siRNA (siCDK9), control siRNA (Con) or transfection reagent alone (Neg). 72 h after transfection, equivalent amounts of protein from the whole cell lysates were used for immunoblot. Top panel, CDK9 staining, bottom, β-actin staining as a loading control.

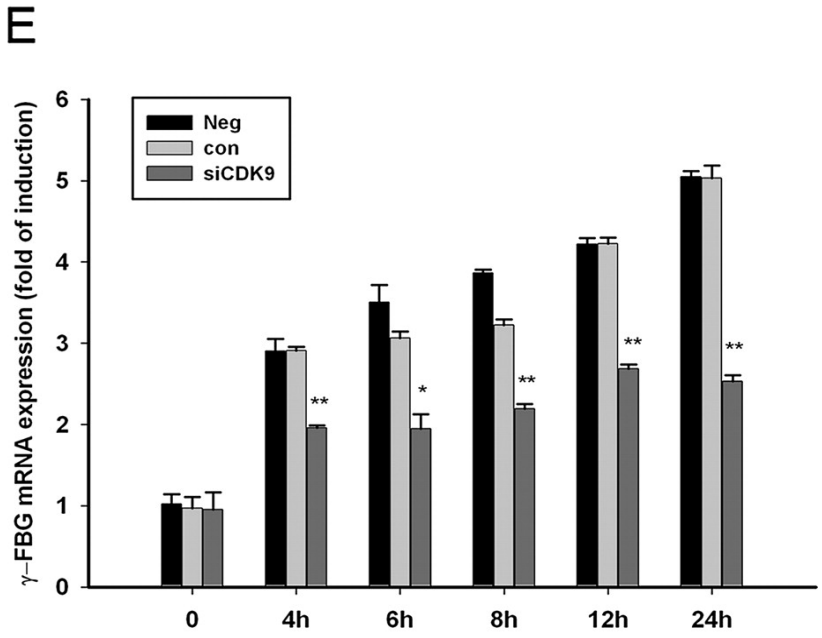

Figure 2.4E, siRNA transfection was performed as described in Fig. 2.4D. 48 h after siRNA transfection, cells were treated with IL-6 (10 ng/ml) for indicated times. The γ-FBG mRNA expression and the fold of induction were measured and calculated as described in Fig. 2.1A. The results from Q-RT-PCR were expressed as means ± SD from triplicates. The data was analyzed by Student's *t* test. *, *p* value < 0.05, **, *p* value < 0.01.

2.2.5 IL-6 induces P-TEFb recruitment to the γ-FBG gene

Three functional type II IL-6 response elements (REs) have been identified on the about 600 bp of the human γ-FBG promoter upstream of the transcription initiation site, and all contribute to full IL-6 inducibility (67). To identify the interaction of STAT3 with these sites, three sets of primers spanning distinct STAT3-responsive region in γ-FBG promoter (RE1, RE2 and RE3) were designed (sequences in Table 1) and optimized by quantitative real time genomic PCR (Q-gPCR) to show a linear dynamic range from 40 ng to 25 μg DNA. Using a two-step ChIP assay that efficiently captures STAT3 binding to genomic DNA (107), we examined the kinetics and amount of IL-6 inducible STAT3 binding to the γ-FBG IL6 REs. This experiment revealed that IL-6 induced a 3.8-fold increase of STAT3 binding to the region containing the first γ-FBG RE, 2.2-fold increase on the RE2 and 3.2-fold increase on the RE3 within 30 min after IL-6 stimulation (Fig. 2.5B).

We next examined the effect of IL-6 on inducible CDK9 binding to the γ-FBG promoter. In a pattern similar to that observed for STAT3, IL-6 induces 2-fold increase of CDK9 binding to the upstream γ-FBG IL6 RE1 (Fig. 2.5C), but no significant recruitment was observed on the RE2 and RE3 (data not shown). The same DNA was examined for changes in CDK9 binding to the TATA box region (spanning nt -66 to +6), exon 5 (nt +2524 to +2606) and exon 7 (nt +4148 to +4239). Here, IL-6 induced 2.3-fold binding to the TATA box, a 4-fold increase on Exon 5 and a 2.5-fold increase on Exon 7 within 30 min after stimulation, suggesting that CDK9 may accompany the elongating polymerase during transcription (Fig. 2.5C).

2.2.6 IL-6 induces Pol II recruitment to the γ-FBG gene

To further understand the role of CDK9 recruitment in IL-6 stimulation, the binding of RNA Pol II and phospho-S2 CTD Pol II was examined by two-step ChIP

assay. IL-6 induced a 3-fold increase in total Pol II binding on the γ-FBG TATA box, and strongly induced Pol II loading on the coding sequences (Fig. 2.5D). Because CDK9 is a kinase for S2 of the Pol II CTD, two-step ChIP was performed using anti-phospho-S2 CTD Pol II Ab. We observed a 3-fold increase of phospho-S2 CTD Pol II binding to the TATA box, and greater than 8-fold increase on exon 5 (Fig. 2.5E). We noted that the distribution pattern of CDK9 was similar to that of phospho-S2 CTD Pol II, supporting the notion that CDK9 is the IL-6 inducible S2-CTD kinase.

To further establish this relationship, we investigated the effects of FP on IL-6 inducible total and phospho-S2 CTD Pol II recruitment. In this experiment, HepG2 cells were pretreated with FP (500 nM) before IL-6 stimulation. The chromatin was processed for two-step ChIP assay using anti-Pol II (Fig. 2.5F) and phospho-S2 CTD Pol II (Fig. 2.5G) Abs. We found that IL-6 induced occupancy of the TATA box, exon 5 and exon 7 by RNA Pol II as well as phospho-S2 CTD Pol II was significantly inhibited by FP. These results suggest that CDK9 is required for RNA Pol II recruitment and licensing it to enter transcription elongation mode, thereby promoting IL-6 inducible γ-FBG expression. To exclude the possibility that FP interferes with STAT3 and CDK9 recruitment, their binding to the γ-FBG gene in presence of FP was assayed by two-step ChIP. IL-6-induced STAT3 and CDK9 occupancy of the γ-FBG promoter and coding region were not significantly affected by FP pretreatment (Fig. 2.5H and 2.5I).

Figure 2.5: Recruitment of CDK9 and Pol II to the γ-FBG gene after IL-6 stimulation.

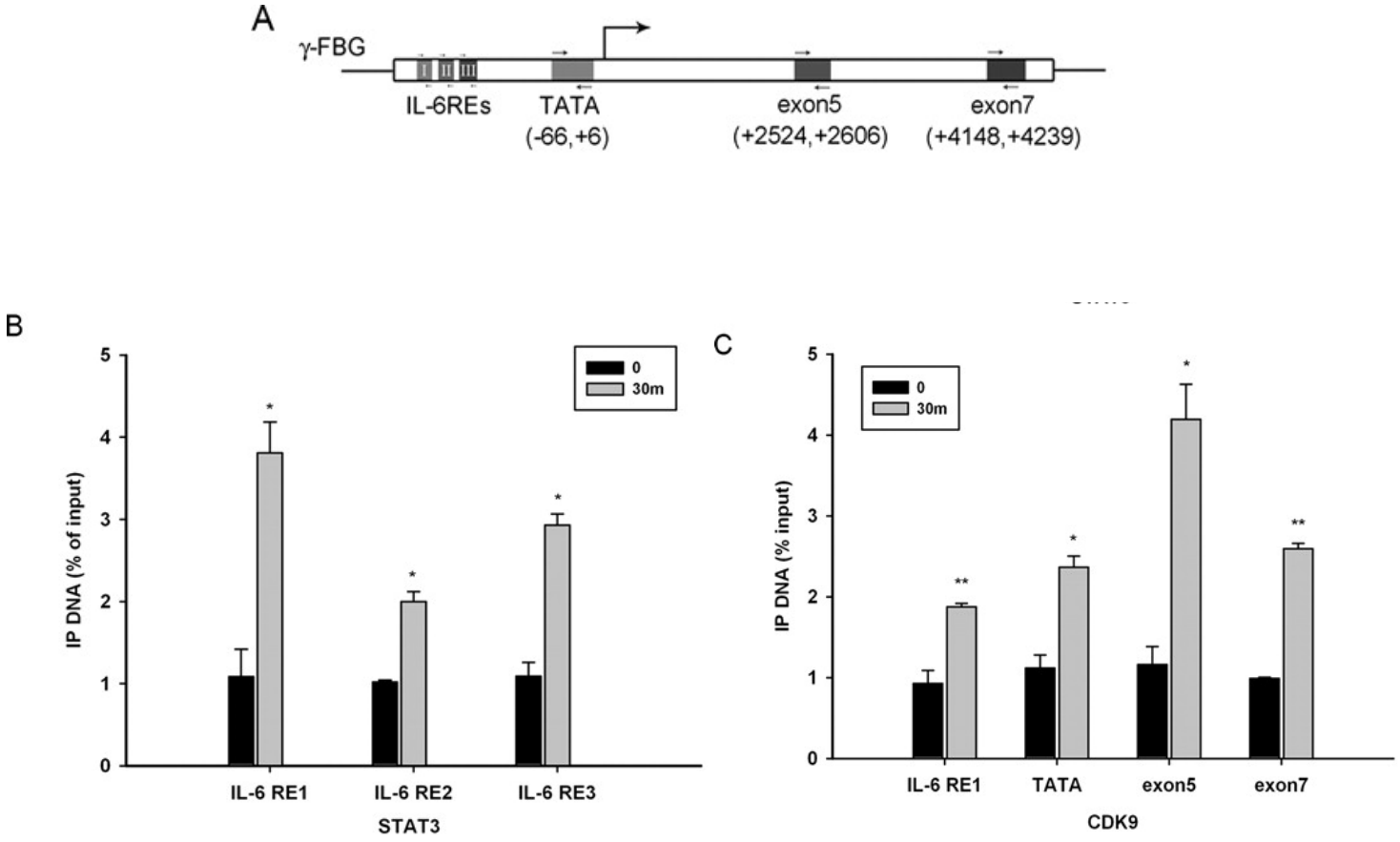

Figure 2.5 A, Schematic diagram of Q-gPCR primers on the γ-FBG promoter. Primer pairs spanning the IL-6REs, TATA box, and exons 5 and 7 were designed and optimized (See Table 1 for sequences). B and C, Serum-starved HepG2 cells were treated with IL-6 (10 ng/ml), and two-step ChIP assay was performed. The sequences in the promoter or coding region of the γ-FBG gene in the immunoprecipitates were amplified by Q-gPCR using specific primer sets. B, STAT3 recruits to IL-6 REs on γ-FBG promoter after IL-6 stimulation. C, IL-6 induces CDK9 recruitment to the IL-6 RE1, TATA box as wells as exons 5 and 7. The results were expressed as means ± SD from triplicates. The data was analyzed by Student's *t* test. *, *p* value < 0.05, **, *p* value < 0.01.

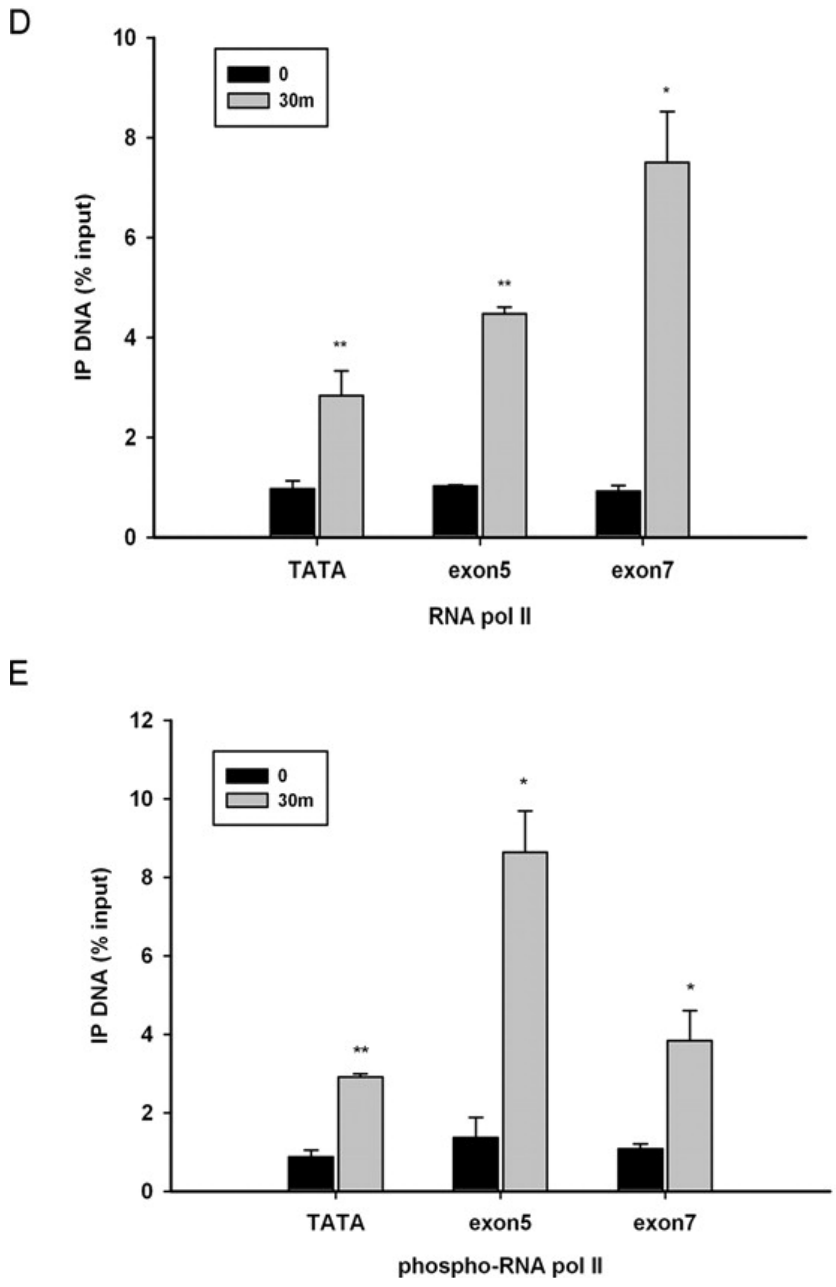

Figure 2.5 D and E, IL-6 increases the Pol II and phospho-S2-CTD Pol II loading to the endogenous γ-FBG gene. The results were expressed as means ± SD from triplicates. The data was analyzed by Student's *t* test. *, *p* value < 0.05, **, *p* value < 0.01.

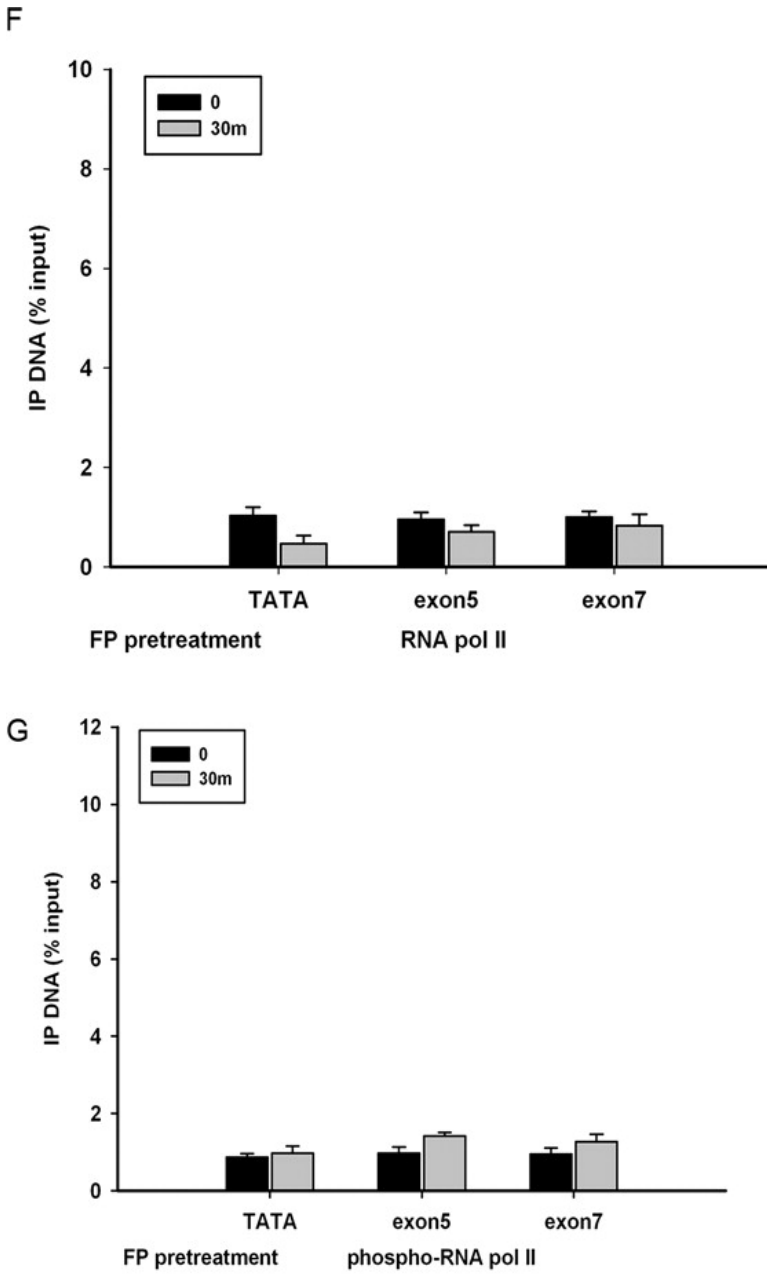

Figure 2.5 F and G, FP inhibits the recruitment of RNA Pol II and phospho-S2 CTD Pol II to the TATA box and coding region. The results were expressed as means ± SD from triplicates. The data was analyzed by Student's *t* test. *, *p* value < 0.05, **, *p* value < 0.01.

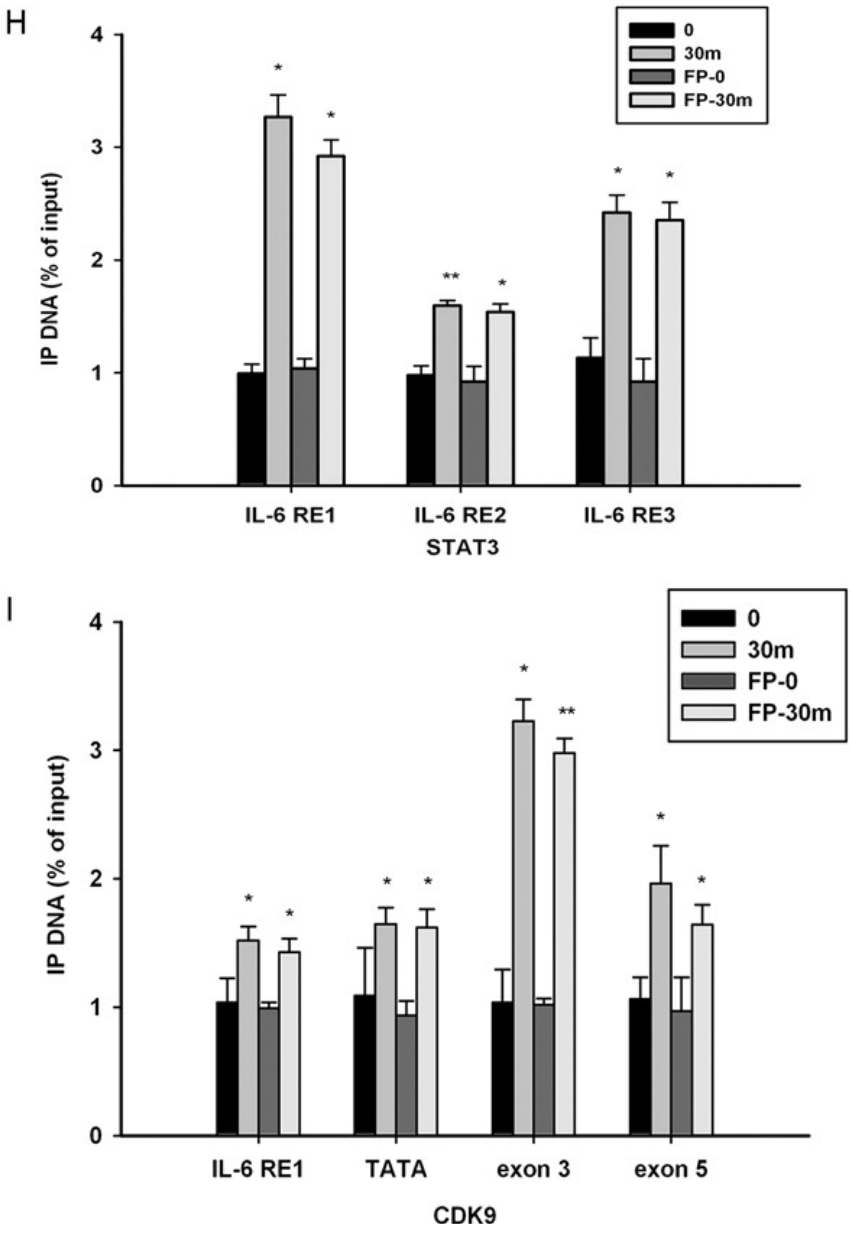

Figure 2.5 H and I, FP pretreatment does not affect the inducible STAT3 and CDK9 binding to the γ-FBG gene. The results were expressed as means ± SD from triplicates. The data was analyzed by Student's *t* test. *, *p* value < 0.05, **, *p* value < 0.01.

2.2.7 FP inhibits basal and IL-6 inducible phospho-S2 CTD Pol II formation

Because RNA Pol II is not the only substrate of CDK9 (29, 108-111), we tested whether CDK9 could also phosphorylate STAT3. HepG2 cells treated in the absence or presence of FP were then IL-6 stimulated. Western Blots were performed using anti-phospho-Y705 and anti-phospho-S727 STAT3 Abs (the latter modification is known to be essential for maximal transcriptional activity of STAT3 (112)). We observed the strong IL-6 inducible STAT3 Y- and S-phosphorylation were unaffected by FP (Fig. 2.6A and 2.6B). As an additional determination, we observed that the IL-6 inducible STAT3·CDK9 association was unaffected by FP treatment (Fig. 2.6C), suggesting that CDK9 kinase activity is not essential for complex formation. Since CDK9 is thought to be a major Pol II S2-CTD kinase we examined its effect on total Pol II- and phospho-S2 CTD Pol II abundance. Although FP did not affect total Pol II abundance (Fig. 2.6D), the general levels of phospho-S2 CTD Pol II was significantly decreased (Fig. 2.6E). We therefore conclude that FP specifically inhibits phospho-S2CTD Pol II formation without affecting STAT3 activation or complex formation with CDK9.

Figure 2.6: Flavopiridol specifically inhibits S2 CTD phosphorylation of Pol II.

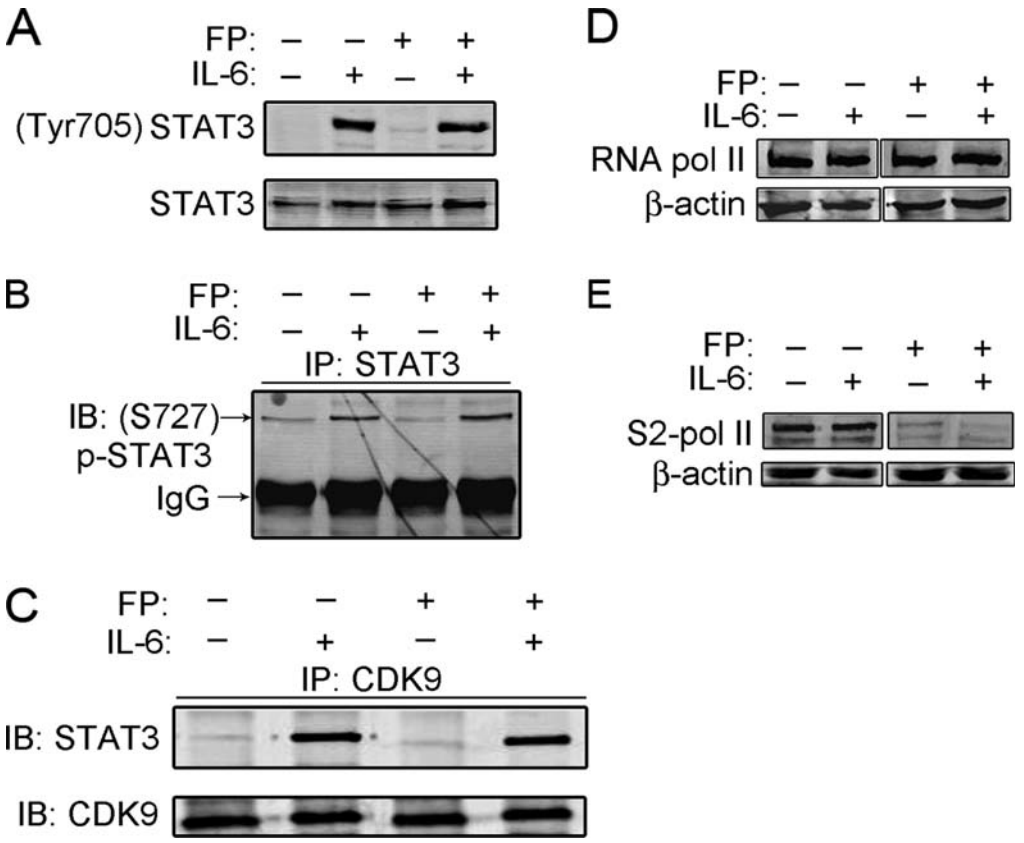

Figure 2.6 HepG2 cells were pretreated with FP (500 nM) for 1 h followed by IL-6 stimulation for 30 min and NEs were isolated. A, FP did not affect Y705 phosphorylation of STAT3. NEs were resolved by 10% SDS-PAGE and assayed by Western blot. Top, Y705 phosphorylation was detected by anti-pY705-STAT3 Ab (B7) and total STAT3 was detected by anti-STAT3 Ab (C-20). B, FP has no effect on S727 phosphorylation of STAT3. NEs were immunoprecipitated by anti-STAT3 Ab (C-20) and pS727-STAT3 was detected by anti-pS-STAT3 Ab. C, STAT3 and CDK9 interaction is not influenced by FP treatment. Immunoprecipitation was performed on NEs from HepG2 cells by using anti-CDK9 Ab, and CDK9-bound STAT3 detected by Western blot. The lower panel showed equal amounts of input protein were used. D, FP did not change the level of total Pol II. RNA Pol II in NE was measured by Western blot using 6% SDS-PAGE and anti-RNA Pol II Ab (N-20). E, FP inhibits S2 phosphorylation of Pol II. NE was fractioned by 6% SDS-PAGE and revealed by anti-pS2 CTD Pol II Ab (H5). β-actin was used as a loading control for both 2.6D and 2.6E.

2.3 Discussion:

FBG is an APP that plays key roles in fibrin clot formation, platelet aggregation and wound repair by binding to cell surface receptors or growth factors through its γ chain. Previous studies have shown the acute phase induction of γ-FBG in liver cells is mainly regulated by the cytokine-inducible STAT3 transcription factor. In this study, we further investigated the molecular mechanism by which IL-6-inducible γ-FBG transcription is regulated by the STAT3·P-TEFb complex. We found that IL-6 induces a formation of STAT3·CDK9 complex mediated by both the STAT3 NH_2-and COOH termini. Moreover, activated pY705-STAT3 and Ac-K87 STAT3 were preferentially complexed with CDK9. Quantitative two-step ChIP assays indicate that IL-6 induces STAT3, CDK9, Pol II and phospho-S2 CTD Pol II recruitment to the γ-FBG gene. Finally, our studies indicate that CDK9 is required for γ-FBG expression because siRNA transfection and inhibition of CDK9 kinase activity both inhibit IL-6 inducible transcription. These studies indicate that P-TEFb is a critical regulator of STAT3 dependent gene activation in the APR.

STAT3 is a central transcription factor in IL-6-induced hepatic APRs. The transcription of APPs controlled by STAT3 is regulated at multiple levels. First, IL-6 induces tyrosine phosphorylation of STAT3 in its COOH-terminus, leading to its dimerization and nuclear translocation. The activated STAT3 then recognizes specific motifs in the promoters of target genes and initiates assembly of the basal transcriptional apparatus (99). At this point, STAT3 recruits p300/CBP coactivators containing histone acetyltransferase activity (HAT) and the BRG1 chromatin-remodeling complex. HAT regulates transcription by acetylating the amino-terminal histone tail, increasing accessibility of chromatin-condensed templates to the transcriptional machinery (113),

whereas chromatin-remodeling complexes function by altering nucleosomal structure and increasing the accessibility of Pol II to the proximal promoter (114). Both these activities promote target gene activation by relieving repression and facilitating the loading of the pre-initiation complex. The findings of our study add a new dimension to how STAT3 mediates gene expression. STAT3 not only induces transcription initiation, but also regulates transcription elongation through its association and recruiting P-TEFb to its target genes.

The P-TEFb complex has been shown to play an important role in Pol II dependent transcription by its ability to release RNA Pol II from transcriptional arrest, allowing production of full length mRNA transcripts (115). Experiments using CDK9 inhibitors strongly indicate that CDK9 activity is required for both HIV transcription and the expression of many cellular genes. Tat, a viral transactivator encoded by HIV and other retroviral genomes (116, 117), is able to recruit the CDK9·cyclinT1 complex to the TAR element of the HIV promoter (37), and position CDK9 to phosphorylate the negative elongation factors as well as the RNA Pol II CTD, thereby enabling transcriptional elongation (30, 117-119). In addition to Tat, recent studies have identified other cellular transcription factors that associate with P-TEFb, including CIITA, NF-κB, c-Myc and p53 (47, 48, 102, 111, 120). The involvement of CDK9 in regulating STAT3 dependent cell cycle regulatory genes was first reported for the p21*waf1* gene (105). The authors found that DRB, another P-TEFb inhibitor, inhibits p21*waf1* expression as well as RNA Pol II recruitment to p21*waf1*. Although these results indicated that CDK9 was required for STAT3's ability to control expression of cell cycle regulatory genes, there may be significant heterogeneity in the mechanisms of transcriptional induction between different classes of STAT3-responsive genes and to what extent the CDK9 was required for activation of the APPs was unknown. Using γ-FBG as a model gene of the APR, our

study here extends the requirement of CDK9 in STAT3 dependent APPs activation. Transient transfection assays revealed that CDK9 activity is required for the activation of γ-FBG promoter transcription (Fig. 2.4A and 2.4C), and Q-RT-PCR showed that CDK9 knockdown significantly suppresses the endogenous γ-FBG expression during the 24 h-time course (Fig. 2.4E).

Although the STAT3-CDK9 interaction was reported before (105), our study extends this previous work by: 1. demonstrating the interaction using an independent technique of confocal colocalization; 2. demonstrating that Y-phosphorylated and K-acetylated STAT3 is found in the complex with CDK9; and, 3. discovering that the STAT3 NH_2 terminus participates in CDK9 complex formation and transcriptional activation.

Co-immunoprecipitation and confocal colocalization showed that the inducible STAT3·CDK9 complex is rapidly formed in the nucleus within 30 min after IL-6 stimulation (Fig. 2.2). Moreover, only the activated, nuclear translocated STAT3 complexes with CDK9, even though CDK9 is also found in the cytoplasm. We interpret this finding to mean that the tyrosine phosphorylation produces a conformational change in STAT3, exposing the CDK9-interacting domains at NH_2 and COOH termini. Currently our data does not prove that the NH_2 terminal of STAT3 binds to CDK9 through a direct protein-protein interaction. Therefore, another possibility could be that the STAT3-CDK9 interaction is indirectly mediated through other protein-protein interactions that are mapped to the STAT3 NH_2 terminus. In this regard, a recent finding from our lab shows that the STAT3 NH_2 terminus is sufficient for the interaction with p300/CBP, an enzyme that acetylates two lysine residues (K49, K87) in this domain (95). These acetylation increase the stability of STAT3·p300/CBP complex, and are indispensable for STAT3 dependent target gene expression (95). This finding indicates the possibility that STAT3

NH_2 terminus-CDK9 interaction is indirectly mediated by p300/CBP. The NH_2-terminal domain is highly conserved in STAT members. According to previous studies, NH_2 terminus is required for cooperative binding of STAT4 dimers to adjacent recognition sites on DNA (121). It also regulates multiple protein-protein interactions important for the functions of STAT1 and STAT2 (98, 122-125). However, little is known about the function of NH_2 terminus in STAT3. Our findings reveal that NH_2 terminal is involved in the interactions between STAT3, the p300/CBP coactivator and the P-TEFb transcriptional elongation complex. The important role of NH_2 terminus for STAT3 function can also be seen in the finding that NH_2-terminal-deleted mutant (ΔN) repressed both the basal and IL-6 inducible activities of γ-FBG-LUC reporter gene (Fig. 2.3H). Although STAT3 (ΔN) remains promoter binding activity, it could not effectively induce transcription because it is unable to successfully recruit coactivators or transcriptional elongation factors.

Although it has known that P-TEFb is generally required for transcription elongation, an unanswered question is whether P-TEFb is recruited to all promoters and regulates downstream gene transcription by similar mechanisms. The existence of eight potential P-TEFb complexes resulting from different combinations of two CDK9 isoforms (31) and four types of cylclins (33) suggest the possibility that unique P-TEFb complexes might be differentially recruited by inducible transcription factors for different genes. Consistent with this notion, the requirement for CDK9 varies widely among genes. For example, HIV replication can be inhibited by FP at concentrations that have no detectable effect on cellular genes transcription (106, 126). Also, a recent study found that some p53 target genes, including p21 and PUMA, are activated when CDK9 activity is inhibited, suggesting a specific subset of p53 target genes can bypass the requirement of CDK9 activity for expression (127). The further study of other STAT3 target genes

may answer the question whether CDK9 activity is generally required for all STAT3 dependent genes. It will be of interest to apply ChIP assays to monitor the kinetics of CDK9 association on different promoters of STAT3 target genes, and determine whether CDK9 utilizes a general mechanism to regulate some or all of STAT3 dependent genes.

Upon P-TEFb recruitment, an important substrate is S2 in the heptad repeat of the RNA Pol II CTD. This notion is supported by our finding that CDK9 binds to TATA box, exon 5 and exon 7 of γ-FBG gene in a similar pattern as phospho-S2 CTD Pol II itself (Fig. 2.5C and 2.5E). Moreover our data show that FP treatment specifically and efficiently suppresses phospho-S2 CTD Pol II formation without affecting STAT3•CDK9 interaction (Fig. 2.6C and 2.6E). Although our data show that there is constitutive S2 CTD phosphorylation, which is globally independent of IL-6 stimulation (Fig. 2.6E), this fraction of phospho- S2 CTD Pol II is not strongly engaged with the γ-FBG promoter. We suggest based on our study that the STAT3-CDK9 interaction results into increased P-TEFb targeting to the γ-FBG gene, producing local Pol II recruitment, CTD phosphorylation and transcriptional elongation. In fact, our experiments indicate that both the recruitment of total Pol II and phospho-S2-CTD Pol II are decreased by CDK inhibition, despite a consistent level of Pol II expression (Fig. 2.5F and Fig. 2.6D). This result implicates that S2 CTD phosphorylation might affect the stability of Pol II binding to chromatin.

In addition to Pol II, CDK9 is a kinase that autophosphorylates as well as phosphorylates other targets that have been partially characterized, including Myo D, hSPT5, and p53 (29, 108-111). In an effort to determine whether STAT3 is also a substrate for CDK9 phosphorylation, our findings that STAT3 phosphorylation at Y705 and S727 are not changed by CDK inhibition (Fig. 2.6A and 2.6B) indicate that these two sites are not CDK9 targets. However, these findings do not rule out the possibility that

STAT3 is a potential substrate of CDK9 at some other site(s) yet to be discovered. Further studies will be necessary to understand whether CDK9 is able to cause phosphorylation of STAT3, especially at its NH_2 terminus and/or COOH terminus.

Interestingly, previous studies show that CDK9 and cyclin T1 expression themselves can be upregulated in T lymphocytes stimulated with cytokines or mitogens (78, 128-131). For example, a combination of IL-2, IL-6 and TNF-α increased both CDK9 and cyclin T1 protein levels in peripheral blood lymphocytes (130). In our study, we did not observe CDK9 induction in response to IL-6, but we have found that cyclin T1 was slightly upregulated by IL-6 (data not shown), which could be another mechanism regulating P-TEFb activity. In addition, a recent finding shows that CDK9 can be acetylated by p300/CBP *in vitro* and this modification affects its ability to phosphorylate Pol II (132). All these findings suggest an additional level of complexity to the regulation of transcriptional elongation.

In summary, we provide evidence that activated STAT3 associates with P-TEFb to stimulate its recruitment and transcription elongation of the γ-FBG gene. CDK9 regulates IL-6-induced γ-FBG transcription via a mechanism involving increased binding of total and phosphorylated RNA Pol II to γ-FBG. Considering the important roles of FBG in inflammation and cancer, this finding has functional significance, making CDK9 is an appealing target for therapeutic intervention.

CHAPTER 3: THE STAT3 NH2-TERMINAL DOMAIN STABILIZES THE ENHANCEOSOME ASSEMBLY BY INTERACTING WITH THE P300 BROMODOMAIN

3.1 Abstract

STAT3 is a latent transcription factor mainly activated by the IL-6 cytokine family. Previous studies have shown that activated STAT3 recruits p300, a coactivator whose intrinsic histone acetyltranferase activity is essential for transcription. Here we investigated the function of the STAT3 NH2-terminal domain and how its interaction with p300 regulates STAT3 signal transduction. In *STAT3-/-* MEFs, a stably expressed NH2-terminal-deficient STAT3 mutant (STAT3-ΔN) was unable to efficiently induce either STAT3-mediated reporter activity or endogenous mRNA expression. ChIP assays were performed to determine whether the NH2-terminal domain regulates p300 recruitment or stabilizes enhanceosome assembly. Despite equivalent levels of STAT3 binding, cells expressing the STAT3-ΔN mutant were unable to recruit p300 and RNA pol II to the native *socs3* promoter as efficiently as those expressing STAT3-full length (FL). We previously reported that the STAT3 NH2-terminal domain is acetylated by p300 at K49 and K87. By introducing K49R/K87R mutations, here we found that the acetylation status of the STAT3 NH2-terminal domain regulates its interaction with p300. In addition, the STAT3 NH2-terminal binding site maps to the p300 bromodomain, a region spanning from aa 1053 to 1156. Finally, a p300 mutant lacking the bromodomain (p300-ΔB) exhibited a weaker binding to STAT3 and the enhanceosome formation on the *socs3* promoter was inhibited when p300-ΔB was overexpressed. Taken together, our data suggest that the STAT3 NH2-terminal domain plays an important role in IL-6

signaling pathway by interacting with the p300 bromodomain, thereby stabilizing enhanceosome assembly.

3.2 Results:

3.2.1 The STAT3 NH2-terminal domain is required for OSM-inducible transcription

Based on our findings that the STAT3 NH2-terminal domain may play an important role in STAT3 function, we generated a V5-epitope tagged STAT3 mutant (V5-STAT3-ΔN), in which the entire NH2-terminal region (aa 1-133) was deleted, and tested its transcriptional activity in luciferase reporter assays. For this purpose, *STAT3-/-* MEFs were used to avoid the interference from endogenous STAT3. First, the loss of STAT3 in *STAT3-/-* MEFs was confirmed by Western Immunoblot shown (Figure 3.1A, left panel). *STAT3-/-* MEFs were then transiently transfected with V5-STAT3-full length (FL) or V5-STAT3-ΔN and ectopically expressed STAT3 measured by Western Immunoblot with anti-V5 Ab. As seen in the right panel of Figure 3.1A, the expression of V5-STAT3-ΔN was not affected by the removal of NH2-terminal domain.

Different doses of V5-STAT3-FL or V5-STAT3-ΔN were then cotransfected with the reporter gene, γ-FBG-LUC, which contains the three native STAT3-binding sites from the *γ-FBG* gene. Because MEFs express low level of IL-6Rα, OSM was used to activate STAT3 signal transduction. Reporter activity was measured in presence or absence of OSM. As little as 0.25 μg of V5-STAT3-FL was able to increase γ-FBG-LUC activity by about 3-fold and further increase to 5-fold was observed when the amount of FL expression vector was increased (Figure 3.1B). In contrast to the behavior of V5-STAT3-FL, V5-STAT3-ΔN was able to induce only a 1.5-fold of increase in reporter activity and a dose-dependent response was not observed (Figure 3.1B). Our findings that the STAT3 NH2-terminal domain is sufficient to associate with p300 raise the possibility

that this domain regulates STAT3 signaling by mediating p300 recruitment. Therefore, we next tested whether the STAT3 NH2-terminal domain was required for the functional cooperation between STAT3 and p300. To this end, different doses of p300 expression vectors were cotransfected with V5-STAT3-FL or the V5-STAT3-ΔN mutant into *STAT3-/-* MEFs. p300 further enhanced γ-FBG-LUC activity induced by V5-STAT3-FL; however, in presence of V5-STAT3-ΔN, p300 was unable to rescue the smaller levels of reporter activity (Figure 3.1C).

Figure 3.1 The STAT3 NH2-terminal domain is required for OSM-inducible transcription.

Figure 3.1A, The left panel is Western Immunoblot showing endogenous STAT3 level in *STAT3*+/- MEFs (C4+/-) and the loss of STAT3 expression in *STAT3-/-* MEFs (L1-/-). In the right panel, the expression of transiently transfected V5-STAT3-FL and V5-STAT3-ΔN in *STAT3-/-* MEFs was measured by Western Immunoblot with anti-V5 Ab. β-actin was used as a loading control.

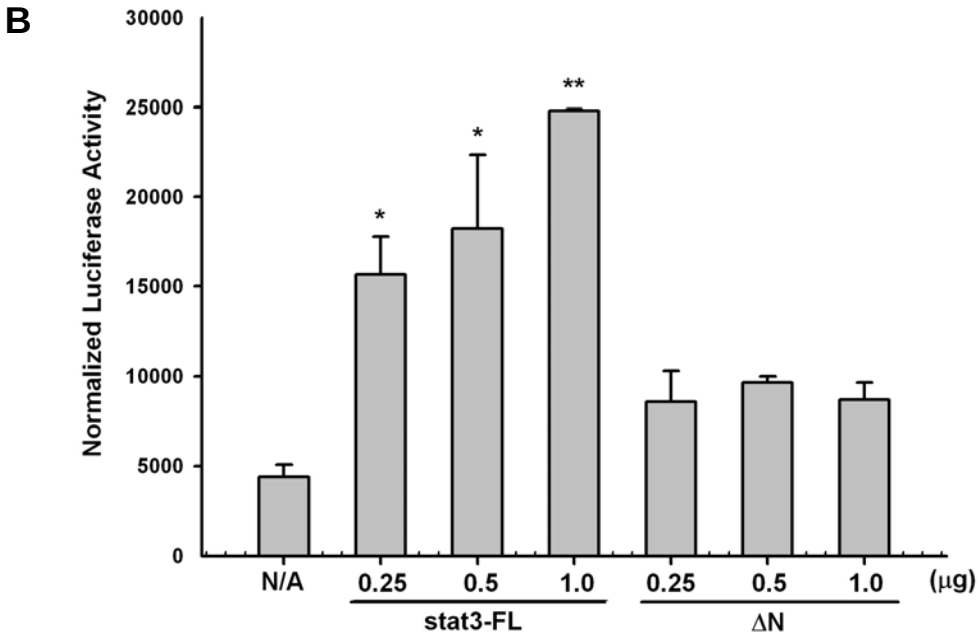

Figure 3.1B, STAT3-/- MEFs were transfected with the γ-FBG-LUC reporter gene together with different doses of STAT3-FL or STAT3-ΔN and then treated with OSM for 24 h followed by reporter gene assay. Data shown were means ± SD from three independent transfections. The data was analyzed by Student's *t* test. The luciferase reporter activities in STAT3-FL-transfected MEFs were compared with that in STAT3-ΔN-transfected MEFs. *, *p* value < 0.05, **, *p* value < 0.01.

C

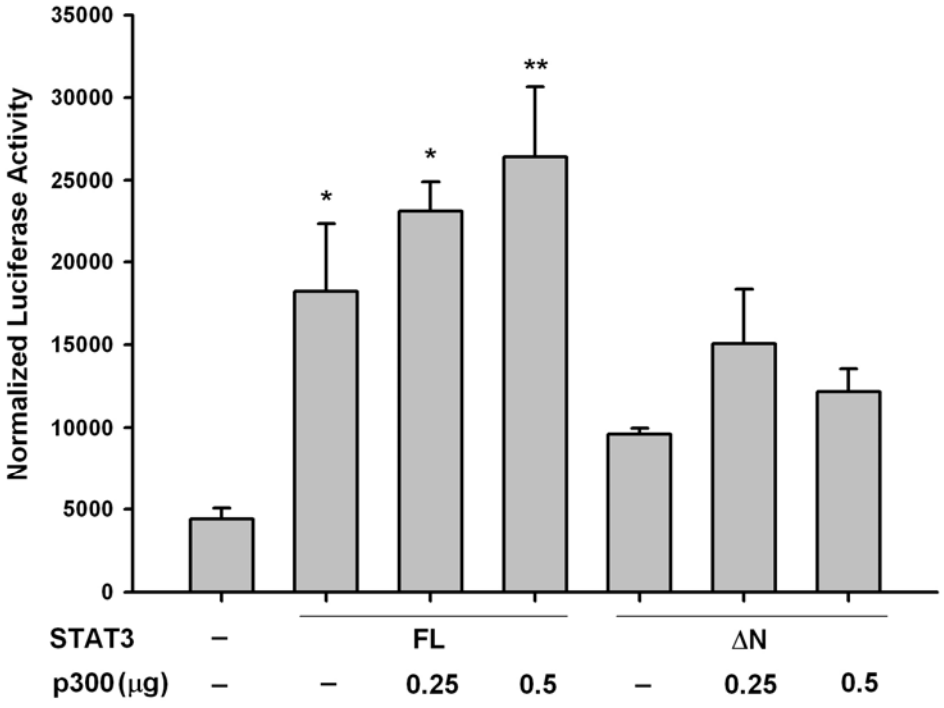

Figure 3.1C, Different doses of pCMVβ p300 were cotransfected with STAT3-FL or STAT3-ΔN together with γ-FBG-LUC reporter followed by OSM stimulation for 24 h. Data shown were means ± SD from three independent transfections. The data was analyzed by Student's *t* test. The luciferase reporter activities in STAT3-FL-transfected MEFs were compared with that in STAT3-ΔN-transfected MEFs. *, *p* value < 0.05, **, *p* value < 0.01.

3.2.2 The STAT3 NH2-terminal domain is required for the OSM-inducible mRNA expression

To further explore the role of the STAT3 NH2 terminus, we analyzed the expression of endogenous STAT3 target genes in MEFs by Quantitative Real-Time PCR (Q-RT-PCR). *Socs3, c-fos* and *p21,* well-established STAT3 dependent genes (133-136), were all significantly and quickly induced by OSM in *STAT3+/-* MEFs, and this inducible upregulation was dramatically decreased in *STAT3-/-* MEFs, indicating that STAT3 was a crucial transactivator for their induction (Figure 3.2A-C). To investigate how the NH2-terminal deletion affects STAT3 target gene expression, we stimulated a population of *STAT3-/-* MEFs stably expressing V5-tagged STAT3-FL or STAT3-ΔN mutant with OSM. In cells expressing STAT3-FL, all three STAT3 target genes were strongly activated by OSM (Figure 3.2D-F). Conversely, cells expressing STAT3-ΔN, despite its equivalent expression as STAT3-FL (insert panel in Figure 3.2D), were defective in gene expression (Figure 3.2D-F). Collectively, these results indicate the necessity of NH2-terminal domain for transcription activation by STAT3 in response to OSM signaling.

Figure 3.2 The STAT3 NH2-terminal domain is required for OSM-inducible mRNA expression

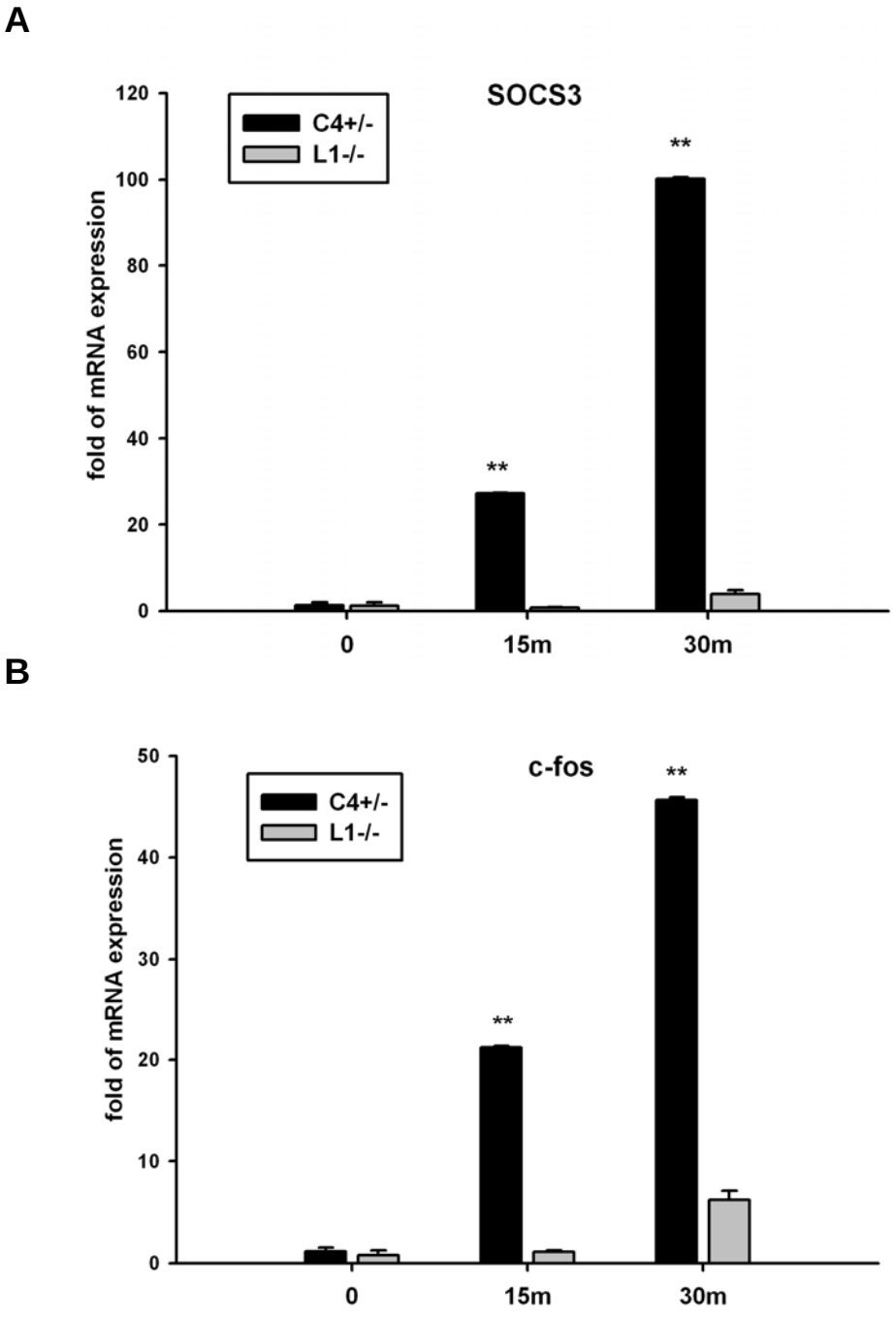

C

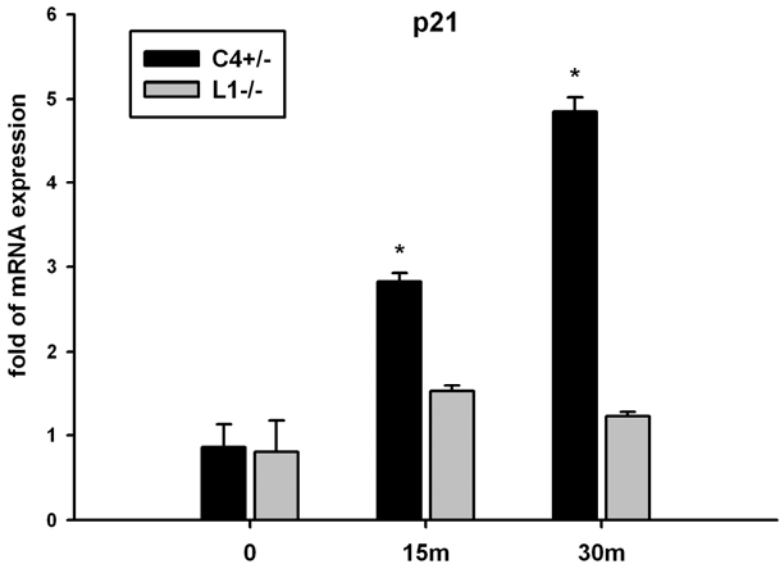

Figure 3.2 A-C, *STAT3+/-* and *STAT3-/-* MEFs were treated with OSM (20 ng/ml) for 15 m or 30 m. Whole cellular mRNA was isolated and the expression of *socs3, c-fos and p21* were measured by Q-RT-PCR. The fold change in OSM-treated cells over OSM-unstimulated control was obtained after correction for the amount of internal control, GAPDH. The mRNA induction in *STAT3+/-* MEFs was compared with that in *STAT3-/-* MEFS. Data shown were means ± SD from triplicates. The data was analyzed by Student's *t* test. *, *p* value < 0.05, **, *p* value < 0.01.

D

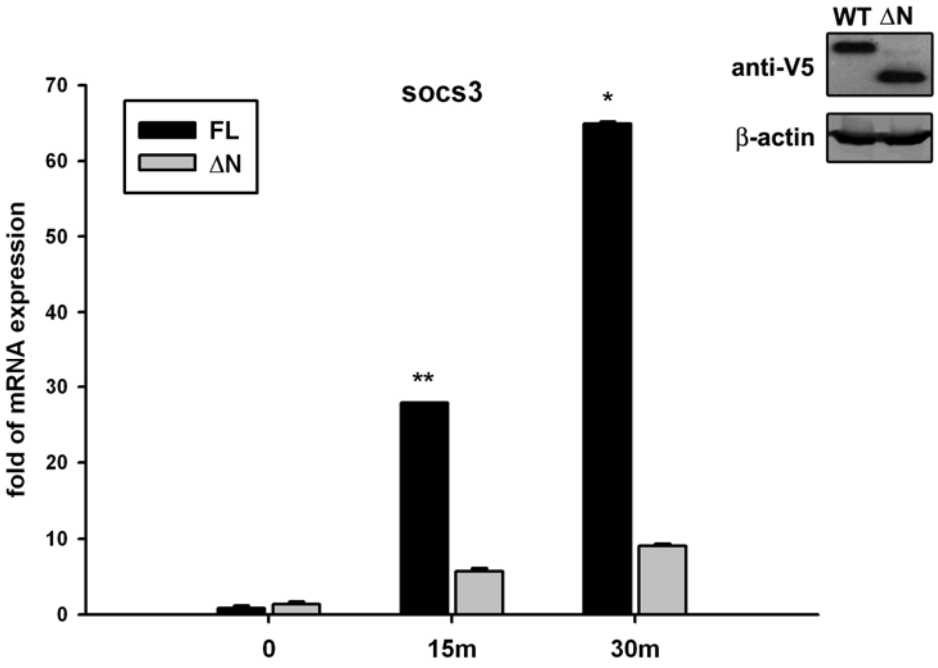
WT ΔN
anti-V5
β-actin
socs3
FL
ΔN
fold of mRNA expression
70
60
50
40
30
20
10
0
*
**
0
15m
30m

E

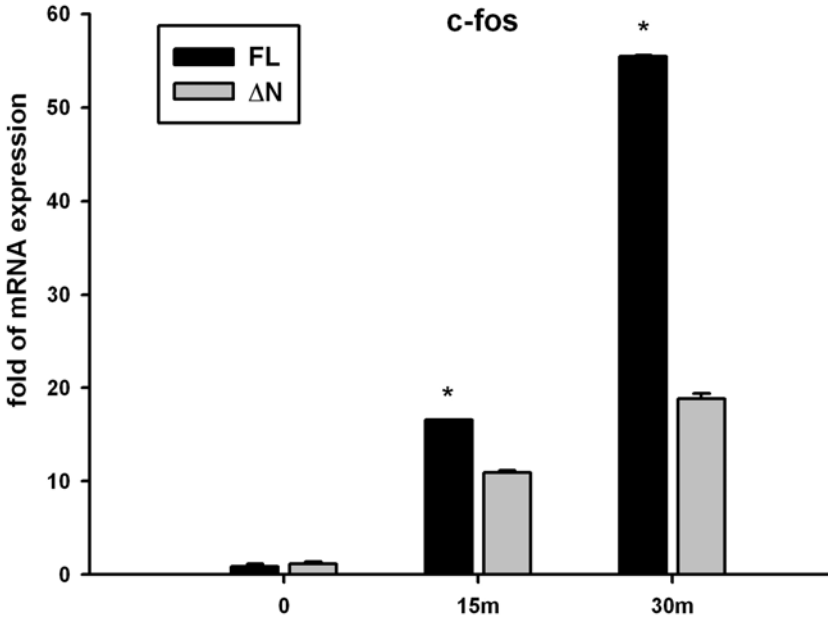
c-fos
FL
ΔN
fold of mRNA expression
60
50
40
30
20
10
0
*
*
0
15m
30m

F

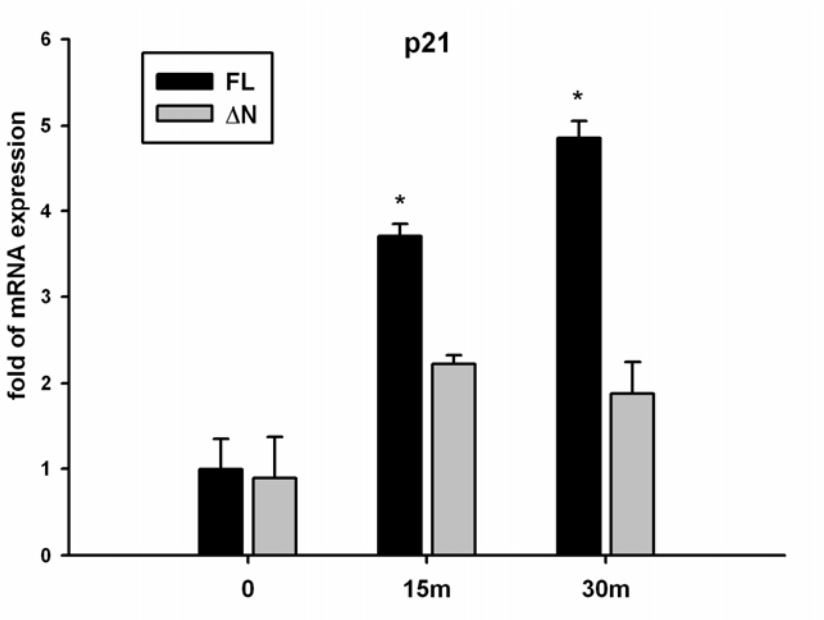

Figure 3.2D-F, *STAT3-/-* MEFs were transfected with pEF6-V5-STAT3-FL or V5-STAT3-ΔN. Positively transfected cells were selected by puromycin at 48 h and pooled. The insert panel in 4D is Western Immunoblot showing the stably expressed STAT3-FL and STAT3-ΔN after antibiotics screening. The STAT3-FL- or STAT3-ΔN-complemented *STAT3-/-* MEFs were stimulated by OSM (20 ng/ml) for 15 m or 30 m. Shown is the result of Q-RT-PCR assays plotting the fold changes of STAT3-dependent genes in OSM treated cells normalized to GAPDH. The mRNA induction in STAT3-FL-complemented *STAT3-/-* MEFs was compared with that in STAT3-ΔN-complemented *STAT3-/-* MEFs. The data was analyzed by Student's *t* test. *, p value < 0.05, **, p value < 0.01.

3.2.3 The NH2 terminal deletion affects enhanceosome assembly on the socs3 promoter

To clarify whether NH2 terminal of STAT3 regulates its transcription activity by mediating p300 recruitment, two-step Chromain Immunoprecipitation (ChIP) assays were performed to analyze p300 binding to the *socs3* promoter. Two STAT3 consensus binding regions have been identified on the *socs3* promoter upstream of the transcription initiation site (133, 134). A pair of primer amplifying both binding sites was designed and optimized by quantitative real time genomic PCR (Q-gPCR) to show a linear dynamic range from 40 ng to 25 μg DNA. First, we examined the OSM inducible STAT3 binding to the *socs3* promoter in *STAT3-/-* MEFs complemented with V5-STAT3-FL or V5-STAT3-ΔN mutant in ChIP experiments by using an anti-V5 as the primary Ab This experiment revealed that both STAT3-FL and STAT3-ΔN associated with the *socs3* promoter within 30 m after OSM stimulation (Figure 3.3A). This finding was consistent with previous studies showing that NH2-terminal deletion did not affect the nuclear translocation or DNA binding activity of STAT3 (95, 137). The ChIP assays were extended further to analyze the effect of OSM on inducible p300 and RNA pol II binding to the *socs3* promoter. As a result, we observed a 2.5-fold increase of p300 binding in response to OSM when *STAT3-/-* MEFs were complemented with V5-STAT3-FL, but no significant p300 recruitment was detected when STAT3-ΔN mutant was stably expressed (Figure 3.3B). In addition, the inducible loading of RNA pol II on the *socs3* gene was also inhibited in MEFs stably expressing STAT3-ΔN (Figure 3.3C). Our explanation for these results is that the reduced p300 binding caused by the NH2-terminal deletion affects the association RNA pol II due to its direct interaction with p300 (138, 139).

Figure 3.3 The STAT3 NH2-terminal domain regulates enhanceosome assembly on the *socs3* promoter.

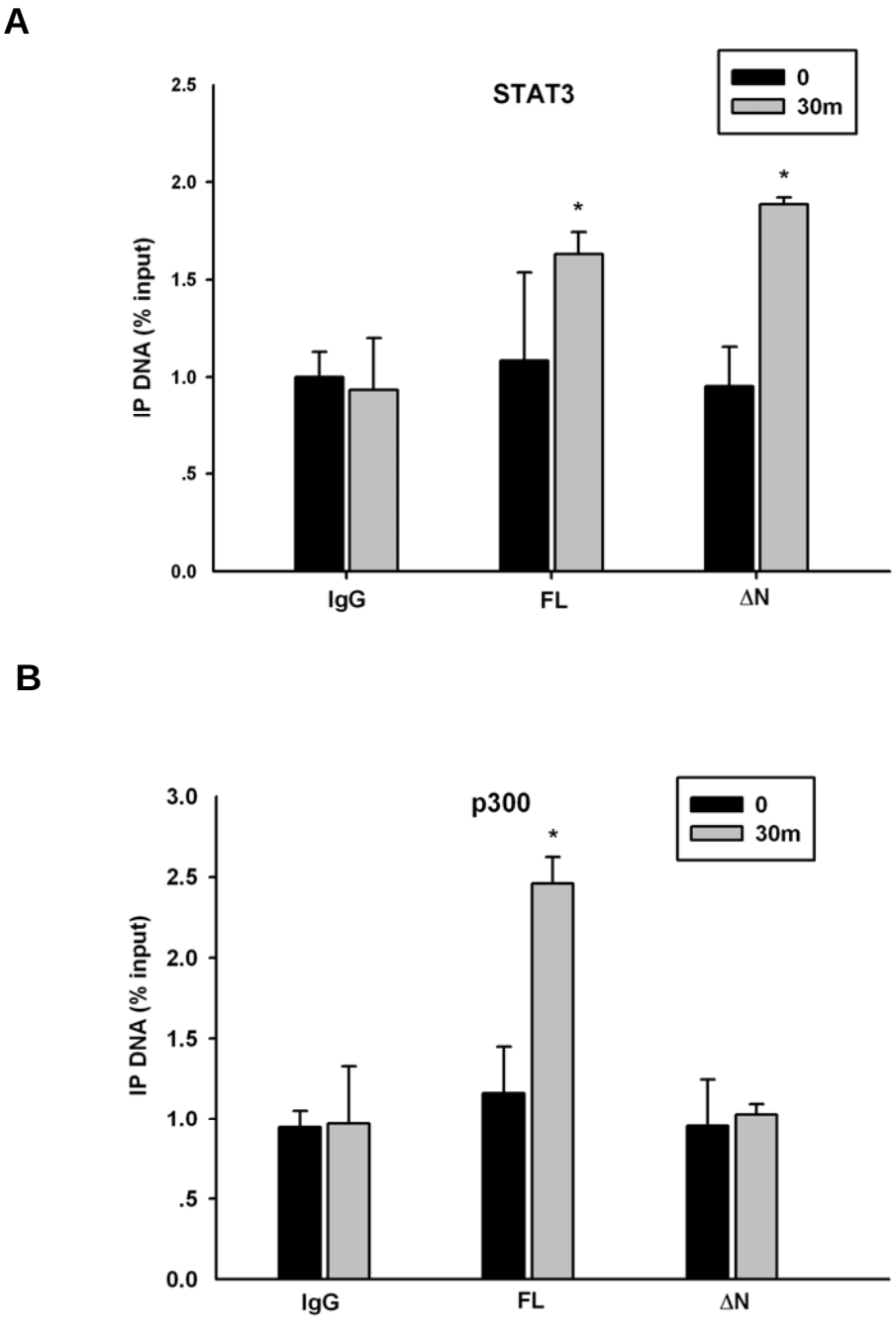

C

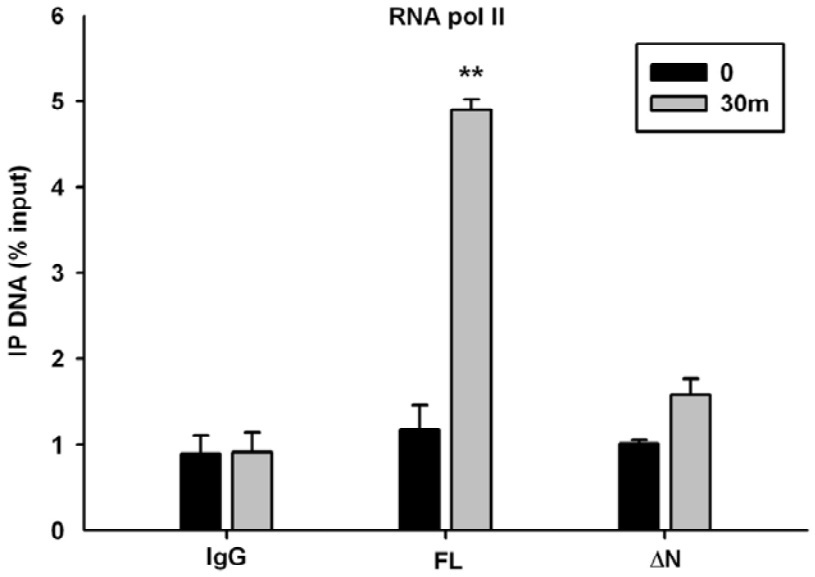

Figure 3.3 *STAT3-/-* MEFs stably expressing V5-STAT3-FL or V5-STAT3-ΔN were treated with OSM (20 ng/ml) for 30 m, and two-step ChIP assay was performed by using Abs specifically recognizing V5 tag (Fig.3.3A), p300 (Fig.3.3B) or RNA pol II (Fig.3.3C). The sequence of the *socs3* promoter in the immunoprecipitates was amplified by Q-RT-gPCR using specific primers. Shown is signal in the immunprecipitates expressed as a percentage of the DNA present in the input. A, Both STAT3-FL and STAT3-ΔN are induced by OSM to bind to the *socs3* promoter. B, The OSM-inducible p300 recruitment to the *socs3* promoter is inhibited in cells stably expressing STAT3-ΔN. C, The OSM-inducible RNA pol II association to the *socs3* promoter is reduced in STAT3-ΔN-complemented MEFs. The results were expressed as means ± SD from triplicates. The signals in OSM-treated cells were compared with non-treated MEFs. The data was analyzed by Student's *t* test. *, p value < 0.05, **, p value < 0.01.

3.2.4 Association between the STAT3 NH2-terminal domain and p300 is regulated by NH2-terminal acetylation

To study the interaction between the STAT3 NH2-terminal domain and p300, we first sought to determine whether the STAT3 NH2-terminus is sufficient for p300 interaction. For this purpose, HepG2 cells were cotransfected with pCMVβ p300 and a plasmid expressing V5-tagged NH2-terminal domain of STAT3 (aa 1-130). Nuclear protein was recovered and immunoprecipitated by anti-p300 Ab followed by Western Immunoblot using anti-V5 Ab. As seen in Figure 3.4A, V5-STAT3 (1-130) was specifically captured by p300 Ab but not by IgG. To determine the effect of STAT3 K49/K87 acetylation on p300 interaction, we generated FLAG-tagged acetylation-deficient (K49R/K87R) and the pseudo-acetylated (K49Q/K87Q) NH2-terminal mutants (aa 1-124), and examined their association with p300. In contrast to the FLAG-STAT3-WT (1-124), the acetylation-deficient FLAG-STAT3 (1-124)-K49R/K87R mutant was barely detectable in p300 immunoprecipitates (Figure 3.4B). Instead, the pseudo-acetylated FLAG-STAT3 (1-124)-K49Q/K87Q mutant exhibited stronger p300 binding despite the fact that its expression level was comparable to FLAG-STAT3-WT (1-124) (Figure 3.4C). These results indicate that the STAT3 NH2-terminal domain is sufficient for p300 interaction and the K49/K87 acetylation increases this association.

Figure 3.4 Interaction between the STAT3 NH2-terminal domain and p300.

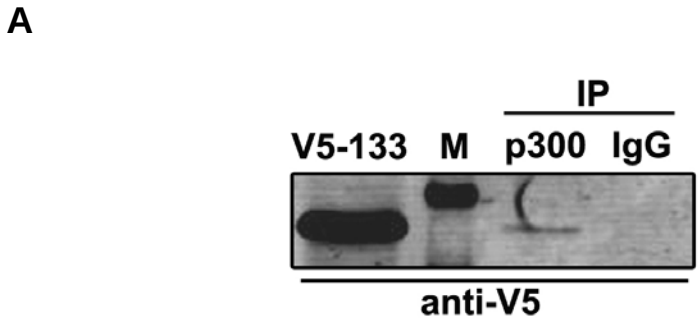

Figure 3.4A, HepG2 cells were cotransfected with pEF6-V5-STAT3 (aa 1-130) with pCMVβ p300. Cells were treated with IL-6 (10 ng/ml) for 30 m before NE was prepared. 2 mg of NE was immunoprecipitated by anti-p300 Ab. p300-bound V5-STAT3 (1-130) was detected by anti-V5 Ab in Western Immunoblot. The first lane is lysate showing the expression of V5-STAT3 (1-130). The second lane is protein standard (indicated by "M" in *Fig. 3.4A*).

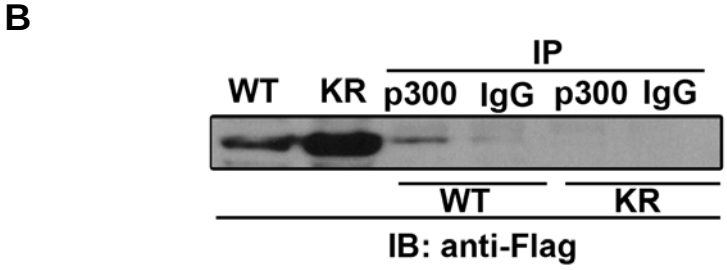

Figure 3.4B, HepG2 cells were cotransfected with either pECFP-FLAG-STAT3-WT (aa 1-124) or STAT3-K49R/K87R mutant (aa 1-124) together with pCMVβ p300. NE was immunoprecipitated with anti-p300 Ab followed by Western Immunoblot with anti-FLAG Ab. The first two lanes show FLAG-STAT3-WT (1-124) and STAT3–K49R/K87R (1-124) expression in nuclear lysate. Lane 3 and lane 4 are immunoprecipitates of FLAG-STAT3-WT (aa 1-124) with anti-p300 Ab (lane 3) or IgG (lane 4). Lane 5 and lane 6 are immunoprecipitates of FLAG-STAT3-K49R/K87R mutant (aa 1-124) with anti-p300 Ab (lane 5) or IgG (lane 6).

C

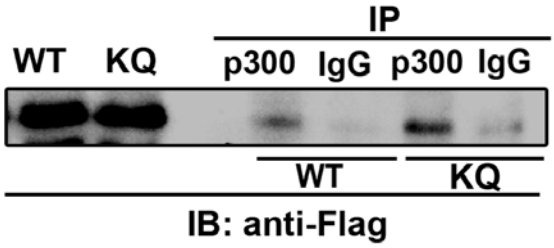

Figure 3.4C, HepG2 cells were cotransfected with either pECFP-FLAG-STAT3-WT (1-124) or STAT3-K49Q/K87Q mutant (1-124) together with pCMVβ p300. Immunoprecipitation was performed as described in *Fig 1B*. The first two lanes show FLAG-STAT3-WT (1-124) and STAT3–K49Q/K87Q (1-124) expression in nuclear lysate. Lane 3 and lane 4 are immunoprecipitates of FLAG-STAT3-WT (aa 1-124) with anti-p300 Ab (lane 3) or IgG (lane 4). Lane 5 and lane 6 are immunoprecipitates of FLAG-STAT3- K49Q/K87Q mutant (aa 1-124) with anti-p300 Ab (lane 5) or IgG (lane 6).

3.2.5 The binding site of STAT3NH2-terminal domain maps to the p300 bromodomain

To determine the domain of p300 responsible for the STAT3 NH2-terminal binding, we generated a panel of FLAG epitope-tagged p300 deletions. The related functional domains included in each truncation are shown in Figure 3.5A. Each of the four NH2-terminal-deleted mutants (p300-ΔN1, -ΔN2, -ΔN3, & -ΔN4) or two COOH-terminal-deleted mutants (p300-ΔC1 & -ΔC2) was individually coexpressed with V5-STAT3 (1-130) and p300-bound-NH2 terminal domain was examined by nondenaturing co-immunoprecipitaiton assays. STAT3 NH2-terminal binding was lost when the region between aa 1047 (p300-ΔN3) and aa 1255 (p300-ΔN4) was deleted (Figure 3.5B, right panel). Importantly, this region, from aa 1047 to aa 1255, contains the p300 bromodomain, spanning from aa 1053 to aa 1156. Consistent with this finding, the lack of bromodomain in ΔC2 (aa 1-1043) abrogated its interaction with the STAT3 NH2-terminal domain, however the bromodomain-containing mutant ΔC1 (aa 1-1264) still complexed with the STAT3 NH2 terminus (Figure 3.5C, right panel). To further confirm

that the p300 bromodomain mediates its interaction with the STAT3 NH2 terminal region, an expression vector encoding p300 with an internal deletion of the bromodomain (p300-ΔB) was generated and tested. As we expected, no interaction was detected between p300-ΔB and the STAT3 NH2-terminal domain (Figure 3.5C, right panel). Taken together, these data suggest that the p300 bromodomain binds the STAT3 NH2-terminal domain and the IL-6 or OSM-inducible NH2-terminal acetylation further stabilize this interaction.

Figure 3.5 The STAT3 NH2-terminal domain is associated with the p300 bromodomain.

A

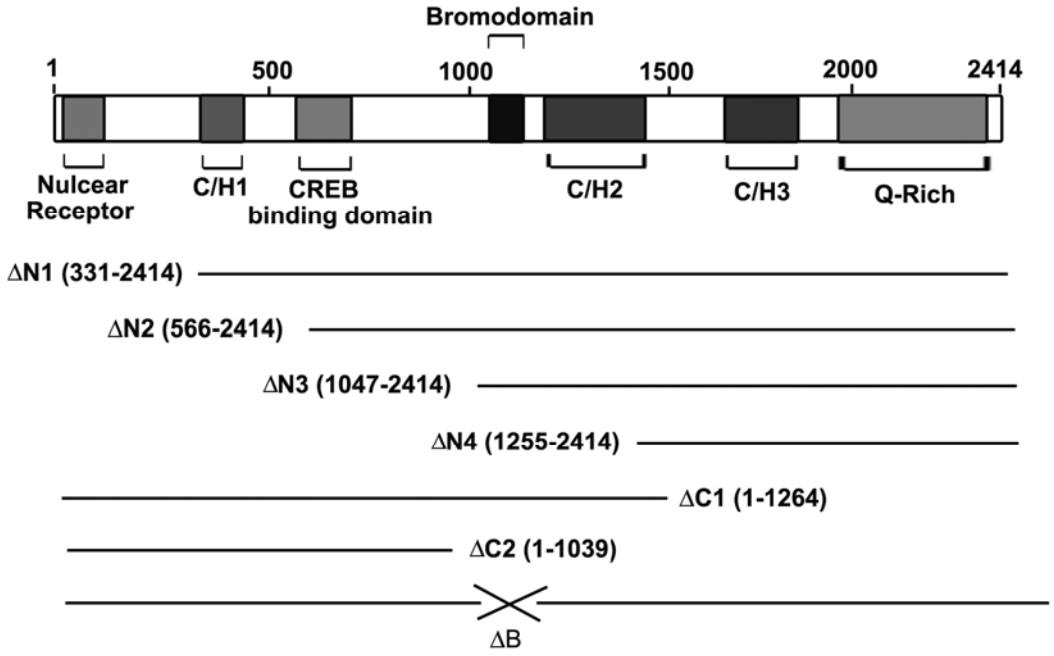

Figure 3.5A A schematic diagram showing different functional domains of p300 and all p300 mutants used in Fig.3.5B & 3.5C.

B

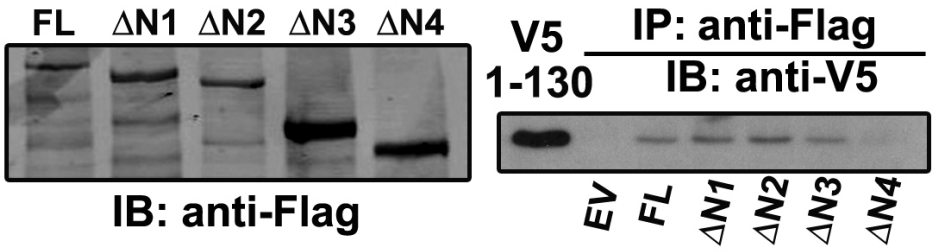

C

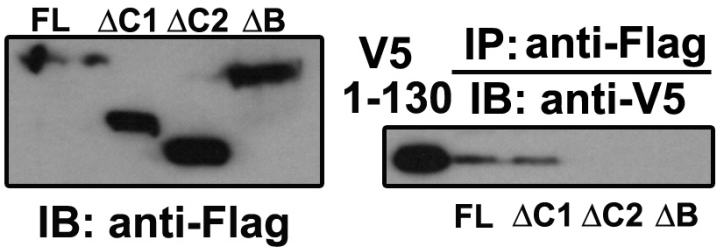

Figure 3.5B&C, The STAT3 NH2-terminal domain associates with the p300 bromodomain. PXFS-FLAG-p300-FL, p300 NH2-terminal deletions (p300-ΔN1, -ΔN2, -ΔN3 and -ΔN4), COOH-terminal deletions (p300-ΔC1 & -ΔC2), or p300 mutant without the bromodomain (p300-ΔB) were individually cotransfected with pEF6-V5-STAT3 (1-130) into HEK 293 cells. Immunoprecipitation was performed by anti-FLAG Ab and the p300-associated STAT3 NH2-terminus was detected by anti-V5 Ab. The left panels are Western Immunoblot showing the expression of each mutant in the cell lysate. The right panels are p300-associated STAT3-NH2 terminus. EV: the empty vector (PXFS-FLAG) was included as a negative control.

3.2.6 The P300 bromodomain facilitates STAT3-dependent transcription

Because the p300 bromodomain was responsible for STAT3 NH2-terminal binding (Figure 3.5), we propose that the p300-STAT3 interaction will be affected when the p300 bromodomain is deleted. To test this, HEK 293 cells were transfected with pEF6-V5 STAT3 together with FLAG-tagged p300-FL or p300-ΔB mutant. The interaction between these two proteins was then accessed by nondenaturing co-immunoprecipitation with anti-FLAG Ab followed by Western Immunoblot with anti-V5 Ab. As we expected, the p300-ΔB mutant showed decreased interaction with STAT3 compared to that of p300-FL (Figure 3.6A, left panel), despite the similar expression level of these two proteins (Figure 3.6A, right panel). The remaining association observed between p300-ΔB and STAT3 indicate multiple domains of p300 are involved in STAT3-p300 interaction. An early study using *in vitro* transcription reactions found that p300 form a stable complex with chromatin templates which is mediated, at least in part, by the bromodomain (140). To confirm this finding *in cellulo*, ChIP experiments were performed to capture the binding of p300 to the endogenous *socs3* promoter after p300-FL or p300-ΔB mutant was transiently transfected into *STAT3+/-* MEFs. As seen in Figure 3.6B, the p300-ΔB mutant exhibited weaker association with the *socs3* promoter than p300-FL. At the same time, reductions in STAT3 and RNA pol II binding were observed in p300-ΔB-transfected cells (Figure 3.6C & 3.6D). To further test the functional role of bromodomain, different doses of p300-FL or p300-ΔB mutant was cotransfected with γ-FBG-LUC reporter gene into HepG2 cells followed by IL-6 treatment for 24h. As a result, the p300-FL expression further enhanced the IL-6-inducible reporter activity in a dose-dependent manner. The p300-ΔB mutant, however, failed to function as a transcriptional coactivator in this assay (Figure 3.6E). Taken

together, our results suggested that the bromodomain plays a critical role in p300 function because it mediates p300 interaction with STAT3 and facilitates the enhanceosome formation.

Figure 3.6 The p300 bromodomain facilitates STAT3-dependent transcriptional activation

A

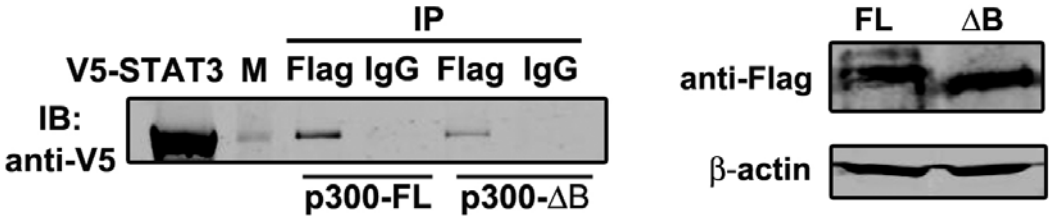

Figure 3.6A The bromodomain deletion in p300 reduces its interaction with STAT3. HEK 293 cells were cotransfected with PXFS-FLAG-p300-FL or p300-ΔB mutant together with pEF6-V5-STAT3-FL. 48 h after transfection, 1 mg of whole cell extract was collected and immunoprecipitated by anti-FLAG Ab followed by Western Immunoblot with anti-V5 Ab. The right panel is Western Immunoblot showing that p300-FL and p300-ΔB mutant had comparable expression level.

B

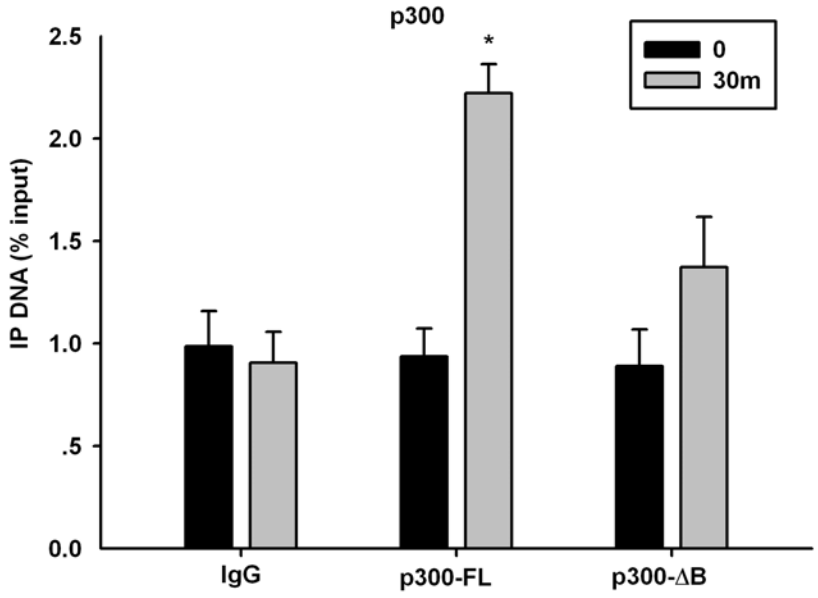

C

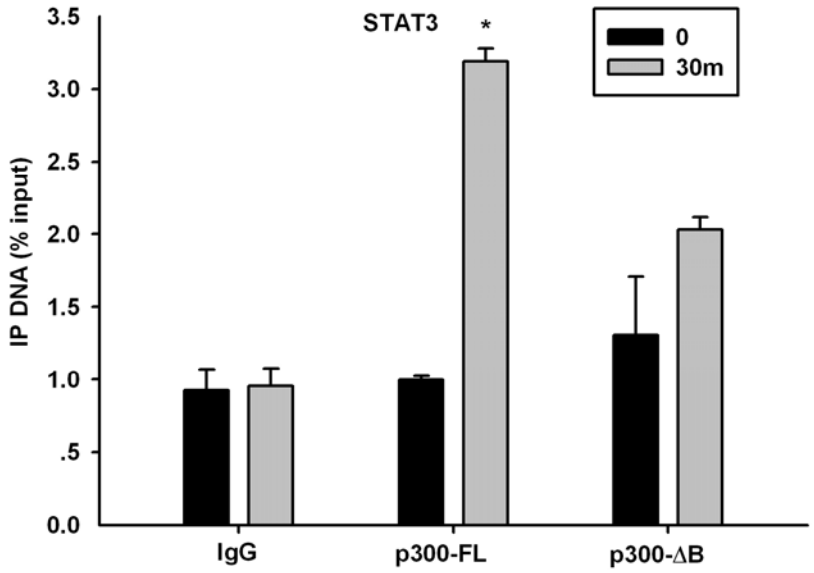

D

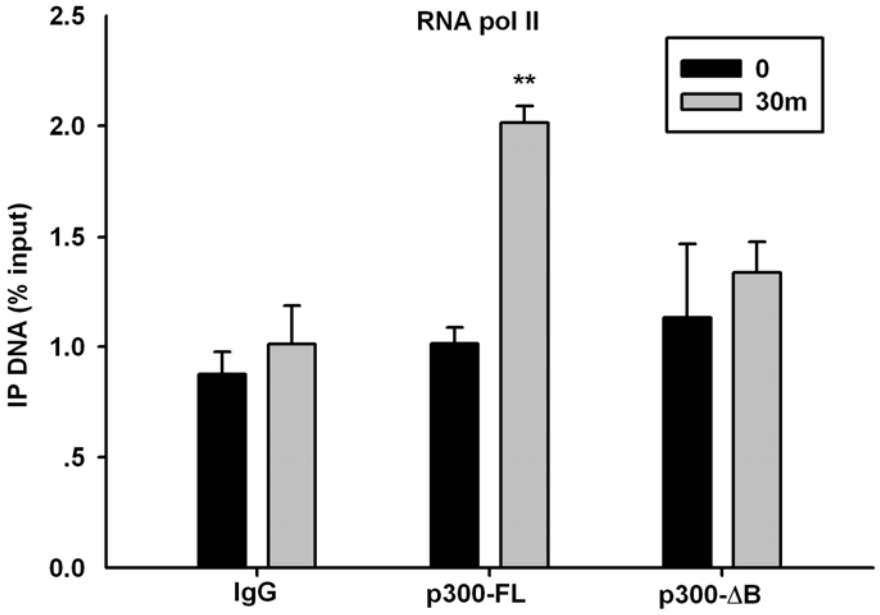

Fgure 3.6B,C&D, The p300 bromodomain stabilizes enhanceosome assembly. *STAT3*+/- MEFs were transiently transfected with PXFS-FLAG-p300-FL or p300-ΔB mutant. 24 h after transfection, cells were treated with OSM (20 ng/ml) for 30 m or left untreated. Two-step ChIP assays were performed by using antibodies specifically recognizing p300 (Fig.3.6B), STAT3 (Fig.3.6C) and RNA pol II (Fig.3.6D).

E

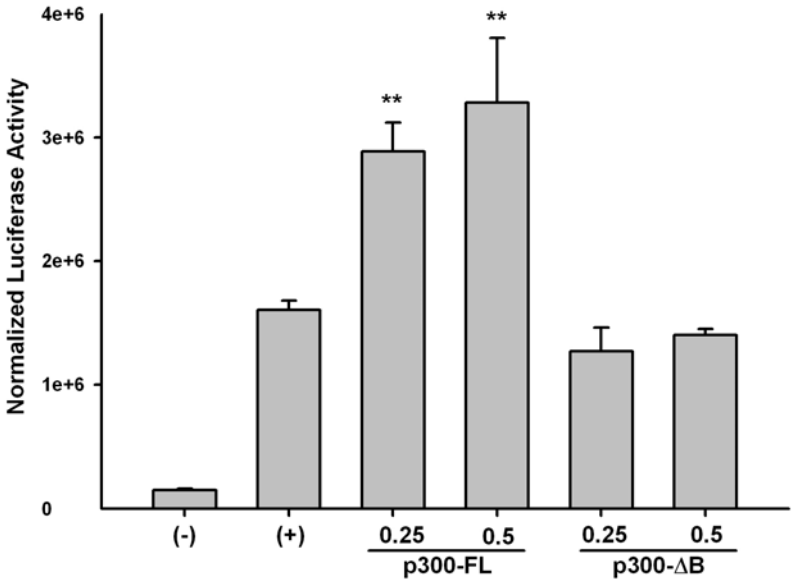

Figure 3.6E HepG2 cells were transfected with different doses of PXFS-FLAG-p300-FL or p300-ΔB mutant together with γ-FBG-LUC reporter gene. 24 h later, cells were treated with IL-6 (10 ng/ml) for another 24 h and then luciferase activity was measured. Data shown were means ± SD from three independent transfections. The luciferase activity in p300-FL-transfected cells is compared with that in p300-ΔB-transfected cells. The data was analyzed by Student's *t* test. *, *p* value < 0.05, **, *p* value < 0.01.

3.3 Discussion

STAT3 is the major transcription factor activated by the IL-6 family of cytokines. Although the STAT3 signaling from the cell membrane to the nucleus is well understood, the molecular events regulating gene transcription need more elucidation. Like many other transcription factors, the activated STAT3 recruits the p300 coactivator after nuclear translocation (27). The p300-induced acetylation on histone tails is coupled with chromatin remodeling, thereby enhancing target gene expression (27, 95, 96). The interaction between p300 and STAT3 is regulated via both the STAT3 NH2-terminal domain and the COOH-terminal TAD (96). In this study, we reported that the NH2-terminal domain plays a critical role in STAT3-mediated signal transduction by regulating enhanceosome assembly at the promoter loci. This conclusion is supported by (1) the NH2-terminal deletion inhibited OSM-induced reporter activity and abolished the cooperation between STAT3 and p300 (Figure 3.1); (2) the expression of endogenous STAT3 target genes, including *socs3, c-fos* and *p21*, was significantly reduced in STAT3-ΔN-complemented *STAT3-/-* MEFs (Figure 3.2); and (3) significantly reduced loading of p300 and RNA pol II to the *socs3* promoter were observed when STAT3-ΔN mutant was stably expressed in *STAT3-/-* MEFs (Figure 3.3). These results suggest that the NH2-terminal deletion disrupts the enhanceosome formation on the *socs3* promoter, resulting into an inhibition in mRNA transcription.

The NH2-terminal domain of STATs comprises approximately the first 130 residues that assembled into an all-helical hook-like structure (141). Although it is highly conserved in the STAT family, NH2-terminal domain is implicated in diverse functions, including STAT dimeration or tetramization, phosphorylation/dephosphorylation, and STAT's interaction with other transcription

factor or coactivators. One of the identified functions of NH2-terminal region is regulating the cooperative binding of STAT dimer·dimer complexes on two tandemly arranged binding sites. This function is conserved in STAT1 (122), STAT4 (121) and STAT5 (142), and recently is also confirmed in STAT3 when it activates the transcription of α2-macroglobulin (*α2-M*) gene (143). A tetrameric STAT3 complex is formed on the α2-M enhancer sequence, which is required for the maximum transcriptional activation (143). Two point mutations in the NH2-terminal region (W37A, Q66A) disrupts the tetramer binding (143). The murine *socs3* promoter also contains two putative STAT3 binding sites which are highly conserved in the human socs3 promoter (133, 144). Both sites are required for the complete activation of the human socs3 promoter stimulated by LIF (144). As for the murine *socs3* promoter, the proximal site localized from nucleotide -72 to -64 is essential for LIF-induced transactivation (133). The distal site from nucleotide -95 to -87, however, has not been directly tested. Although two STAT3 motifs on the murine *socs3* promoter are tandemly linked, STAT3 binding is only detected on the proximal site and no obvious dimer·dimer interaction is observed (137). This excludes the possibility that the defective activity of STAT3-ΔN mutant in activating the *socs3* expression (Figure 3.2) is caused by the disruption of STAT3 tetramerization.

Here we describe a new level of STAT3 NH2-terminal function achieved through its interaction with the p300 bromodomain. p300 is known to function as a bridging factor connecting sequence-specific transcription factor with the basal transcription machinery (86). The direct association between p300 and RNA pol II in mammary cells has long been known (138, 139). In this interaction, p300 specifically interacts with the unphosphorylated form of RNA pol II which is able to form transcription preinitiation complex (138, 145). Our study show that the STAT3 NH2-terminal deletion significantly decreases p300 recruitment to the *socs3* promoter (Figure 3.3B), resulting in an inhibition

in RNA pol II binding (Figure 3.3C). These results reveal the function of NH2-terminal domain to integrate the enhancer binding proteins and facilitate the assembly of transcription preinitiation complex.

The recent finding that STAT3 is also a direct target of p300 for acetylation drew more attention to the study of p300-STAT3 interaction. STAT3 is acetylated by p300 at multiple lysine residues. The reversible acetylation on K 685 within TAD is essential for STAT3 dimeration and DNA-binding ability (96). Our earlier studies identified another two acetylation sites (K49 and K87) localized in the NH2-terminal domain of STAT3, sites whose acetylation are also indispensable for STAT3-mediated transactivation (95). Interestingly, this NH2-terminal acetylation, however, have no effect on the inducible STAT3 binding to DNA (95).

In this study, we demonstrate that the STAT3 NH2-terminal domain is sufficient for p300 interaction (Figure 3.4A) and show that the NH2-terminal acetylation increase the p300-NH2-terminal interaction (Figure 3.4B & 3.4C). Here we report the discovery that the p300 bromodomain is the site for NH2-terminal association (Figure 3.5). The bromodomain represents a highly conserved protein module that is commonly found in many chromatin-associated proteins and nearly all HATs (146). The function of bromodomain as an acetyl-Lysine binding domain was discovered soon after its three-dimensional structure was elucidated. The solution structure of the bromodomain from P/CAF revealed an unusual left-handed four-helix bundle (147), a unique structural fold that was conserved in other chromatin-associated proteins, such as human TAFII250 (148) and the *Saccharomyces cerevisiae* Gcn5p (149). Although the acetyl-Lysine is the direct recognition site of the bromodomain, residues flanking both sides of acetyl-lysine are also important for the interaction and contribute to the ligand selectivity of bromodomains (150). The acetylation-enhanced interaction (Figure 3.4B & 3.4C)

indicates that the acetylation on K49 and K87 provide binding motif for the bromodomain of p300, leading to a stable complex formation and efficient HAT recruitment to the promoter. There is also a possibility that the NH2-terminal acetylation induce conformational changes in residues flanking the acetyl-Lysine that positively affect p300-STAT3 interaction. Interestingly, the acetylation-dependent interaction is also observed between MyoD and the bromodomain of p300/CBP (82). p300/CBP selectively recognizes the acetylated form of MyoD in cell and mutations of acetylation sites in MyoD decrease its ability to cooperate with p300/CBP (82). This suggests that acetylation is probably a common strategy that p300/CBP utilizes to facilitate their interaction with non-histone proteins.

The bromodomain is also reported to mediate p300 binding to chromatin. p300 forms a stable complex with *in vitro* transcription template and this association is regulated at least partially by the bromodomain (140). Our ChIP result in Figure 3.6B confirmed this finding *in cellulo* by showing that the bromdomain deletion decreased p300 occupancy on the endogenous *socs3* promoter. We also noticed that the bromodomain-deficient mutant (p300-ΔB) was still bound to STAT3 (Figure 3.6A) although the interaction was significantly weaker than that of p300-FL and STAT3. This data indicates that more than one domain of p300 are involved in mediating p300-STAT3 interaction. It has been shown that TAD of STAT3 also associates with p300 although the binding site on p300 has not been identified yet (27, 96). Similarly, the interaction between STAT1 and p300/CBP is also mediated by two contact regions. The STAT1 NH2-terminal region is recognized by the CREB-binding domain of p300/CBP and the binding site of TAD maps to the p300/CBP domain that recruits adenovirus E1A protein (98).

In summary, we have provided evidence that the STAT3 NH2-terminal domain interacts with the p300 bromodomain in an acetylation-dependent manner. IL-6 or OSM-induced acetylation on K49 and K87 trigger the recognition of substrate by the p300 bromodomain, resulting in a strengthened association between p300 and STAT3. This interaction further stabilizes the recruitment of other transcription components like RNA pol II to efficiently initiate the transcription of STAT3 target genes.

CHAPTER 4: MATERIALS AND METHODS

4.1 Antibodies and Reagents:

Polyclonal anti-CDK9 (c-20), STAT3 (c-20), anti-phospho-Y STAT3 (B7), cyclin T1 (H-245), anti-p300 (N-15) and RNA Pol II (N-20) Abs were purchased from Santa Cruz Biotechnology. Anti-V5 and Flag Abs were obtained from Invitrogen and Sigma, respectively. Monoclonal anti-phospho-S2 carboxy terminal domain (CTD) Pol II Ab (H5) was from Covance. Anti-Ac-Lys87 STAT3 Ab was described before(95). Recombinant human IL-6 was from PEPROTECH. Recombinant mouse OSM was provided by R&D Systems.

4.2 Cell Culture and Treatment

The human hepatoblastoma cell-line HepG2 (ATCC, Manassas, VA) was cultured in DMEM (GIBCO, Invitrogen) supplemented with 10% (vol/vol) fetal bovine serum, 2 mM L-glutamine, 0.1 mM nonessential amino acids, 1 mM sodium pyruvate, and penicillin (100 U/ml)/streptomycin (100 μg/ml). *STAT3 +/-* and *STAT3-/-* MEFs were generous gifts from Dr. Stephanie Watowich in M.D. Anderson. MEFs and human HEK 293 cells were cultured in DMEM (GIBCO, Invitrogen) supplemented with 10% (vol/vol) fetal bovine serum, 2 mM L-glutamine and penicillin (100U/ml)/streptomycin (100μg/ml). Cells are maintained at 37^{o}C in a humidified atmosphere of 5% CO2. Cells were serum starved for at least 16 h before treatment with IL-6 or OSM. FP was added 1 h before IL-6 stimulation.

4.3 Plasmid Construction

For the γ-FBG-LUC reporter, 643 bp of the 5' flanking human γ-FBG promoter was amplified from HepG2 cell genomic DNA by PCR using the forward primer 5'-CGCGGGATCCCTCCTGAGAAGTGAGAGCCTA-3' and reverse primer 5'-GCCCAAGCTTGAGCTCCGAGCCTTGTAGTG-3'. The PCR product was digested with Bam HI and Hind III, gel purified and ligated into the same sites in the pOLUC plasmid (151).

The pEF6-V5-STAT3 wild type and dominant-negative (DN) STAT3 were constructed as described before (52). The V5 epitope-tagged NH2- and COOH-truncated STAT3 expression vectors (amino acids 1-585, 1-688, 130-770(ΔN)) were previously described (95). The V5 STAT3 (1-130, 1-320, 1-488, and 130-688) expression vectors were produced by PCR and cloned into pEF6/V5-His (InVitrogen). Primers 5'-GGAAATGGCCCAATGGAATCAGCTACAG-3′ and 5'-GTTGGCCTGGCCCCCTTGCTG-3' were used for 1-130; primers 5'-GGAAATGGCCCAATGGAATCAGCTACAG-3′ and 5'-GGCACTTT TCATTAAGTTTCT-3' were used for 1-320; primers 5'-GTTGGCCTGGCCCCCTTGCTG-3' and 5'-GGAGATCACCACAACTGGCAA-3' were used for 1-488; primers 5'-GGTTATGGCAGCCGTGGTGACGGAGAAG-3' and 5'-TGCCTCCTCCTTGGGAATGTCAGGATAGAG-3' are used for 130-688.

Flag-tagged WT-124, KR-124 and KQ-124 were produced by PCR using pEFF6-V5-WT-STAT3, KR (48/97)-STAT3 and KQ (48/97)-STAT3(95) as templates respectively. The primers used for this purpose were: sense primer 5' CATCGATGGATCCATGGACTACAAAGACGATGACGATAAGGCCCAATGGAAT CAGCTACAG 3' and antisense primer 5'

CGTACCTCTAGACTACTGGGCCGCAGTGGCTGCAGTCTG 3'. The PCR products were digested with Bam HI and Xba I endonuleases, gel purified and cloned into pECFP-Nuc (Clonetech) restricted with the same endonuleases.

The FLAG-mStraw CDK9 expression plasmid was constructed in two steps. First, the monomeric strawberry (mStraw) cDNA (a generous gift of R. Tsien (152)) was PCR amplified using primers to introduce a Bgl II restriction endonuclease site upstream of the initiator methionine, remove the stop codon and insert multiple cloning sites. The sequence of these primers was 5'-CAGTCAGATCTATGGTGTAGCAAGGGCGAGGAGAATAACATG-3' (upstream), and 5'-GTCAACAAGCTTGTGGATCCAGCTTTCTTGTACAGCTCGTCCATGCC-3' (downstream). The mStraw PCR product was digested with Bgl II and Hind III endonucleases, gel purified and cloned into pcDNA-FLAG (52) digested with BamH1 and Hind III, producing pcDNA-FLAG-Straw. Second, the full length human CDK-9 cDNA was produced by amplification of oligo-dT primed cDNA from HeLa cell RNA. The sequence of the primers was: 5'-CATGCAAGCTTGCAAAGCAGTA CGACTCTGGTGGAG-3' (upstream), and 5'-GTCATTCTAGAGGATCCTCAGAAGACGCGCTCAAACTCCGTCTGG-3' (downstream). The CDK9 cDNA was then restricted with Hind III and Xba I and cloned into the pcDNA-FLAG-Straw plasmid restricted with the same endonucleases, producing pcDNA-FStraw-CDK9.

For pEYFP-Flag-CDK9, The CDK9 cDNA was amplified from oligo-dT-primed Hela cDNA using sense primer 5' AGTCTGAAGCTTGCAAAGCAGTACGACTCGGTG 3' and antisense primer 5' TACCAGGGATCCTCAGAAGACGCGCTCAAACTCCGTCTGGTTGG 3'. The PCR fragment was digested with Hind III and Bam HI and cloned into a modified pEYFP-C1

plasmid (Clonetech) containing a Flag epitope inserted upstream of multiple cloning site to generate pEYFP-Flag-CDK9.

The DN-CDK9 (Asp167 to Asn, D167N) was produced from wild type CDK9 as a template using site-directed mutagenesis (QuickChange, Stratagene (153)). The sequence of primers used was (mutations underlined): 5'-CCTGAAGCTGGCAAACTTTGGGCTGGCCCGGG-3' (sense) and 5'-CCCGGGCC AGCCCAAAGTTTGCCAGCTTCAGG-3' (antisense).

The expression vector used for PXFS-Flag-p300 constructs was described(154). The full length of p300 cDNA was amplified from pCMVβ p300 (155) using the following primers: sense: 5'-CAGTCTAGACGTAAGCTTGCCGAGAATGTGGTGGAACCGG-3' and antisense: 5'-CTCGTAGATATCCTAGTGTATGTCTAGTGTACTC-3'. The PCR product was restricted with HindIII and EcoRV and cloned into the vector of PXFS-Flag. The four NH2-terminal-deleted truncates (p300-ΔN1, p300-ΔN2, p300-ΔN3 and p300-ΔN4) were produced from FL p300 by PCR using the same antisense primer : 5'-CATGAACTACTCTAACAGTGACC-3'-and different sense primers as following: sense 5'-GGTTCTGGAGCAAAGCTTGCTGATCCAGAGAAGCGCAAGCTCATCC-3' for p300-ΔN1; sense 5'-CCATCCACTACTAAGCTTCGGAAACAGTGGCACGAAGATATTAC-3' for p300-ΔN2; sense 5'-GTCAAAGAAAAAGCTTTTCAAACCCAGAAGAACTACGACAG-3' for p300-ΔN3; sense 5'-GCGGAAGAAAGATGAAGCTTATCTGTGTCCTTCACCATGAGATC-3' for p300-ΔN4. All the PCR fragments were restricted by HindIII and XbaI and cloned into the PXFS-Straw-Flag plasmid restricted with the same endonucleases. The two COOH-terminal-deleted truncates (p300-ΔC1 & p300-ΔC2) were amplified from FL p300 using

the same sense primer as 5'-ACGTCTAGACGTAAGCTTGCCGAGAATGTGGTGGAACCGG-3' and different antisense primers as following: antisense 5'-GATATCCTAGATCTCATGGTGAAGGACACAG-3' for p300-ΔC1 and antisense 5'-GATATCCTACGGAGATGACTGGGTAGCT-3' for p300-ΔC2. The PCR products were digested with HindIII and EcoRV and ligated into the PXFS-Straw-Flag plasmid restricted with the same endonucleases. p300-ΔB mutant was generated by two steps. First the fragment containing the sequences encoding aa 1 to aa 994 was produced by using primer set: sense 5'-CAGTCTAGACGTAAGCTTGCCGAGAATGTGGTGGAACCGG-3' and antisense: 5-CTGAAATAAGCTTCGGCTGAGTATCTGCTGG-3' from FL p300, producing a PCR product overhang with HindIII site on both 5' and 3'. This PCR product was then restricted with HindIII and fused into pXFS-straw-Flag-ΔN4 upstream of the sequences encoding aa 1255 of p300, finally producing a plasmid encoding p300 mutant without aa 995 to aa 1255 was deleted.

All plasmids were purified by ion exchange chromatography and sequenced prior to transfection.

4.4 Transfection and Luciferase Activity Assay

Transient transfection was performed using Lipofectamine PLUS reagent (Life Technologies, Inc.) in HepG2 and HEK 293 cells according to the manufacturer's instruction. For reporter assay, cells were plated into 6-well plates and cotransfected with γ-FBG-LUC reporter gene and the transfection efficiency control plasmid pSV2PAP. Twenty-four hours later, cells were stimulated with the cytokine. Both luciferase and alkaline phosphatase activities were measured 48 h after transfection. All transfections

are carried out in three independent experiments. For co-immunoprecipitation, indicated expression plasmids were co-transfected into 10-cm^2 dishes using the same protocol. Cells were treated with the cytokine at 24 h after transfection prior to protein extraction. MEFs were transfected by electroporation (Amaxa, Cologne, Germany). 2 x 10^6 cells were combined with 100 µl of MEF nucleofector soluction 2 and 3-5 µg of purified plasmids. Cells were transfected by using the program of A23 and then transferred into culture dish with fresh medium.

4.5 Preparation of Subcellular Extracts

Cells were collected in 1ml of cold PBS and centrifuged at 9000 rpm for 1minute at 4^{o}C. The pellets were resuspended by adding double cell volume of solution A(95) [50 mM HEPES (pH 7.9), 10 mM KCl, 1 mM EDTA, 1 mM EGTA, 1 mM dithiothreitol (DTT), 0.5 mM phenylmethylsulfonyl fluoride (PMSF), 20 mM NaF, 1 mM $Na_4P_20_7$, 1 mM Na_3VO_4] with protease inhibitor mix (1:100, vol/vol, Sigma Aldrich). After incubation on ice for 10 minutes, 10% Trixon-X 100 was added to a final concentration of 0.5%. The lysates were centrifuged at 6000×g for 1 minute at 4^{o}C and the supernatants were saved as cytoplasmic fraction. The nuclear pellets were resuspended in solution B (solution A with 1.0 M sucrose) and centrifuged again at 12,000×g at 4^{o}C for 10 minutes. After supernatants were removed, the purified nuclear pellets were incubated in solution C [10% glycerol, 50 mM HEPES (pH 7.9), 400 mM KCl, 1 mM EDTA, 1 mM EGTA, 1 mM DTT, 0.5 mM PMSF, 20 mM NaF, 1 mM $Na_4P_20_7$, 1 mM Na_3VO_4] with protease inhibitor mix (1:100, vol/vol, Sigma Aldrich), and vortexed at 4^{o}C for 20 minutes. After centrifugation at 12,000×g at 4^{o}C for 20 minutes, the supernatants were saved as nuclear extract. The protein concentrations were measured by coomassie dye binding (Protein Reagent, BioRad).

4.6 Western Blotting

Proteins were fractionated by SDS-PAGE, and transferred to polyvinylidene difluoride (PVDF) membranes (Millipore, Bedford, Mass). Membranes were blocked in 5% milk for 0.5-1 h and incubated with indicated primary Ab at 4°C overnight. Membranes were washed in TBS-0.1% Tween 20 and incubated with secondary Ab at 20 °C for 1 h. Signals were detected by the enhanced chemiluminescence assay (ECL; Amersham) or visualized by the Odyssey Infrared Imaging system. ß-actin is used as a loading control.

4.7 Co-immunoprecipitation

1-2 mg NE or WCE were precleared with 40 µl protein A-Sepharose beads (Sigma) for 1 h at 4 ^{o}C. Immunoprecipitation was performed in the presence of 5 µg of the indicated primary Ab at 4^{o}C overnight. Immune complexes were captured by adding 50 µl protein A-Sepharose beads and rotated at 4^{o}C for 2 h. After supernatant was discarded, protein A-Sepharose beads were washed with cold PBS for 4-5 times and immunoprecipitates were fractionated by SDS-PAGE.

4.8 siRNA Transfection

HepG2 cells were plated into 6-well plates at a density of 2.5x10^{5} cells/well. On the following day the cells were transfected with either siRNA targeting human CDK9 or the negative control siRNA (Ambion, Austin, TX) using TransIT-siQUEST transfection reagent (Mirus, Madison, WI) according to the manufacturer's instructions. 48 h later, the transfected cells were exposed to IL-6 stimulation prior to total cellular RNA extraction for Real-Time (RT) - PCR.

4.9 Two-Step ChIP Assay

4-6 x106 cells per 100mm dish were plated on the day before experiment and serum starved in 0.5% BSA-containing DMEM medium before treatment. Cells were stimulated for indicated times and washed twice with PBS. Double cross-linking was performed with DSG (Pierce) for 45 minutes and with 1% formaldehyde in PBS solution for 15 minutes at room temperature(107). After cells were washed and collected in 1ml PBS, pellets were lysed by SDS lysis buffer (1% SDS, 10 mM EDTA, 50 mM Tris-HCl, pH 8.0) with protease inhibitor cocktail mix (Sigma Aldrich) and sonicated 4 times, 15 seconds each at setting 4 with 10 seconds break on ice in-between until DNA fragments lengths were between 200 to 1000 bp. Equal amounts of DNA were immunoprecipitated overnight at 4^{o}C with 4µg indicated antibodies in ChIP dilution buffer (150 mM NaCl, 1% Triton X-100, 10% glycerol, 10 mM HEPES, pH 7.4, 1 mM EDTA). Immunoprecipitates were collected with 40 ul protein-A magnetic beads (Dynal Inc., Brown Deer, WI), and washed sequentially with ChIP dilution buffer, high-salt buffer (0.1% SDS, 1% Triton X-100, 2 mM EDTA, 20 mM Tris-HCl, pH 8.1, 500 mM NaCl), LiCl wash buffer (0.25 M LiCl, 1% Triton X-100, 1% deoxycholate, 1 mM EDTA, 10 mM Tris-HCl, pH 8.0), and finally in 1x TE buffer (10 mM Tris-HCl, 1 mM EDTA, pH 8.0). DNA was eluted in 250µl elution buffer containing 0.1 M NaHCO3 and 1% SDS for 15 minutes at room temperature. Samples were de-cross-linked in de-cross-linking mixture (20µl 5 M NaCl, 20µl 0.2 M EDTA, 20µl 1M HEPES, pH 7.4, 1 µl proteinase K) at 65^{o}C for 2 hours. DNA was exacted by phenol/chloroform, precipitated by 100% ethanol and used for RT-PCR.

4.10 Quantitative Real-Time PCR (Q-RT-PCR)

Total cellular RNA was extracted by Tri Reagent (Sigma). 2 μg of RNA was used for reverse transcription using SuperScript III First-Strand Synthesis System from Invitrogen. Two μl of cDNA products was amplified in 20 μl reaction system containing 10 μl iQ SYBR Green Supermix (BioRad) and 400 nM primer mix. All the primers were designed by PrimerExpress v2.0. For γ-FBG mRNA expression, the primers 5'-GGCAACTGTGCTGAACAGGAT-3' and 5'-GATGGCCAGCGTGACACTT-3' were used. The primer sequences for socs3, c-fos and p21 mRNA detection were shown in Table 3. All the reactions were processed in MyiQ Single Color Real-Time PCR thermocycler using two-step plus melting curve program and the results were analyzed by iQ5 program (BioRad). For quantitative real-time genomic PCR (Q-gPCR), a standard curve was generated using a dilution series of genomic DNA (from 40 ng – 25 μg) for each primer pair. The fold change of DNA in each immunoprecipitate was determined by normalizing the absolute amount to input DNA reference and calculating the fold change relative to that amount in unstimulated cells. The sequences of primer sets used in genomic assays are shown in Table 1 and Table 2.

4.11 Immunofluoresent Staining

HepG2 cells were grown in 6-well tissue culture plates containing sterile coverslips (Fisher). After treatment, cells on coverslips were rinsed by PBS twice and fixed with 4% paraformadehyde for 20 min at room temperature. After fixation, cells were washed with PBS three times and treated with 0.2% Trion X-100 for 15 min at room temperature prior to immunostaining. All slips were blocked with blocking buffer containing 1% BSA and 0.1% Triton X-100 for 1h and then washed once with PBS. The primary antibody was diluted in blocking buffer (1:50 for anti-pY705 STAT3, 1:100 for

anti-STAT3 (c-20) and 1:200 for anti-CDK9 (c-20)) and applied to the cells on coverslips. Cells were incubated in the primary antibody at 4 ^{o}C overnight. Next day, all slips were washed three times for 10 minutes each with PBS and then incubated with the diluted fluorescence-labeled secondary antibody (1:100, secondary antibodies for STAT3 and pY705STAT3 were from Jackson ImmunoResearch, secondary antibody for CDK9 staining was from Invitrogen) in blocking buffer for 1h at room temperature in the dark. Cells were washed three times with PBS in low lighting and dried at room temperature. Coverslips were mounted on slides using DakoCytomation Fluorescent Mounting Medium and observed under confocal microscope (Zeiss LSM510 META system). Images were captured at a magnification of 40X or 60X.

Table1. Primer sets used for Q-RT-gPCR in ChIP assay (γ-FBG gene)

Amplified Region	Primer sequences	
	forward	reverse
IL-6RE1	ACAGAGGGACAGGAATGTATTTCC	TGGCAGGAGGAGACTGACTTC
IL-6RE2	CTTAGTTCGAGGTCATATCTGTTTGC	AGTCCTGGAGGCTGTGTGATG
IL-6RE3	GAGCTTCAACCTGTGTGCAAAAT	CCGTTCCTTTTTCCTCATCCT
TATA	CCTCTCAGGCTCCAATTGTC	GTGATCAGCTCCAGCCATTT
Exon 5	ATGCATATGGGATGGCAGAC	CTGTCTCCTACTGGCACAACAG
Exon 7	CATCAGTTACCTTTCCCAGTGA	GAGAAGGTAGCCCAGCTTGA

Table 2. Primer sets used for RT-PCR

Target genes	Sense	Anti-sense
socs3	5’ CCGCGGGCACCTTTC 3’	5’ TTGACGCTCAACGTGAAGAAGT 3’
c-fos	5’ CCTGCCCCTTCTCAACGA 3’	5’ TCCACGTTGCTGATGCTCTT 3’
p21	5’ TTCCGCACAGGAGCAAAGT 3’	5’ CGGCGCAACTGCTCACT 3’

CHAPTER 5 SUMMARY AND FUTURE STUDY

5.1 Summary

The JAK/STAT3 signaling pathway is one of the handful pleiotropic cascades that translates extracellular signal into a transcription response. Because of its important role in multiple biological processes, including the immune response to injury or infection (6, 24, 25, 154), haematopoiesis (156-158) and embryonic development(9, 159), the JAK/STAT3 pathway has been extensively investigated. Although the principal components in the JAK/STAT3 cascade have been identified, there remain substantial unanswered questions about how this signaling pathway is activated and regulated. One of the gaps in our understanding of JAK/STAT3 signal transduction is how the activated STAT3 modulates gene transcription once it is translocated into nucleus. The transcriptional regulation in eukaryotes involves the coordinated interaction of a large group of proteins including the sequence-specific transcription factors, chromatin remodeling complexes and components of the basic transcriptional apparatus. Consistent with this theory, numerous studies have reported the robust interaction between STAT3 and other transcriptional regulators, including other enhancer-specific transcription factors (160-162), nuclear receptors (135, 163, 164) and HATs (27, 95, 96, 165). It becomes apparent now that STAT3-mediated transactivation is a complicated process that is highly regulated by the protein-protein and protein-DNA interactions. Despite the extensive study, the molecular mechanism governing STAT3 downstream gene expression is far from being fully understood.

In Chapter 2, we reported an inducible association between STAT3 and CDK9, the kinase subunit of P-TEFb complex, which activates the transcription elongation by

phosphorylating the CTD of RNA Pol II and negative elongation factors. For the first time, we described that CDK9 interacts with STAT3 via both its NH2-terminal domain and COOH-terminal domain. Our data also showed that CDK9 acts as a functional coactivator in STAT3-dependent enhanceosome because CDK9 inhibition causes a dramatic decrease in IL-6 induced APP expression exampled by γ-FBG. Finally, we clarified the mechanism how CDK9 regulates STAT3-dependent transcription by ChIP assays. The model we propose in Chapter 2 suggests that the activated STAT3 recruits CDK9 in nucleus which induces the subsequent activation of RNA Pol II by the CTD phosphorylation, leading to the productive transcription elongation. The importance of this study is to add a new level of STAT3 function as a regulator of transcription elongation by interacting with CDK9. Therefore, targeting CDK9 could be a potential approach to interfere with APR induction regulated by STAT3 signal transduction.

Like many other transcription factors, STAT3 also recruits HATs including p300 as coactivators to remodel chromatin structure and facilitates gene transcription (27, 95, 96, 165). However, the mechanism by which p300 regulates transcriptional activation is not well understood. There is a growing body of evidence suggesting that the p300 function is not limited to acetylate histone tails and relax chromatin structure. As a large protein, p300 contacts with multiple components in the basic transcriptional machinery and brings other cofactors into the close proximity [72, 89-94]. Our recent studies found that STAT3 not only interacts with p300 but also is a direct substrate of p300 for acetylation. In Chapter 3, we showed that the NH2-terminal acetylation on K49 and K87 stabilizes the association between STAT3 and p300. For the first time, we reported that the STAT3 NH2-terminal domain is bound to the p300 bromodomain, a domain recognizing acetyl-lysine. When we further investigate the function of NH2-terminal domain, we found that the STAT3 NH2-terminus-deficient mutant (STAT3-ΔN) reduces

the OSM inducible γ-FBG reporter activity and the endogenous STAT3 target gene expression, indicating the necessity of NH2-terminal domain in STAT3 function. ChIP experiments reveal that the STAT3 NH2-terminal deletion regulates gene transcription by mediating p300 and RNA Pol II recruitment to the promoter loci. Therefore, our study in Chapter 3 propose a model in which the inducible acetylation on the STAT3 NH2-teminal domain increases its binding affinity to the p300 bromodomain, thereby stabilizing enhanceosome assembly on the promoter and facilitating transcriptional activation.

5.2 Future study

CDK9/cyclin T are not constitutively active complexes; instead their activity and expression are regulated at several levels. For example, it was reported that cyclin T1 levels were upregulated in peripheral blood lymphocytes (PBLs) in response to PMA and/or PHA (128-130). This upregulation of cyclin T1 is related to hyperphosphorylation of RNA Pol II and results into HIV replication in stimulated PBLs (128). Also, the kinase activity of CDK9 is negatively regulated by two inhibitors, 7SK small nuclear RNA (7SK snRNA) (166, 167) and a protein called HEXIM 1(hexamehylene bisacetamide-induced protein 1) (168, 169). It has been shown that in Hela cells, about 50% of CDK9/cyclin T complexes are silenced by interacting with 7SK snRNA (166). Both UV irradiation and inhibition of transcription by actinomycin D can release CDK9 from 7SK snRNA inhibition (166, 167). Finally, the maturation of CDK9/cyclin T is regulated by a chaperone mechanism in which the newly synthesized CDK9 is transferred from Heat Shock Protein (HSP) to cyclin T1 (170). Therefore, the active pool of CDK9/cyclin T1 is tightly regulated in cells, which limits the availability of P-TEFb complex under certain cellular instances. It is unknown how the regulation of CDK9/cyclin T1 affects the

activity of transcription factors that interact with them. We noticed that cyclin T1 is upregulated by IL-6 in HepG2 cells. It will be interesting to test whether this induction has any effect on STAT3-depedent transcription. It has been shown that the upregulation of HEXIM 1 induced by HMBA (hexamethylene bisacetamide) in vasucular smooth muscle cells is correlated with grow arrest and suppression of NF-κB-dependent gene expression (171). It will also be interesting to examine whether overexpression of HEXIM will affect STAT3 signal transduction.

Cyclin is an important regulatory subunit of CDK9 complexes and four different types of cyclin have been identified up to now, including cyclin T1, cyclin T2a, cyclin T2b and cyclin K (35). The three T-type cyclins contain a NH2-terminal domain, a coiled-coil domain, a His-rich motif and a COOH-terminal PEST sequence (33, 172). The NH2-terminal cyclin box is highly conserved in cyclin T protein, whereas the carboxyl terminus is much less conserved (33). Although each of the T-type cyclin T/CDK9 complexes can phosphorylate the RNA pol II CTD, numerous studies have shown that the three cyclin T proteins have different functions. For example, cyclin T1/CDK9 is the only complexes that are able to bind HIV Tat because cyclin T1 contains a unique Tat:TAR Recognition Motif (TRM) that is not present in cyclin T2a and cyclin T2b(172). Cyclin T2 is highly expressed in human adult skeletal muscle cells and its expression level reaches to the peak during muscle cells differentiation(173), suggesting that cyclin T2a/CDK9complex might promote myogenic differentiation. This finding suggests that all the cyclins do not have redundant function and each of them plays a specific role in different gene transcription. In the future, it will be interesting to test the STAT3 interaction with other types of cycin/CDK9 complexes and how this interaction specifically regulates the STAT3-dependent transcription.

Although the previous study found that the P-TEFb is broadly required for RNA pol II-regulated transcription (126), the recent finding implicates that some gene expression is not dependent on CDK9 activity. For example, the inhibition of P-TEFb kinase activity in human colon carcinoma cells selectively blocks a subset group of genes controlled by the p53 pathway (127). The CDK9 activity and the S2 phosphorylation on the RNA pol II CTD are dispensable for p21 mRNA transcription (127). This finding indicates that P-TEFb is differentially required for activation of distinct p53 target genes. There is a possibility that some genes within IL-6 signaling pathway could also bypass the requirement of P-TEFb to activate mRNA synthesis. Measurement of the changes in other STAT3-dependent gene expression in response to CDK9 inhibition will help clarify this question.

CDK9 is recently identified as a substrate of HATs for acetylation. CDK9 is an acetylatable protein in cells and is aceylated by p300 *in vitro* (132, 174). Interestingly, two independent groups identified two distinct acetylation sites on CDK9 which play different roles in regulating CDK9 activity. The acetyaltion on K44 is required for the CDK9 kinase activity to phosphorylate the CTD of RNA Pol II (132). The acetylation on K48, however, inhibits the kinase function of CDK9 and transcriptional activity of P-TEFb (174). In our study, we also detected an interaction between CDK9 and p300 (data not shown), which raises the possibility that p300 regulates STAT3-dependent transcription by inducing posttranslational modification on CDK9 and modulating its kinase activity. In future study, the CDK9 mutants containing K44R or K48R substitution can be generated and tested for their effects on STAT3-dependent transcription.

Both CDK9 and p300 interact with the STAT3 NH2-terminal domain, indicating the important role of NH2-terminal region in recruiting STAT3 coactivators. A recent study reported that synthetic analogs of the STAT3 second α-helix specifically binds to

STAT3 and inhibits STAT3-dependent cancer cell survival and growth (175). Since the crystal structure of STAT3 NH2-terminal domain is not available yet, the inhibitor used in this study was designed based on the structure data from the STAT4 NH2-terminal region (175). This study suggests that the STAT3 NH2-terminal domain is a promising drug target for cancer treatment. Future study centering on the high resolution structure of STAT3 NH2-terminal domain will provide more rationality in designing STAT3 inhibitors.

Appendix: List of Abbreviations

STAT	signal transducers and activators of transcription
CDK	cyclin dependent kinase
IL-6	interleukin-6
OSM	oncostatin M
FL	Full length
IL-6Rα□	IL-6 receptor α chain
CTD	COOH terminal domain (of Pol II)
FBG	fibrinogen
FP	flavopiridol
IL6 RE	IL-6 response elements
RNA Pol II	RNA polymerase II
HATs	histone acetyltranferase
CBP	CREB-binding protein
P-TEFb	Positive Transcription Elongation Factor b complex
Q-RT-gPCR	quantitative real time genomic PCR
ChIP	chromatin immunoprecipitation assay
WT	wildtype
NE	Nuclear extract
NAP	nucleosome assembly proteins
DSIF	DRB-sensitivity-inducing factor
NELF	the negative elongation factor

REFERENCES

1. Ernst, M., and B. J. Jenkins. 2004. Acquiring signalling specificity from the cytokine receptor gp130. *Trends Genet* 20:23-32.
2. Heinrich, P. C., I. Behrmann, S. Haan, H. M. Hermanns, G. Muller-Newen, and F. Schaper. 2003. Principles of interleukin (IL)-6-type cytokine signalling and its regulation. *Biochem J* 374:1-20.
3. Murray, P. J. 2007. The JAK-STAT signaling pathway: input and output integration. *J Immunol* 178:2623-2629.
4. Heinrich, P. C., I. Behrmann, G. Muller-Newen, F. Schaper, and L. Graeve. 1998. Interleukin-6-type cytokine signalling through the gp130/Jak/STAT pathway. *Biochem J* 334 (Pt 2):297-314.
5. Hou, T., B. C. Tieu, S. Ray, A. Recinos, R. Cui, R. G. Tilton, and A. R. Brasier. 2008. Roles of IL-6-gp130 signaling in vascular inflammation. *Current Cardiology Reviews* 4:179-192.
6. Ishihara K, H. T. 2002. IL-6 in autoimmune disease and chronic inflammatory proliferative disease. *Cytokine Growth Factor Rev* 13:357-368.
7. Hong DS, A. L., Kurzrock R. 2007. Interleukin-6 and its receptor in cancer: implications for Translational Therapeutics. *Cancer* 110:1911-1928.
8. Baraldi-Junkins CA, B. A., Rothstein G. 2000. Hematopoiesis and cytokines. Relevance to cancer and aging. *Hematol Oncol Clin North Am* 14:45-61.
9. Taga T, F. S. 2005. Role of IL-6 in the neural stem cell differentiation. *Clin Rev Allergy Immunol.* 28:249-256.
10. Seiler P, P. G., Deng MC. 2001. The interleukin-6 cytokine system in embryonic development, embryo-maternal interactions and cardiogenesis. *Eur Cytokine Netw.* 12:15-21.
11. Yamasaki, K., T. Taga, Y. Hirata, H. Yawata, Y. Kawanishi, B. Seed, T. Taniguchi, T. Hirano, and T. Kishimoto. 1988. Cloning and expression of the human interleukin-6 (BSF-2/IFN beta 2) receptor. *Science* 241:825-828.
12. Murakami, M., M. Hibi, N. Nakagawa, T. Nakagawa, K. Yasukawa, K. Yamanishi, T. Taga, and T. Kishimoto. 1993. IL-6-induced homodimerization of gp130 and associated activation of a tyrosine kinase. *Science* 260:1808-1810.
13. Lutticken, C., U. M. Wegenka, J. Yuan, J. Buschmann, C. Schindler, A. Ziemiecki, A. G. Harpur, A. F. Wilks, K. Yasukawa, T. Taga, and et al. 1994. Association of transcription factor APRF and protein kinase Jak1 with the interleukin-6 signal transducer gp130. *Science* 263:89-92.

14. Radtke, S., H. M. Hermanns, C. Haan, H. Schmitz-Van De Leur, H. Gascan, P. C. Heinrich, and I. Behrmann. 2002. Novel role of Janus kinase 1 in the regulation of oncostatin M receptor surface expression. *J Biol Chem* 277:11297-11305.

15. Stahl, N., T. G. Boulton, T. Farruggella, N. Y. Ip, S. Davis, B. A. Witthuhn, F. W. Quelle, O. Silvennoinen, G. Barbieri, S. Pellegrini, and et al. 1994. Association and activation of Jak-Tyk kinases by CNTF-LIF-OSM-IL-6 beta receptor components. *Science* 263:92-95.

16. Gerhartz, C., B. Heesel, J. Sasse, U. Hemmann, C. Landgraf, J. Schneider-Mergener, F. Horn, P. C. Heinrich, and L. Graeve. 1996. Differential activation of acute phase response factor/STAT3 and STAT1 via the cytoplasmic domain of the interleukin 6 signal transducer gp130. I. Definition of a novel phosphotyrosine motif mediating STAT1 activation. *J Biol Chem* 271:12991-12998.

17. Stahl, N., T. J. Farruggella, T. G. Boulton, Z. Zhong, J. E. Darnell, Jr., and G. D. Yancopoulos. 1995. Choice of STATs and other substrates specified by modular tyrosine-based motifs in cytokine receptors. *Science* 267:1349-1353.

18. Kaptein, A., V. Paillard, and M. Saunders. 1996. Dominant negative stat3 mutant inhibits interleukin-6-induced Jak-STAT signal transduction. *J Biol Chem* 271:5961-5964.

19. Shuai, K., G. R. Stark, I. M. Kerr, and J. E. Darnell, Jr. 1993. A single phosphotyrosine residue of Stat91 required for gene activation by interferon-gamma. *Science* 261:1744-1746.

20. Honda, M., S. Yamamoto, M. Cheng, K. Yasukawa, H. Suzuki, T. Saito, Y. Osugi, T. Tokunaga, and T. Kishimoto. 1992. Human soluble IL-6 receptor: its detection and enhanced release by HIV infection. *J Immunol* 148:2175-2180.

21. Muller-Newen, G., C. Kohne, R. Keul, U. Hemmann, W. Muller-Esterl, J. Wijdenes, J. P. Brakenhoff, M. H. Hart, and P. C. Heinrich. 1996. Purification and characterization of the soluble interleukin-6 receptor from human plasma and identification of an isoform generated through alternative splicing. *Eur J Biochem* 236:837-842.

22. Lust, J. A., K. A. Donovan, M. P. Kline, P. R. Greipp, R. A. Kyle, and N. J. Maihle. 1992. Isolation of an mRNA encoding a soluble form of the human interleukin-6 receptor. *Cytokine* 4:96-100.

23. Mullberg, J., H. Schooltink, T. Stoyan, M. Gunther, L. Graeve, G. Buse, A. Mackiewicz, P. C. Heinrich, and S. Rose-John. 1993. The soluble interleukin-6 receptor is generated by shedding. *Eur J Immunol* 23:473-480.

24. Mitsuyama, K., M. Sata, and S. Rose-John. 2006. Interleukin-6 trans-signaling in inflammatory bowel disease. *Cytokine Growth Factor Rev* 17:451-461.

25. Scheller, J., N. Ohnesorge, and S. Rose-John. 2006. Interleukin-6 trans-signalling in chronic inflammation and cancer. *Scand J Immunol* 63:321-329.

26. Paulson, M., S. Pisharody, L. Pan, S. Guadagno, A. L. Mui, and D. E. Levy. 1999. Stat protein transactivation domains recruit p300/CBP through widely divergent sequences. *J Biol Chem* 274:25343-25349.

27. Ray, S., C. T. Sherman, M. Lu, and A. R. Brasier. 2002. Angiotensinogen gene expression is dependent on signal transducer and activator of transcription 3-mediated p300/cAMP response element binding protein-binding protein coactivator recruitment and histone acetyltransferase activity. *Mol Endocrinol* 16:824-836.

28. Kwon, M. C., B. K. Koo, J. S. Moon, Y. Y. Kim, K. C. Park, N. S. Kim, M. Y. Kwon, M. P. Kong, K. J. Yoon, S. K. Im, J. Ghim, Y. M. Han, S. K. Jang, M. Shong, and Y. Y. Kong. 2008. Crif1 is a novel transcriptional coactivator of STAT3. *Embo J* 27:642-653.

29. Grana, X., A. De Luca, N. Sang, Y. Fu, P. P. Claudio, J. Rosenblatt, D. O. Morgan, and A. Giordano. 1994. PITALRE, a nuclear CDC2-related protein kinase that phosphorylates the retinoblastoma protein in vitro. *Proc Natl Acad Sci U S A* 91:3834-3838.

30. Zhu, Y., T. Pe'ery, J. Peng, Y. Ramanathan, N. Marshall, T. Marshall, B. Amendt, M. B. Mathews, and D. H. Price. 1997. Transcription elongation factor P-TEFb is required for HIV-1 tat transactivation in vitro. *Genes Dev* 11:2622-2632.

31. Shore, S. M., S. A. Byers, W. Maury, and D. H. Price. 2003. Identification of a novel isoform of Cdk9. *Gene* 307:175-182.

32. Peng, J., N. F. Marshall, and D. H. Price. 1998. Identification of a cyclin subunit required for the function of Drosophila P-TEFb. *J Biol Chem* 273:13855-13860.

33. Peng, J., Y. Zhu, J. T. Milton, and D. H. Price. 1998. Identification of multiple cyclin subunits of human P-TEFb. *Genes Dev* 12:755-762.

34. Lin, X., R. Taube, K. Fujinaga, and B. M. Peterlin. 2002. P-TEFb containing cyclin K and Cdk9 can activate transcription via RNA. *J Biol Chem* 277:16873-16878.

35. Garriga, J., and X. Grana. 2004. Cellular control of gene expression by T-type cyclin/CDK9 complexes. *Gene* 337:15-23.

36. Zawel, L., K. P. Kumar, and D. Reinberg. 1995. Recycling of the general transcription factors during RNA polymerase II transcription. *Genes Dev* 9:1479-1490.

37. Akoulitchev, S., T. P. Makela, R. A. Weinberg, and D. Reinberg. 1995. Requirement for TFIIH kinase activity in transcription by RNA polymerase II. *Nature* 377:557-560.

38. Dvir, A., R. C. Conaway, and J. W. Conaway. 1997. A role for TFIIH in controlling the activity of early RNA polymerase II elongation complexes. *Proc Natl Acad Sci U S A* 94:9006-9010.

39. Lei, L., D. Ren, A. Finkelstein, and Z. F. Burton. 1998. Functions of the N- and C-terminal domains of human RAP74 in transcriptional initiation, elongation, and recycling of RNA polymerase II. *Mol Cell Biol* 18:2130-2142.

40. Tan, S., T. Aso, R. C. Conaway, and J. W. Conaway. 1994. Roles for both the RAP30 and RAP74 subunits of transcription factor IIF in transcription initiation and elongation by RNA polymerase II. *J Biol Chem* 269:25684-25691.

41. Yamaguchi, Y., N. Inukai, T. Narita, T. Wada, and H. Handa. 2002. Evidence that negative elongation factor represses transcription elongation through binding to a DRB sensitivity-inducing factor/RNA polymerase II complex and RNA. *Mol Cell Biol* 22:2918-2927.

42. Yamaguchi, Y., T. Takagi, T. Wada, K. Yano, A. Furuya, S. Sugimoto, J. Hasegawa, and H. Handa. 1999. NELF, a multisubunit complex containing RD, cooperates with DSIF to repress RNA polymerase II elongation. *Cell* 97:41-51.

43. Marshall, N. F., J. Peng, Z. Xie, and D. H. Price. 1996. Control of RNA polymerase II elongation potential by a novel carboxyl-terminal domain kinase. *J Biol Chem* 271:27176-27183.

44. Shim, E. Y., A. K. Walker, Y. Shi, and T. K. Blackwell. 2002. CDK-9/cyclin T (P-TEFb) is required in two postinitiation pathways for transcription in the C. elegans embryo. *Genes Dev* 16:2135-2146.

45. Sims, R. J., 3rd, R. Belotserkovskaya, and D. Reinberg. 2004. Elongation by RNA polymerase II: the short and long of it. *Genes Dev* 18:2437-2468.

46. Majello, B., and G. Napolitano. 2001. Control of RNA polymerase II activity by dedicated CTD kinases and phosphatases. *Front Biosci* 6:D1358-1368.

47. Barboric, M., R. M. Nissen, S. Kanazawa, N. Jabrane-Ferrat, and B. M. Peterlin. 2001. NF-kappaB binds P-TEFb to stimulate transcriptional elongation by RNA polymerase II. *Mol Cell* 8:327-337.

48. Kanazawa, S., T. Okamoto, and B. M. Peterlin. 2000. Tat competes with CIITA for the binding to P-TEFb and blocks the expression of MHC class II genes in HIV infection. *Immunity* 12:61-70.

49. Jiang, S. L., D. Samols, J. Sipe, and I. Kushner. 1992. The acute phase response: overview and evidence of roles for both transcriptional and post-transcriptional mechanisms. *Folia Histochem Cytobiol* 30:133-135.

50. Ramji, D. P., A. Vitelli, F. Tronche, R. Cortese, and G. Ciliberto. 1993. The two C/EBP isoforms, IL-6DBP/NF-IL6 and C/EBP delta/NF-IL6 beta, are induced by IL-6 to promote acute phase gene transcription via different mechanisms. *Nucleic Acids Res* 21:289-294.

51. Hagihara, K., T. Nishikawa, Y. Sugamata, J. Song, T. Isobe, T. Taga, and K. Yoshizaki. 2005. Essential role of STAT3 in cytokine-driven NF-kappaB-mediated serum amyloid A gene expression. *Genes Cells* 10:1051-1063.

52. Sherman, C. T., and A. R. Brasier. 2001. Role of signal transducers and activators of transcription 1 and -3 in inducible regulation of the human angiotensinogen gene by interleukin-6. *Mol Endocrinol* 15:441-457.

53. Rooney, M. M., L. V. Parise, and S. T. Lord. 1996. Dissecting clot retraction and platelet aggregation. Clot retraction does not require an intact fibrinogen gamma chain C terminus. *J Biol Chem* 271:8553-8555.

54. Ernst, E., and K. L. Resch. 1993. Fibrinogen as a cardiovascular risk factor: a meta-analysis and review of the literature. *Ann Intern Med* 118:956-963.

55. Amrani, D. L. 1990. Regulation of fibrinogen biosynthesis: glucocorticoid and interleukin-6 control. *Blood Coagulation and Fibrinolysis* 1:443-336.

56. Hu, C. H., J. E. Harris, E. W. Davie, and D. W. Chung. 1995. Characterization of the 5'-flanking region of the gene for the alpha chain of human fibrinogen. *J Biol Chem* 270:28342-28349.

57. Mizuguchi, J., C. H. Hu, Z. Cao, K. R. Loeb, D. W. Chung, and E. W. Davie. 1995. Characterization of the 5'-flanking region of the gene for the gamma chain of human fibrinogen. *J Biol Chem* 270:28350-28356.

58. Zhang, Z., N. L. Fuentes, and G. M. Fuller. 1995. Characterization of the IL-6 responsive elements in the gamma fibrinogen gene promoter. *J Biol Chem* 270:24287-24291.

59. Anderson, G. M., A. R. Shaw, and J. A. Shafer. 1993. Functional characterization of promoter elements involved in regulation of human B beta-fibrinogen expression. Evidence for binding of novel activator and repressor proteins. *J Biol Chem* 268:22650-22655.

60. Dalmon, J., M. Laurent, and G. Courtois. 1993. The human beta fibrinogen promoter contains a hepatocyte nuclear factor 1-dependent interleukin-6-responsive element. *Mol Cell Biol* 13:1183-1193.

61. Gervois, P., N. Vu-Dac, R. Kleemann, M. Kockx, G. Dubois, B. Laine, V. Kosykh, J. C. Fruchart, T. Kooistra, and B. Staels. 2001. Negative regulation of human fibrinogen gene expression by peroxisome proliferator-activated receptor alpha agonists via inhibition of CCAAT box/enhancer-binding protein beta. *J Biol Chem* 276:33471-33477.

62. Hawiger, J. 1995. Adhesive ends of fibrinogen and its antiadhesive peptides: the end of a sage? *Semin Hematol* 32:99-109.

63. Ugarova, T. P., V. K. Lishko, N. P. Podolnikova, N. Okumura, S. M. Merkulov, V. P. Yakubenko, V. C. Yee, S. T. Lord, and T. A. Haas. 2003. Sequence gamma 377-395(P2), but not gamma 190-202(P1), is the binding site for the alpha MI-domain of integrin alpha M beta 2 in the gamma C-domain of fibrinogen. *Biochemistry* 42:9365-9373.

64. Sahni, A., and C. W. Francis. 2000. Vascular endothelial growth factor binds to fibrinogen and fibrin and stimulates endothelial cell proliferation. *Blood* 96:3772-3778.

65. Sahni, A., O. D. Altland, and C. W. Francis. 2003. FGF-2 but not FGF-1 binds fibrin and supports prolonged endothelial cell growth. *J Thromb Haemost* 1:1304-1310.

66. Sahni, A., M. Guo, S. K. Sahni, and C. W. Francis. 2004. Interleukin-1beta but not IL-1alpha binds to fibrinogen and fibrin and has enhanced activity in the bound form. *Blood* 104:409-414.

67. Duan, H. O., and P. J. Simpson-Haidaris. 2003. Functional analysis of interleukin 6 response elements (IL-6REs) on the human gamma-fibrinogen promoter: binding of hepatic Stat3 correlates negatively with transactivation potential of type II IL-6REs. *J Biol Chem* 278:41270-41281.

68. Ray, A. 2000. A SAF binding site in the promoter region of human gamma-fibrinogen gene functions as an IL-6 response element. *J Immunol* 165:3411-3417.

69. Duan, H. O., and P. J. Simpson-Haidaris. 2006. Cell type-specific differential induction of the human gamma-fibrinogen promoter by interleukin-6. *J Biol Chem* 281:12451-12457.

70. Bayle, J. H., and G. R. Crabtree. 1997. Protein acetylation: more than chromatin modification to regulate transcription. *Chem Biol* 4:885-888.

71. Brownell, J. E., J. Zhou, T. Ranalli, R. Kobayashi, D. G. Edmondson, S. Y. Roth, and C. D. Allis. 1996. Tetrahymena histone acetyltransferase A: a homolog to yeast Gcn5p linking histone acetylation to gene activation. *Cell* 84:843-851.

72. Ogryzko, V. V., R. L. Schiltz, V. Russanova, B. H. Howard, and Y. Nakatani. 1996. The transcriptional coactivators p300 and CBP are histone acetyltransferases. *Cell* 87:953-959.

73. Yang, X. J., V. V. Ogryzko, J. Nishikawa, B. H. Howard, and Y. Nakatani. 1996. A p300/CBP-associated factor that competes with the adenoviral oncoprotein E1A. *Nature* 382:319-324.

74. Mizzen, C. A., X. J. Yang, T. Kokubo, J. E. Brownell, A. J. Bannister, T. Owen-Hughes, J. Workman, L. Wang, S. L. Berger, T. Kouzarides, Y. Nakatani, and C. D. Allis. 1996. The TAF(II)250 subunit of TFIID has histone acetyltransferase activity. *Cell* 87:1261-1270.

75. Garcia-Ramirez, M., C. Rocchini, and J. Ausio. 1995. Modulation of chromatin folding by histone acetylation. *J Biol Chem* 270:17923-17928.

76. Tse, C., T. M. Fletcher, and J. C. Hansen. 1998. Enhanced transcription factor access to arrays of histone H3/H4 tetramer.DNA complexes in vitro: implications for replication and transcription. *Proc Natl Acad Sci U S A* 95:12169-12173.

77. Tse, C., T. Sera, A. P. Wolffe, and J. C. Hansen. 1998. Disruption of higher-order folding by core histone acetylation dramatically enhances transcription of nucleosomal arrays by RNA polymerase III. *Mol Cell Biol* 18:4629-4638.

78. Yang, X., M. O. Gold, D. N. Tang, D. E. Lewis, E. Aguilar-Cordova, A. P. Rice, and C. H. Herrmann. 1997. TAK, an HIV Tat-associated kinase, is a member of the cyclin-dependent family of protein kinases and is induced by activation of peripheral blood lymphocytes and differentiation of promonocytic cell lines. *Proc Natl Acad Sci U S A* 94:12331-12336.

79. Herrera, J. E., K. Sakaguchi, M. Bergel, L. Trieschmann, Y. Nakatani, and M. Bustin. 1999. Specific acetylation of chromosomal protein HMG-17 by PCAF alters its interaction with nucleosomes. *Mol Cell Biol* 19:3466-3473.

80. Munshi, N., M. Merika, J. Yie, K. Senger, G. Chen, and D. Thanos. 1998. Acetylation of HMG I(Y) by CBP turns off IFN beta expression by disrupting the enhanceosome. *Mol Cell* 2:457-467.

81. Soutoglou, E., N. Katrakili, and I. Talianidis. 2000. Acetylation regulates transcription factor activity at multiple levels. *Mol Cell* 5:745-751.

82. Polesskaya, A., I. Naguibneva, A. Duquet, E. Bengal, P. Robin, and A. Harel-Bellan. 2001. Interaction between acetylated MyoD and the bromodomain of CBP and/or p300. *Mol Cell Biol* 21:5312-5320.

83. Leo, C., and J. D. Chen. 2000. The SRC family of nuclear receptor coactivators. *Gene* 245:1-11.

84. Xu, L., C. K. Glass, and M. G. Rosenfeld. 1999. Coactivator and corepressor complexes in nuclear receptor function. *Curr Opin Genet Dev* 9:140-147.

85. Hampsey, M., and D. Reinberg. 1999. RNA polymerase II as a control panel for multiple coactivator complexes. *Curr Opin Genet Dev* 9:132-139.

86. Chan, H. M., and N. B. La Thangue. 2001. p300/CBP proteins: HATs for transcriptional bridges and scaffolds. *J Cell Sci* 114:2363-2373.

87. Gu, W., and R. G. Roeder. 1997. Activation of p53 sequence-specific DNA binding by acetylation of the p53 C-terminal domain. *Cell* 90:595-606.

88. Martinez-Balbas, M. A., U. M. Bauer, S. J. Nielsen, A. Brehm, and T. Kouzarides. 2000. Regulation of E2F1 activity by acetylation. *Embo J* 19:662-671.

89. Goodman, R. H., and S. Smolik. 2000. CBP/p300 in cell growth, transformation, and development. *Genes Dev* 14:1553-1577.

90. Shikama, N., H. M. Chan, M. Krstic-Demonacos, L. Smith, C. W. Lee, W. Cairns, and N. B. La Thangue. 2000. Functional interaction between nucleosome assembly proteins and p300/CREB-binding protein family coactivators. *Mol Cell Biol* 20:8933-8943.

91. Yao, T. P., G. Ku, N. Zhou, R. Scully, and D. M. Livingston. 1996. The nuclear hormone receptor coactivator SRC-1 is a specific target of p300. *Proc Natl Acad Sci U S A* 93:10626-10631.

92. Chen, H., R. J. Lin, R. L. Schiltz, D. Chakravarti, A. Nash, L. Nagy, M. L. Privalsky, Y. Nakatani, and R. M. Evans. 1997. Nuclear receptor coactivator ACTR is a novel histone acetyltransferase and forms a multimeric activation complex with P/CAF and CBP/p300. *Cell* 90:569-580.

93. Ito, T., T. Ikehara, T. Nakagawa, W. L. Kraus, and M. Muramatsu. 2000. p300-mediated acetylation facilitates the transfer of histone H2A-H2B dimers from nucleosomes to a histone chaperone. *Genes Dev* 14:1899-1907.

94. Shikama, N., C. W. Lee, S. France, L. Delavaine, J. Lyon, M. Krstic-Demonacos, and N. B. La Thangue. 1999. A novel cofactor for p300 that regulates the p53 response. *Mol Cell* 4:365-376.

95. Ray, S., I. Boldogh, and A. R. Brasier. 2005. STAT3 NH2-terminal acetylation is activated by the hepatic acute-phase response and required for IL-6 induction of angiotensinogen. *Gastroenterology* 129:1616-1632.

96. Yuan, Z. L., Y. J. Guan, D. Chatterjee, and Y. E. Chin. 2005. Stat3 dimerization regulated by reversible acetylation of a single lysine residue. *Science* 307:269-273.

97. Bhattacharya, S., R. Eckner, S. Grossman, E. Oldread, Z. Arany, A. D'Andrea, and D. M. Livingston. 1996. Cooperation of Stat2 and p300/CBP in signalling induced by interferon-alpha. *Nature* 383:344-347.

98. Zhang, J. J., U. Vinkemeier, W. Gu, D. Chakravarti, C. M. Horvath, and J. E. Darnell, Jr. 1996. Two contact regions between Stat1 and CBP/p300 in interferon gamma signaling. *Proc Natl Acad Sci U S A* 93:15092-15096.

99. Levy, D. E., and J. E. Darnell, Jr. 2002. Stats: transcriptional control and biological impact. *Nat Rev Mol Cell Biol* 3:651-662.

100. Kammerer, R. A. 1997. Alpha-helical coiled-coil oligomerization domains in extracellular proteins. *Matrix Biol* 15:555-565; discussion 567-558.

101. Shuai, K., C. M. Horvath, L. H. Huang, S. A. Qureshi, D. Cowburn, and J. E. Darnell, Jr. 1994. Interferon activation of the transcription factor Stat91 involves dimerization through SH2-phosphotyrosyl peptide interactions. *Cell* 76:821-828.

102. Eberhardy, S. R., and P. J. Farnham. 2002. Myc recruits P-TEFb to mediate the final step in the transcriptional activation of the cad promoter. *J Biol Chem* 277:40156-40162.

103. Lee, D. K., H. O. Duan, and C. Chang. 2001. Androgen receptor interacts with the positive elongation factor P-TEFb and enhances the efficiency of transcriptional elongation. *J Biol Chem* 276:9978-9984.

104. Iankova, I., R. K. Petersen, J. S. Annicotte, C. Chavey, J. B. Hansen, I. Kratchmarova, D. Sarruf, M. Benkirane, K. Kristiansen, and L. Fajas. 2006. Peroxisome proliferator-activated receptor gamma recruits the positive transcription elongation factor b complex to activate transcription and promote adipogenesis. *Mol Endocrinol* 20:1494-1505.

105. Giraud, S., A. Hurlstone, S. Avril, and O. Coqueret. 2004. Implication of BRG1 and cdk9 in the STAT3-mediated activation of the p21waf1 gene. *Oncogene* 23:7391-7398.

106. Chao, S. H., K. Fujinaga, J. E. Marion, R. Taube, E. A. Sausville, A. M. Senderowicz, B. M. Peterlin, and D. H. Price. 2000. Flavopiridol inhibits P-TEFb and blocks HIV-1 replication. *J Biol Chem* 275:28345-28348.

107. Nowak, D. E., B. Tian, and A. R. Brasier. 2005. Two-step cross-linking method for identification of NF-kappaB gene network by chromatin immunoprecipitation. *Biotechniques* 39:715-725.

108. Song, A., Q. Wang, M. G. Goebl, and M. A. Harrington. 1998. Phosphorylation of nuclear MyoD is required for its rapid degradation. *Mol Cell Biol* 18:4994-4999.

109. Kim, J. B., and P. A. Sharp. 2001. Positive transcription elongation factor B phosphorylates hSPT5 and RNA polymerase II carboxyl-terminal domain independently of cyclin-dependent kinase-activating kinase. *J Biol Chem* 276:12317-12323.

110. Radhakrishnan, S. K., and A. L. Gartel. 2006. CDK9 phosphorylates p53 on serine residues 33, 315 and 392. *Cell Cycle* 5:519-521.

111. Claudio, P. P., J. Cui, M. Ghafouri, C. Mariano, M. K. White, M. Safak, J. B. Sheffield, A. Giordano, K. Khalili, S. Amini, and B. E. Sawaya. 2006. Cdk9 phosphorylates p53 on serine 392 independently of CKII. *J Cell Physiol* 208:602-612.

112. Wen, Z., Z. Zhong, and J. E. Darnell, Jr. 1995. Maximal activation of transcription by Stat1 and Stat3 requires both tyrosine and serine phosphorylation. *Cell* 82:241-250.

113. Kouzarides, T. 1999. Histone acetylases and deacetylases in cell proliferation. *Curr Opin Genet Dev* 9:40-48.

114. Roberts, C. W., and S. H. Orkin. 2004. The SWI/SNF complex--chromatin and cancer. *Nat Rev Cancer* 4:133-142.

115. Price, D. H. 2000. P-TEFb, a cyclin-dependent kinase controlling elongation by RNA polymerase II. *Mol Cell Biol* 20:2629-2634.

116. Rana, T. M., and K. T. Jeang. 1999. Biochemical and functional interactions between HIV-1 Tat protein and TAR RNA. *Arch Biochem Biophys* 365:175-185.

117. Wimmer, J., K. Fujinaga, R. Taube, T. P. Cujec, Y. Zhu, J. Peng, D. H. Price, and B. M. Peterlin. 1999. Interactions between Tat and TAR and human

immunodeficiency virus replication are facilitated by human cyclin T1 but not cyclins T2a or T2b. *Virology* 255:182-189.

118. Ping, Y. H., and T. M. Rana. 2001. DSIF and NELF interact with RNA polymerase II elongation complex and HIV-1 Tat stimulates P-TEFb-mediated phosphorylation of RNA polymerase II and DSIF during transcription elongation. *J Biol Chem* 276:12951-12958.

119. Bieniasz, P. D., T. A. Grdina, H. P. Bogerd, and B. R. Cullen. 1998. Recruitment of a protein complex containing Tat and cyclin T1 to TAR governs the species specificity of HIV-1 Tat. *Embo J* 17:7056-7065.

120. Eberhardy, S. R., and P. J. Farnham. 2001. c-Myc mediates activation of the cad promoter via a post-RNA polymerase II recruitment mechanism. *J Biol Chem* 276:48562-48571.

121. Xu, X., Y. L. Sun, and T. Hoey. 1996. Cooperative DNA binding and sequence-selective recognition conferred by the STAT amino-terminal domain. *Science* 273:794-797.

122. Vinkemeier, U., S. L. Cohen, I. Moarefi, B. T. Chait, J. Kuriyan, and J. E. Darnell, Jr. 1996. DNA binding of in vitro activated Stat1 alpha, Stat1 beta and truncated Stat1: interaction between NH2-terminal domains stabilizes binding of two dimers to tandem DNA sites. *Embo J* 15:5616-5626.

123. Leung, S., S. A. Qureshi, I. M. Kerr, J. E. Darnell, Jr., and G. R. Stark. 1995. Role of STAT2 in the alpha interferon signaling pathway. *Mol Cell Biol* 15:1312-1317.

124. Murphy, T. L., E. D. Geissal, J. D. Farrar, and K. M. Murphy. 2000. Role of the Stat4 N domain in receptor proximal tyrosine phosphorylation. *Mol Cell Biol* 20:7121-7131.

125. Strehlow, I., and C. Schindler. 1998. Amino-terminal signal transducer and activator of transcription (STAT) domains regulate nuclear translocation and STAT deactivation. *J Biol Chem* 273:28049-28056.

126. Chao, S. H., and D. H. Price. 2001. Flavopiridol inactivates P-TEFb and blocks most RNA polymerase II transcription in vivo. *J Biol Chem* 276:31793-31799.

127. Gomes, N. P., G. Bjerke, B. Llorente, S. A. Szostek, B. M. Emerson, and J. M. Espinosa. 2006. Gene-specific requirement for P-TEFb activity and RNA polymerase II phosphorylation within the p53 transcriptional program. *Genes Dev* 20:601-612.

128. Garriga, J., J. Peng, M. Parreno, D. H. Price, E. E. Henderson, and X. Grana. 1998. Upregulation of cyclin T1/CDK9 complexes during T cell activation. *Oncogene* 17:3093-3102.

129. Herrmann, C. H., R. G. Carroll, P. Wei, K. A. Jones, and A. P. Rice. 1998. Tat-associated kinase, TAK, activity is regulated by distinct mechanisms in peripheral blood lymphocytes and promonocytic cell lines. *J Virol* 72:9881-9888.

130. Ghose, R., L. Y. Liou, C. H. Herrmann, and A. P. Rice. 2001. Induction of TAK (cyclin T1/P-TEFb) in purified resting CD4(+) T lymphocytes by combination of cytokines. *J Virol* 75:11336-11343.

131. Marshall, R. M., D. Salerno, J. Garriga, and X. Grana. 2005. Cyclin T1 expression is regulated by multiple signaling pathways and mechanisms during activation of human peripheral blood lymphocytes. *J Immunol* 175:6402-6411.

132. Fu, J., H. G. Yoon, J. Qin, and J. Wong. 2007. Regulation of P-TEFb Elongation Complex Activity by CDK9 Acetylation. *Mol Cell Biol* 27:4641-4651.

133. Auernhammer, C. J., C. Bousquet, and S. Melmed. 1999. Autoregulation of pituitary corticotroph SOCS-3 expression: characterization of the murine SOCS-3 promoter. *Proc Natl Acad Sci U S A* 96:6964-6969.

134. Paul, C., I. Seiliez, J. P. Thissen, and A. Le Cam. 2000. Regulation of expression of the rat SOCS-3 gene in hepatocytes by growth hormone, interleukin-6 and glucocorticoids mRNA analysis and promoter characterization. *Eur J Biochem* 267:5849-5857.

135. Yang, E., L. Lerner, D. Besser, and J. E. Darnell, Jr. 2003. Independent and cooperative activation of chromosomal c-fos promoter by STAT3. *J Biol Chem* 278:15794-15799.

136. Bellido, T., C. A. O'Brien, P. K. Roberson, and S. C. Manolagas. 1998. Transcriptional activation of the p21(WAF1,CIP1,SDI1) gene by interleukin-6 type cytokines. A prerequisite for their pro-differentiating and anti-apoptotic effects on human osteoblastic cells. *J Biol Chem* 273:21137-21144.

137. Zhang, L., D. B. Badgwell, J. J. Bevers, 3rd, K. Schlessinger, P. J. Murray, D. E. Levy, and S. S. Watowich. 2006. IL-6 signaling via the STAT3/SOCS3 pathway: functional analysis of the conserved STAT3 N-domain. *Mol Cell Biochem* 288:179-189.

138. Cho, H., G. Orphanides, X. Sun, X. J. Yang, V. Ogryzko, E. Lees, Y. Nakatani, and D. Reinberg. 1998. A human RNA polymerase II complex containing factors that modify chromatin structure. *Mol Cell Biol* 18:5355-5363.

139. Neish, A. S., S. F. Anderson, B. P. Schlegel, W. Wei, and J. D. Parvin. 1998. Factors associated with the mammalian RNA polymerase II holoenzyme. *Nucleic Acids Res* 26:847-853.

140. Manning, E. T., T. Ikehara, T. Ito, J. T. Kadonaga, and W. L. Kraus. 2001. p300 forms a stable, template-committed complex with chromatin: role for the bromodomain. *Mol Cell Biol* 21:3876-3887.

141. Vinkemeier, U., I. Moarefi, J. E. Darnell, Jr., and J. Kuriyan. 1998. Structure of the amino-terminal protein interaction domain of STAT-4. *Science* 279:1048-1052.

142. John, S., U. Vinkemeier, E. Soldaini, J. E. Darnell, Jr., and W. J. Leonard. 1999. The significance of tetramerization in promoter recruitment by Stat5. *Mol Cell Biol* 19:1910-1918.

143. Zhang, X., and J. E. Darnell, Jr. 2001. Functional importance of Stat3 tetramerization in activation of the alpha 2-macroglobulin gene. *J Biol Chem* 276:33576-33581.

144. He, B., L. You, K. Uematsu, M. Matsangou, Z. Xu, M. He, F. McCormick, and D. M. Jablons. 2003. Cloning and characterization of a functional promoter of the human SOCS-3 gene. *Biochem Biophys Res Commun* 301:386-391.

145. Lu, H., O. Flores, R. Weinmann, and D. Reinberg. 1991. The nonphosphorylated form of RNA polymerase II preferentially associates with the preinitiation complex. *Proc Natl Acad Sci U S A* 88:10004-10008.

146. Zeng, L., and M. M. Zhou. 2002. Bromodomain: an acetyl-lysine binding domain. *FEBS Lett* 513:124-128.

147. Dhalluin, C., J. E. Carlson, L. Zeng, C. He, A. K. Aggarwal, and M. M. Zhou. 1999. Structure and ligand of a histone acetyltransferase bromodomain. *Nature* 399:491-496.

148. Jacobson, R. H., A. G. Ladurner, D. S. King, and R. Tjian. 2000. Structure and function of a human TAFII250 double bromodomain module. *Science* 288:1422-1425.

149. Owen, D. J., P. Ornaghi, J. C. Yang, N. Lowe, P. R. Evans, P. Ballario, D. Neuhaus, P. Filetici, and A. A. Travers. 2000. The structural basis for the recognition of acetylated histone H4 by the bromodomain of histone acetyltransferase gcn5p. *Embo J* 19:6141-6149.

150. Mujtaba, S., Y. He, L. Zeng, A. Farooq, J. E. Carlson, M. Ott, E. Verdin, and M. M. Zhou. 2002. Structural basis of lysine-acetylated HIV-1 Tat recognition by PCAF bromodomain. *Mol Cell* 9:575-586.

151. Brasier, A. R., J. E. Tate, and J. F. Habener. 1989. Optimized use of the firefly luciferase assay as a reporter gene in mammalian cell lines. *Biotechniques* 7:1116-1122.

152. Shaner, N. C., R. E. Campbell, P. A. Steinbach, B. N. Giepmans, A. E. Palmer, and R. Y. Tsien. 2004. Improved monomeric red, orange and yellow fluorescent proteins derived from Discosoma sp. red fluorescent protein. *Nat Biotechnol* 22:1567-1572.

153. Madore, S. J., and B. R. Cullen. 1993. Genetic analysis of the cofactor requirement for human immunodeficiency virus type 1 Tat function. *J Virol* 67:3703-3711.

154. Hou, T., S. Ray, and A. R. Brasier. 2007. The functional role of an interleukin 6-inducible CDK9.STAT3 complex in human gamma-fibrinogen gene expression. *J Biol Chem* 282:37091-37102.

155. Eckner, R., M. E. Ewen, D. Newsome, M. Gerdes, J. A. DeCaprio, J. B. Lawrence, and D. M. Livingston. 1994. Molecular cloning and functional analysis of the adenovirus E1A-associated 300-kD protein (p300) reveals a protein with properties of a transcriptional adaptor. *Genes Dev* 8:869-884.

156. Ishibashi, T., H. Kimura, T. Uchida, S. Kariyone, P. Friese, and S. A. Burstein. 1989. Human interleukin 6 is a direct promoter of maturation of megakaryocytes in vitro. *Proc Natl Acad Sci U S A* 86:5953-5957.

157. Bruno, E., R. J. Cooper, R. A. Briddell, and R. Hoffman. 1991. Further examination of the effects of recombinant cytokines on the proliferation of human megakaryocyte progenitor cells. *Blood* 77:2339-2346.

158. Wallace, P. M., J. F. MacMaster, J. R. Rillema, J. Peng, S. A. Burstein, and M. Shoyab. 1995. Thrombocytopoietic properties of oncostatin M. *Blood* 86:1310-1315.

159. Hirano, T., K. Ishihara, and M. Hibi. 2000. Roles of STAT3 in mediating the cell growth, differentiation and survival signals relayed through the IL-6 family of cytokine receptors. *Oncogene* 19:2548-2556.

160. Cantwell, C. A., E. Sterneck, and P. F. Johnson. 1998. Interleukin-6-specific activation of the C/EBPdelta gene in hepatocytes is mediated by Stat3 and Sp1. *Mol Cell Biol* 18:2108-2117.

161. Zhang, X., M. H. Wrzeszczynska, C. M. Horvath, and J. E. Darnell, Jr. 1999. Interacting regions in Stat3 and c-Jun that participate in cooperative transcriptional activation. *Mol Cell Biol* 19:7138-7146.

162. Nakashima, K., M. Yanagisawa, H. Arakawa, N. Kimura, T. Hisatsune, M. Kawabata, K. Miyazono, and T. Taga. 1999. Synergistic signaling in fetal brain by STAT3-Smad1 complex bridged by p300. *Science* 284:479-482.

163. Ueda, T., N. Bruchovsky, and M. D. Sadar. 2002. Activation of the androgen receptor N-terminal domain by interleukin-6 via MAPK and STAT3 signal transduction pathways. *J Biol Chem* 277:7076-7085.

164. De Miguel, F., S. O. Lee, S. A. Onate, and A. C. Gao. 2003. Stat3 enhances transactivation of steroid hormone receptors. *Nucl Recept* 1:3.

165. Giraud, S., F. Bienvenu, S. Avril, H. Gascan, D. M. Heery, and O. Coqueret. 2002. Functional interaction of STAT3 transcription factor with the coactivator NcoA/SRC1a. *J Biol Chem* 277:8004-8011.

166. Nguyen, V. T., T. Kiss, A. A. Michels, and O. Bensaude. 2001. 7SK small nuclear RNA binds to and inhibits the activity of CDK9/cyclin T complexes. *Nature* 414:322-325.

167. Yang, Z., Q. Zhu, K. Luo, and Q. Zhou. 2001. The 7SK small nuclear RNA inhibits the CDK9/cyclin T1 kinase to control transcription. *Nature* 414:317-322.

168. Michels, A. A., V. T. Nguyen, A. Fraldi, V. Labas, M. Edwards, F. Bonnet, L. Lania, and O. Bensaude. 2003. MAQ1 and 7SK RNA interact with CDK9/cyclin T complexes in a transcription-dependent manner. *Mol Cell Biol* 23:4859-4869.

169. Yik, J. H., R. Chen, R. Nishimura, J. L. Jennings, A. J. Link, and Q. Zhou. 2003. Inhibition of P-TEFb (CDK9/Cyclin T) kinase and RNA polymerase II transcription by the coordinated actions of HEXIM1 and 7SK snRNA. *Mol Cell* 12:971-982.

170. O'Keeffe, B., Y. Fong, D. Chen, S. Zhou, and Q. Zhou. 2000. Requirement for a kinase-specific chaperone pathway in the production of a Cdk9/cyclin T1 heterodimer responsible for P-TEFb-mediated tat stimulation of HIV-1 transcription. *J Biol Chem* 275:279-287.

171. Ouchida, R., M. Kusuhara, N. Shimizu, T. Hisada, Y. Makino, C. Morimoto, H. Handa, F. Ohsuzu, and H. Tanaka. 2003. Suppression of NF-kappaB-dependent gene expression by a hexamethylene bisacetamide-inducible protein HEXIM1 in human vascular smooth muscle cells. *Genes Cells* 8:95-107.

172. Wei, P., M. E. Garber, S. M. Fang, W. H. Fischer, and K. A. Jones. 1998. A novel CDK9-associated C-type cyclin interacts directly with HIV-1 Tat and mediates its high-affinity, loop-specific binding to TAR RNA. *Cell* 92:451-462.

173. De Luca, A., A. Tosolini, P. Russo, A. Severino, A. Baldi, L. De Luca, I. Cavallotti, F. Baldi, A. Giordano, J. R. Testa, and M. G. Paggi. 2001. Cyclin T2a gene maps on human chromosome 2q21. *J Histochem Cytochem* 49:693-698.

174. Sabo, A., M. Lusic, A. Cereseto, and M. Giacca. 2008. Acetylation of conserved lysines in the catalytic core of cyclin-dependent kinase 9 inhibits kinase activity and regulates transcription. *Mol Cell Biol* 28:2201-2212.

175. Timofeeva, O. A., V. Gaponenko, S. J. Lockett, S. G. Tarasov, S. Jiang, C. J. Michejda, A. O. Perantoni, and N. I. Tarasova. 2007. Rationally designed inhibitors identify STAT3 N-domain as a promising anticancer drug target. *ACS Chem Biol* 2:799-809.

Vita

Tieying Hou was born in Liaocheng, Shandong Province, P.R. China on July 17, 1977. Her father is Shouxi Hou and her mother is Yulian Zeng. Ms. Hou obtained her M.D. degree from School of Medicine, Qingdao University in 2000 and her M.S. degree from Shandong University in 2003. During her Ph.D. study, Ms. Hou has published three papers on peer-reviewed journals including one first-authored paper. Ms. Hou can be reached at 250 Del Medio Ave, Apt 205, Mountain View, CA, 77555.

PULICATIONS:

1. Ray, S., Lee, C., **Hou, T.**, Boldogh, I., and Brasier, A.R. Requirement of Histone Deacetylase (HDAC1) in Signal Transducer and Activator of Transcription 3 (STAT3) nucleocytoplasmic distribution. *Nucleic Acids Res* 2008 Jul 8. [Epub ahead of print]
2. **Hou, T.**, Ray, S., Brasier, A.R. 2007. The Functional Role of an Interleukin 6-inducible CDK9·STAT3 Complex in Human gamma-Fibrinogen Gene Expression. *J Biol Chem* 282(51):37091
3. Recinos, A., Lejeune, W.S., Sun, H., Lee, C., Tieu, B.C., Lu, M., **Hou, T.**, Boldogh, I., Tilton, R.G,, Brasier, A.R. 2007. Angiotensin II induces IL-6 expression and the Jak-STAT3 pathway in aortic adventitia of LDL receptor-deficient mice. *Atherosclerosis* 194(1):125
4. **Hou, T.**, Tieu, B.C., Ray, S.,Recinos, A., Cui, R., Tilton, R.G. and Brasier, A.R. Roles of IL-6-gp130 Signaling in Vascular Inflammation. *Current Cardiology Reviews* 2008, 4: 179-192

This dissertation was typed by Tieying Hou.